NGA DEVELOPERS' RESPONSES TO QUESTIONS BY THE U.S. GEOLOGICAL SURVEY (USGS) AND CALIFORNIA GEOLOGICAL SURVEY (CGS) SEPTEMBER 1, 2006

PREFACE

The U.S. Geological Survey (USGS), working cooperatively with the California Geological Survey (CGS), conducted a review of the NGA relations. The review was focused on the potential use of the NGA relations in national ground motion hazard mapping. Review workshops were held in 2005 and 2006, with the principal and final review workshop held on September 25, 2006. Participants at this meeting included USGS and CGS reviewers, an external review panel formed by USGS, and NGA developers and other NGA project team members. Prior to the final review workshop, NGA developers responded in writing to questions from USGS and CGS reviewers and provided the responses to all reviewers. The questions and responses are provided in this document. Responses to specific questions by specific NGA developer teams can be accessed by clicking on the questions and responses in the Table of Contents. Where there are multiple responses to a question, the question is repeated before each response.

TABLE OF CONTENTS

TABLE OF CONTENTS
(continued)

Page

RESPONSES TO MARK PETERSEN'S QUESTIONS

MARK PETERSEN'S QUESTION #1

Do you consider your ground motion prediction equations appropriate for seismic hazard assessments of California and throughout the western U.S.? Please explain. If you had left out international data and only used California data would you get a significantly different answer? Please explain.

CAMPBELL-BOZORGNIA RESPONSE

There are really two issues to address regarding your question. One is the potential difference between extensional and non-extensional tectonic regimes and the other is the potential difference between different geographic regions. The issue regarding different tectonic regimes is important since much of California is in a non-extensional tectonic regime whereas most of the WUS is in an extensional tectonic regime. This issue is addressed by showing plots of inter-event residuals versus magnitude segregated by tectonic regime. The latter issue is addressed by showing plots of inter-event residuals versus magnitude and intra-event residuals versus distance (R_{RUP}) and 30m shear-wave velocity (V_{S30}) segregated by geographic region.

Regional Distribution of Database

Before responding to the question, we would first like to summarize the geographical distribution of our database. The distribution of the database by magnitude, distance and geographic region is given in Figure 1. The regions identified in this figure are California, the western United States outside of California (WUS), Alaska and Taiwan. All other regions are combined into a single category called Other. Figure 1 clearly shows that the database for $\mathbf{M} < 7.3$ is dominated by strong-motion recordings from California. The limited amount of WUS data fall within the data cloud for California. At larger magnitudes, the data from Taiwan, Alaska, and the remaining regions predominate. The extent to which the different geographic regions might have influenced our model is discussed below.

Distribution of Inter-Event Residuals by Geographic Region

The distribution of the inter-event residuals (source terms) by geographic region plotted against magnitude is shown in Figures 2–5 for PGA and SA at periods of 0.2, 1.0 and 3.0s, respectively. One might argue that the residuals show a slight bias towards under-predicting ground motions for California earthquakes. But the average residuals for California indicate that there is only a +5% bias in the predicted ground motions at short periods and a +9% bias in the predicted ground motions at long periods. The biggest biases are for Alaska, where ground motions are over-predicted at all periods, and the WUS, where ground motions are grossly over-predicted at long periods. The Taiwan (1999 Chi-Chi) earthquake (**M** 7.6) is over-predicted at short periods but is well-predicted at long periods. Of course, these biases are based on the assumption that the magnitude scaling predicted by the model is correct.

A second concern is whether the magnitude scaling at large magnitudes is biased. It appears that the California bias might be larger for events with $\mathbf{M} > 6.7$. If this is true, the magnitude scaling would need to be adjusted. However, there are only five California earthquakes between $\mathbf{M} = 6.7$ and 7.4, which are not enough to constrain magnitude scaling at large magnitudes. It is primarily the Alaska earthquakes that are responsible for offsetting the California events. We see no reason why these Alaska events are not a suitable analogue for California. In fact, many seismologists have used the 2002 Denali (**M** 7.9) earthquake as an analogue for a large earthquake on the San Andreas Fault. One of the more spectacular results is the very low residuals (near –1.0) at periods of 1.0 and 3.0s for two WUS earthquakes. A potential reason for this bias is discussed in the next section.

Distribution of Inter-Event Residuals by Tectonic Regime

The distribution of the inter-event residuals (source terms) by tectonic regime plotted against magnitude is shown in Figures 6–9 for PGA and SA at periods of 0.2, 1.0 and 3.0s, respectively. It should be noted that the classification of a region as extensional or non-extensional was taken directly from the NGA database. In this database, the 1999 Kocaeli (**M** 7.5) and 1999 Duzce (**M** 7.1) earthquakes, both from western Turkey, and the 1992 Landers (**M** 7.3) and the 1999 Hector Mine (**M** 7.1) earthquakes, both from the Mojave Desert in California, are classified as coming from a non-extensional regime. Art Frankel of the USGS and John Anderson of the University of Nevada (Reno) have suggested that both of these regions might be extensional rather than non-extensional.[1]

The figures show that there does not appear to be a significant bias between extensional and non-extensional regimes at short periods. Nor does there appear to be a bias associated with the four earthquakes of questionable tectonic regime classification. One of the more spectacular results is the very low residuals (near –1.0) at 1.0 and 3.0s periods for two WUS earthquakes: 1983 Borah Peak (**M** 6.9) and 1992 Little Skull Mtn. (**M** 5.7). Both events occurred in the extensional tectonic regime of the Basin and Range Province and have residuals at short periods that are not out of line with the other earthquakes. Both of these earthquakes occurred in a region dominated by volcanic rock, possibly at or very near the surface, which is likely to have a very shallow sediment depth (i.e., a small value of $Z_{2.5}$). However, our database does not contain estimates of sediment depth for the sites that recorded these earthquakes. Our model predicts very low long-period ground motions for sites with $Z_{2.5} < 1$ km, which might explain the observed biases. Because of this, we did not allow these events to bias the normal-faulting factor at long periods in our model. See the discussion of this issue in our report.

Distribution of Intra-Event Residuals by Distance and 30m Shear-Wave Velocity

The distribution of the intra-event residuals by geographic region plotted against distance (R_{RUP}) is shown in Figures 10–13 for PGA and SA at periods of 0.2, 1.0 and 3.0s, respectively. The plots are shown in terms of log distance to be consistent with how the parameter is used in the regression and to emphasize those recordings at short distances that are of greater

[1] After this response was written, Paul Spudich and Dave Boore of the USGS investigated the four earthquakes in question and determined that they occurred within a non-extensional regime.

engineering interest. These figures indicate that there does not appear to be a regional bias in any of the residuals.

The distribution of the intra-event residuals by geographic region plotted against 30m shear-wave velocity (V_{S30}) is shown in Figures 14–17. Similar to the plots with distance, these figures indicate that there does not appear to be a regional bias in any of the residuals, except for a tendency to under-predict 3.0s spectral accelerations at $V_{S30} > 1000$ m/s in both California and Taiwan. The reason for this under-prediction is unknown at the present time. It is interesting to note that in general the model seems valid for predicting ground motions for NEHRP E sites, even though we have recommended in our report that the user exercise caution when predicting ground motions for such low-velocity sites. We made this recommendation to bring attention to the fact that the shaking response of some NEHRP E sites is problematic at high values of ground motion and are best addressed using site-specific response analyses.

Conclusion

Based on the results and discussion presented above, we believe that our empirical ground motion model is appropriate for predicting ground motions in California for purposes of seismic hazard assessment. Its validity in the WUS is more problematic, because there are only three earthquakes in our database that are outside of California and all three come from the extensional Basin and Range Province. Two of these events have long-period ground motions that are grossly over-predicted at long periods, which we attribute to shallow sediments of unknown depth. Aside from these two earthquakes, we believe that our residuals show that our ground-motion predictions do not appear to have a significant regional bias and that earthquakes from regions outside of California and the WUS are appropriate for estimating ground motions in these regions.

The question of whether our results would have been significantly different had we used only California data is difficult to answer without the painstaking task of re-running our analysis and re-interpreting the results. This question gets at the appropriateness of our predicted magnitude scaling at $\mathbf{M} > 6.7$, which is based on only five California earthquakes, the largest being 7.4. We believe that the five California earthquakes in our database within this magnitude range are insufficient to constrain magnitude scaling at large magnitudes, so we would not recommend re-running our analysis with only California earthquakes. Assuming the same magnitude scaling predicted by our model, we find a bias of only 5–9%, depending on period, in the predicted California ground motions, which we do not find to be significant. We do acknowledge that the magnitude scaling at large magnitudes is less certain that that at smaller magnitudes, which is appropriately addressed by increasing the epistemic uncertainty at these magnitudes. In our opinion, restricting the database to the few California earthquakes at $\mathbf{M} > 6.7$ would more likely significantly bias the magnitude scaling and, therefore, the median predictions of ground motion at large magnitudes at the expense of reducing both the aleatory and epistemic uncertainty.

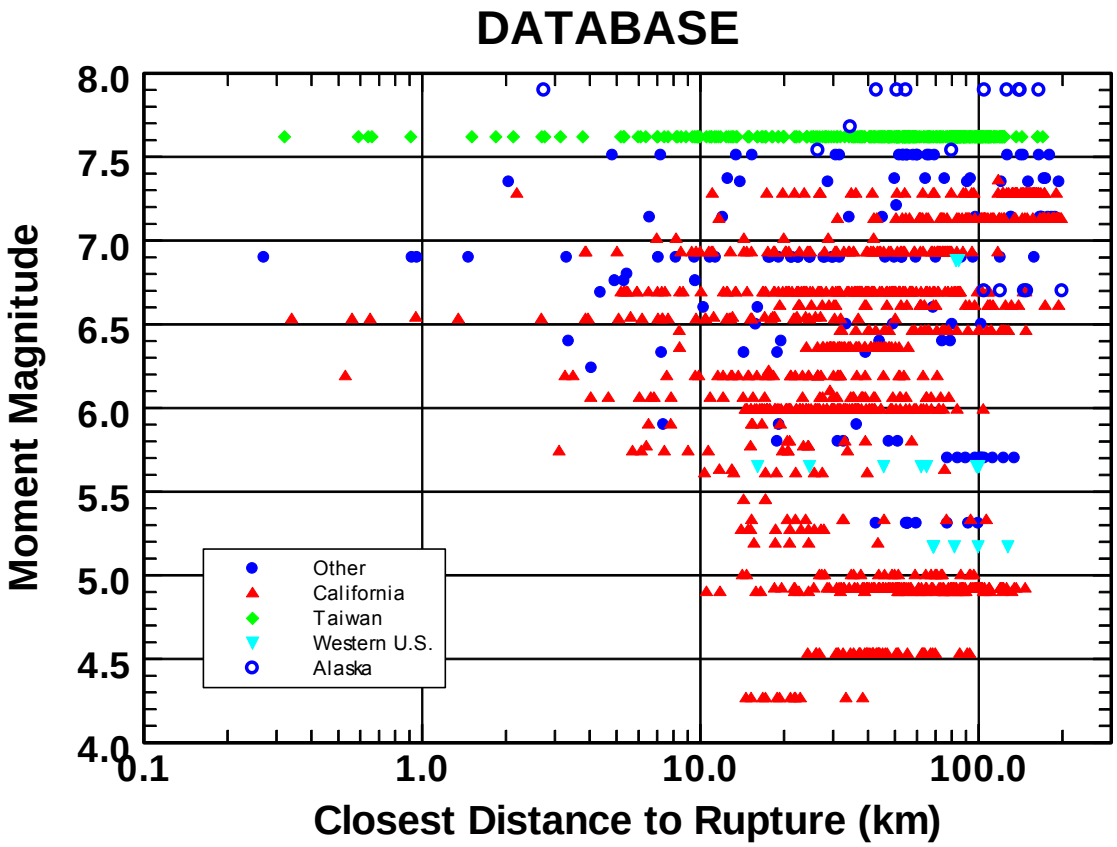

Figure 1: Plot of the distribution of recordings with respect to magnitude, distance and geographic region for the Campbell-Bozorgnia (CB06) NGA database. The regions identified in the legend include: California, the western United States outside of California, Alaska, Taiwan, and all other regions.

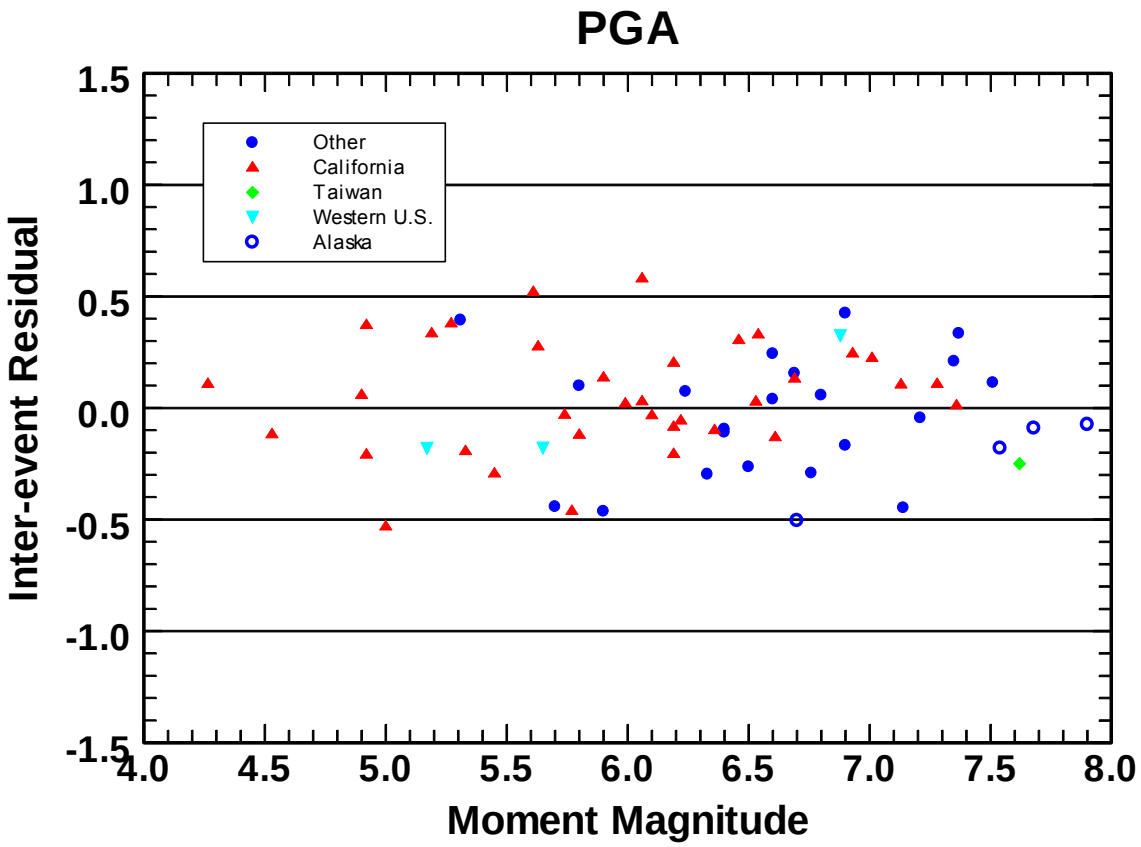

Figure 2: Plot of inter-event residuals for PGA for the Campbell and Bozorgnia (CB06) NGA model showing their distribution with respect to geographic region.

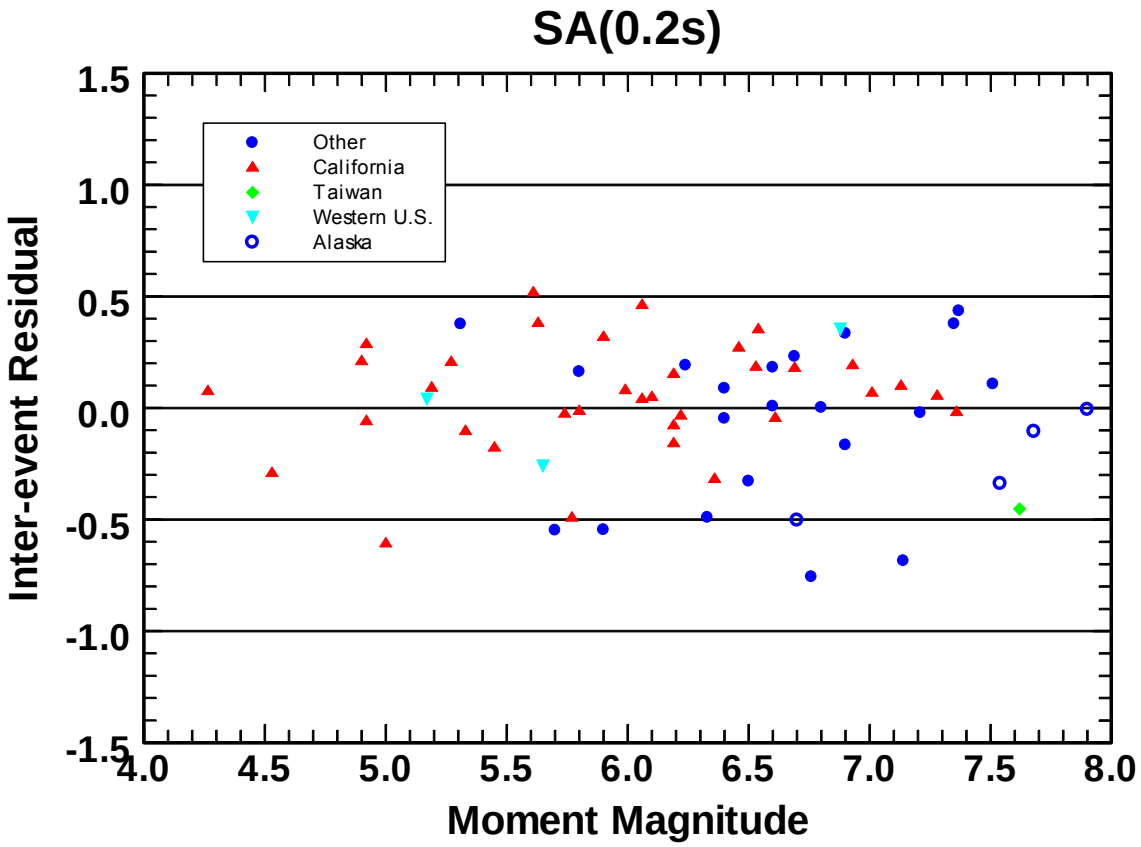

Figure 3: Plot of inter-event residuals for 0.2s spectral acceleration for the Campbell and Bozorgnia (CB06) NGA model showing their distribution with respect to geographic region.

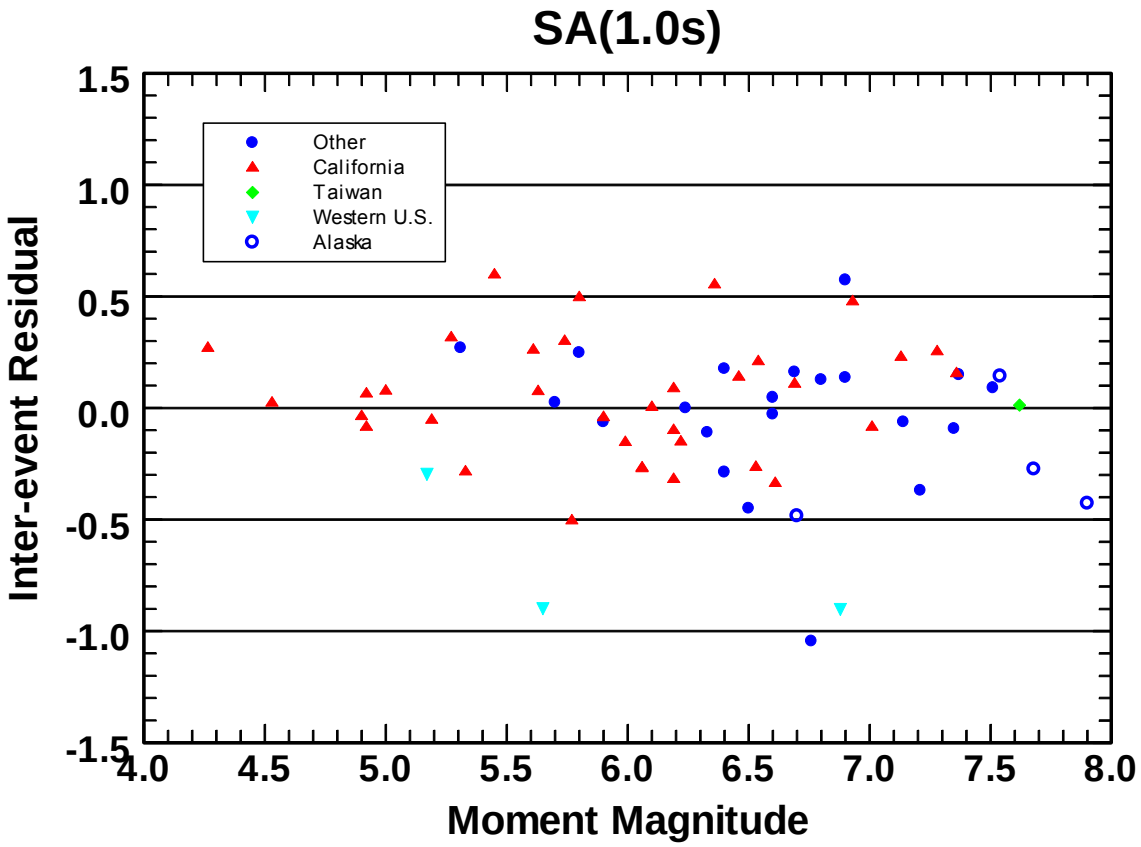

Figure 4: Plot of inter-event residuals for 1.0s spectral acceleration for the Campbell and Bozorgnia (CB06) NGA model showing their distribution with respect to geographic region.

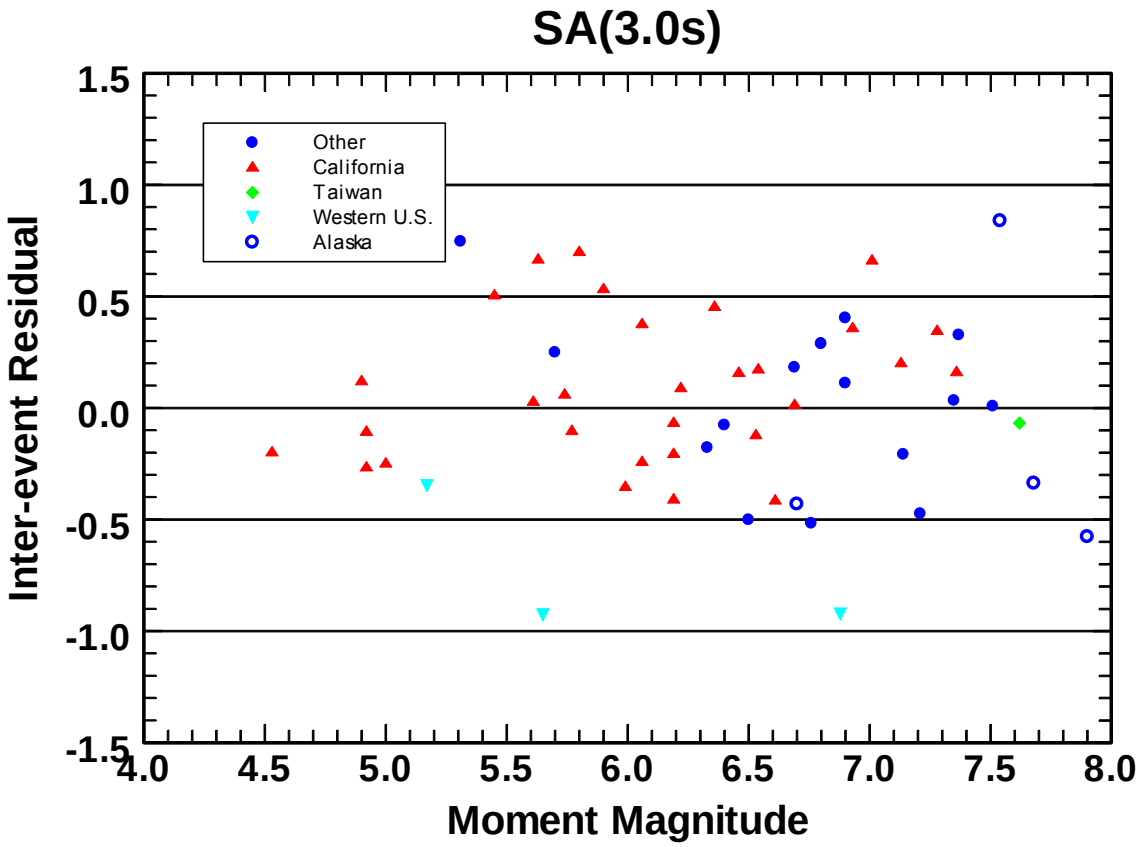

Figure 5: Plot of inter-event residuals for 3.0s spectral acceleration for the Campbell and Bozorgnia (CB06) NGA model showing their distribution with respect to geographic region.

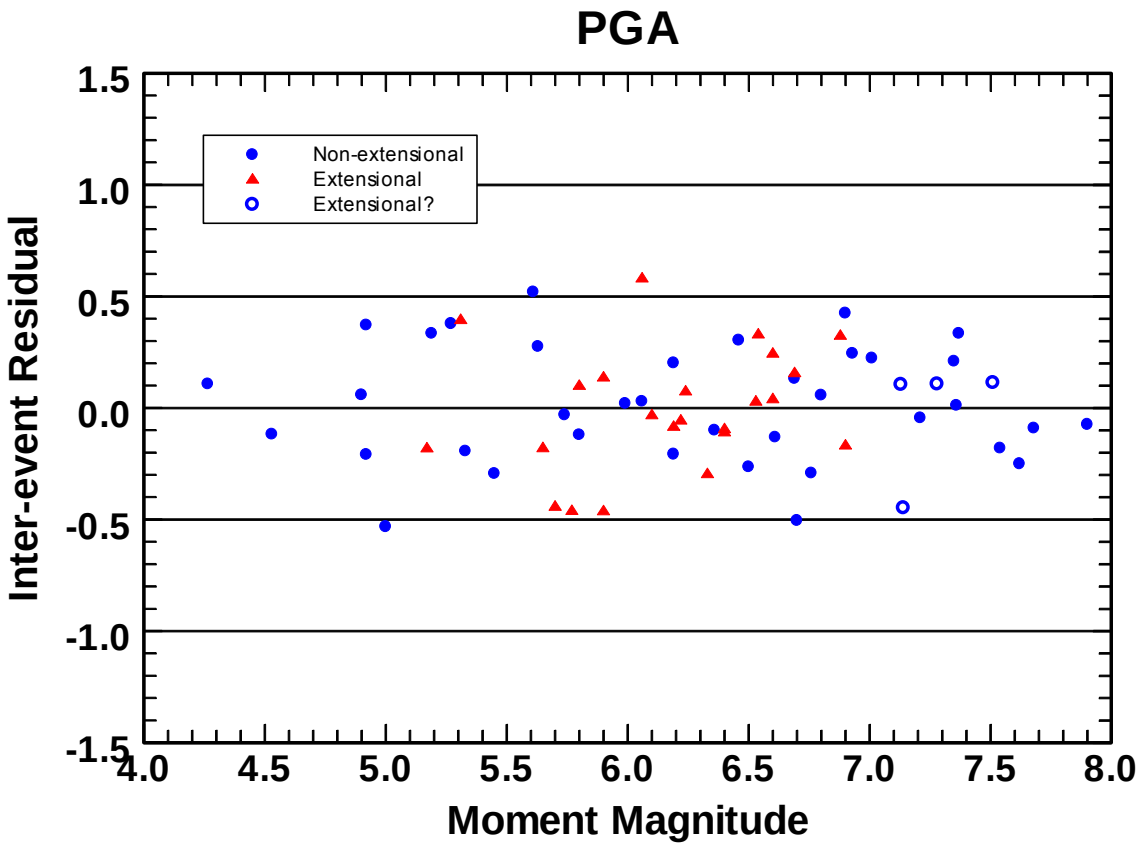

Figure 6: Plot of inter-event residuals for PGA for the Campbell and Bozorgnia (CB06) NGA model showing their distribution with respect to tectonic regime.

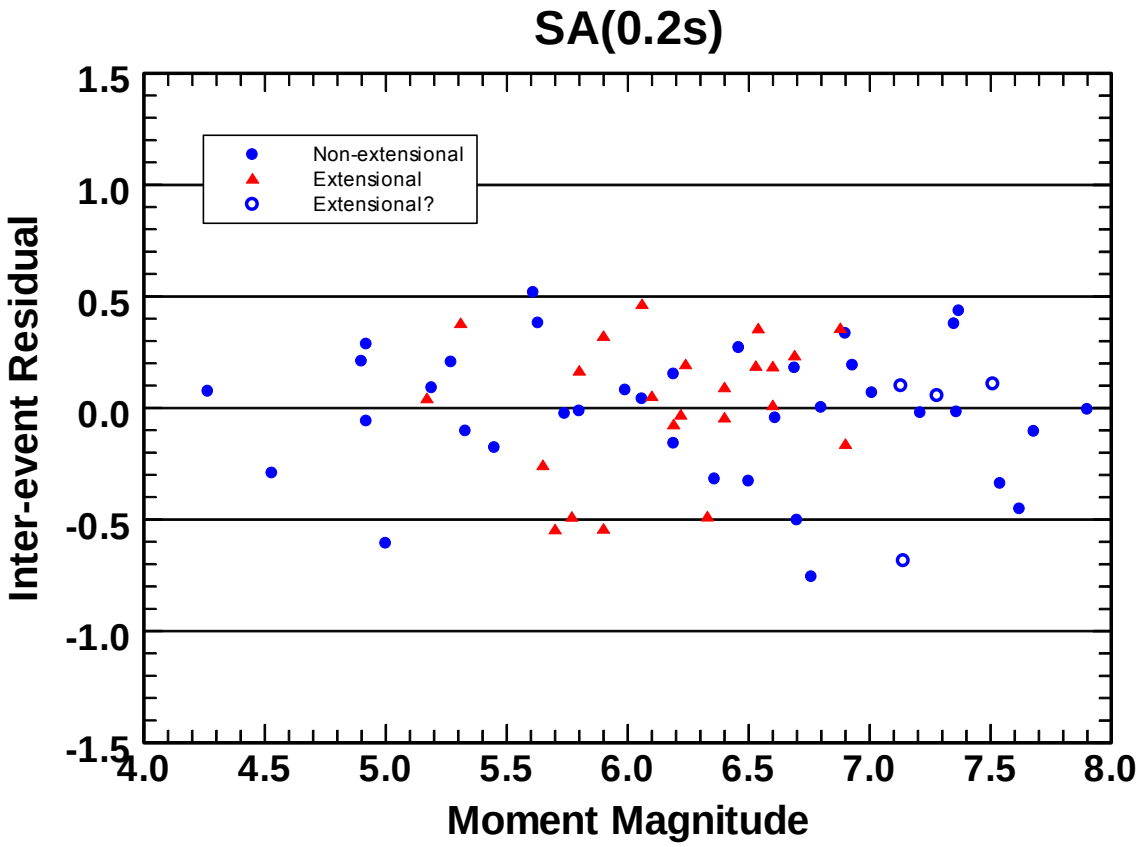

Figure 7: Plot of inter-event residuals for 0.2s spectral acceleration for the Campbell and Bozorgnia (CB06) NGA model showing their distribution with respect to tectonic regime.

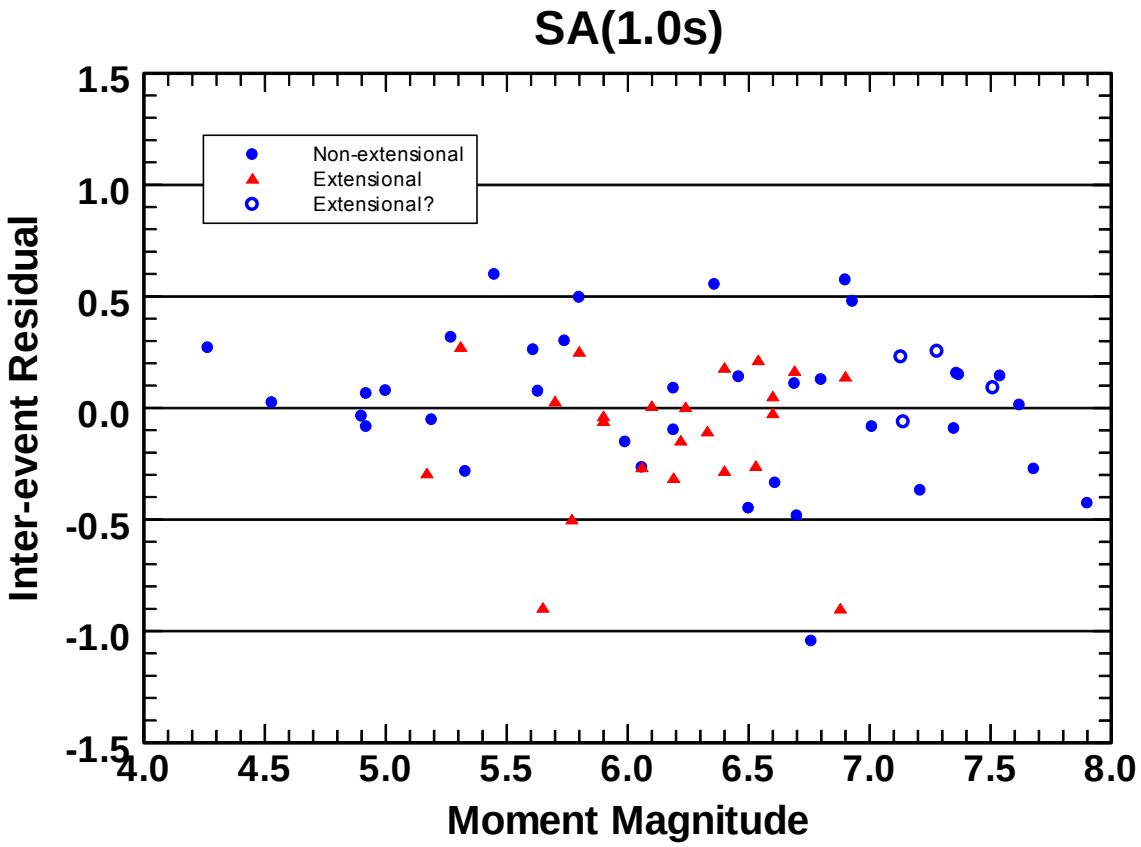

Figure 8: Plot of inter-event residuals for 1.0s spectral acceleration for the Campbell and Bozorgnia (CB06) NGA model showing their distribution with respect to tectonic regime.

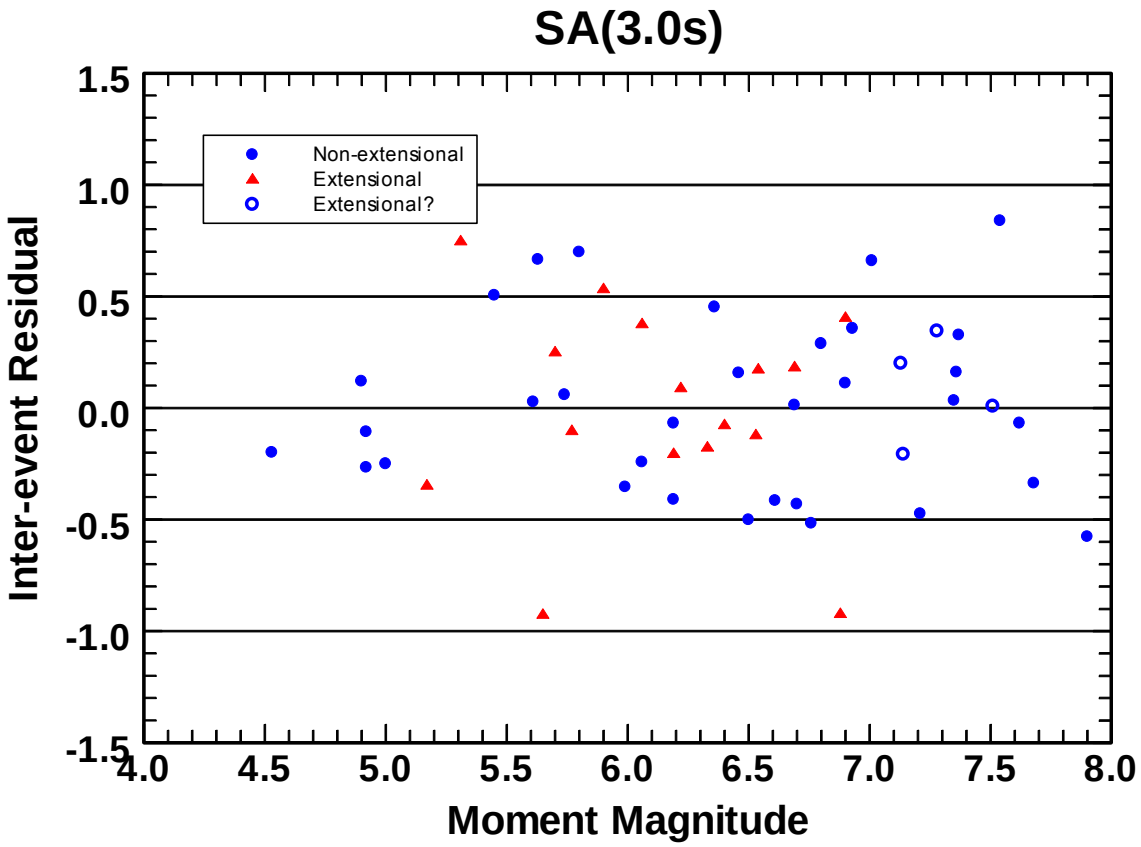

Figure 9: Plot of inter-event residuals for 3.0s spectral acceleration for the Campbell and Bozorgnia (CB06) NGA model showing their distribution with respect to tectonic regime.

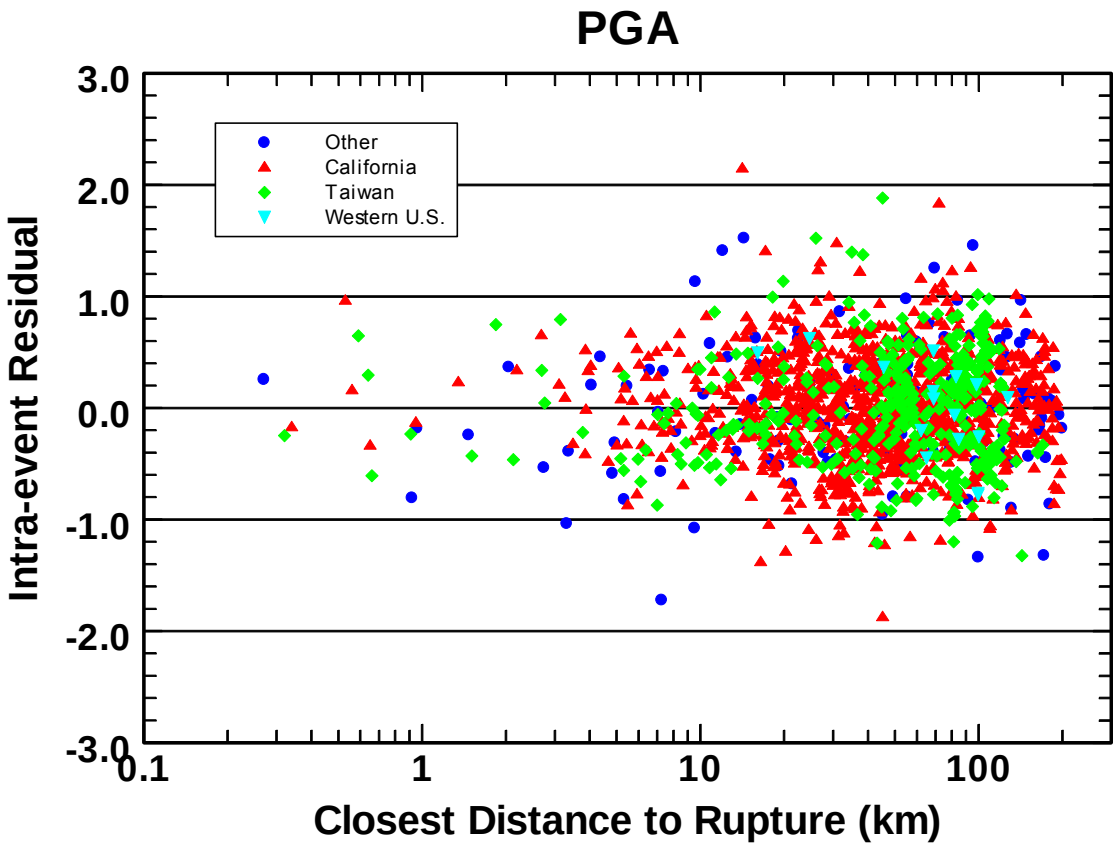

Figure 10: Plot of intra-event residuals for PGA for the Campbell and Bozorgnia (CB06) NGA model showing their distribution with respect to distance.

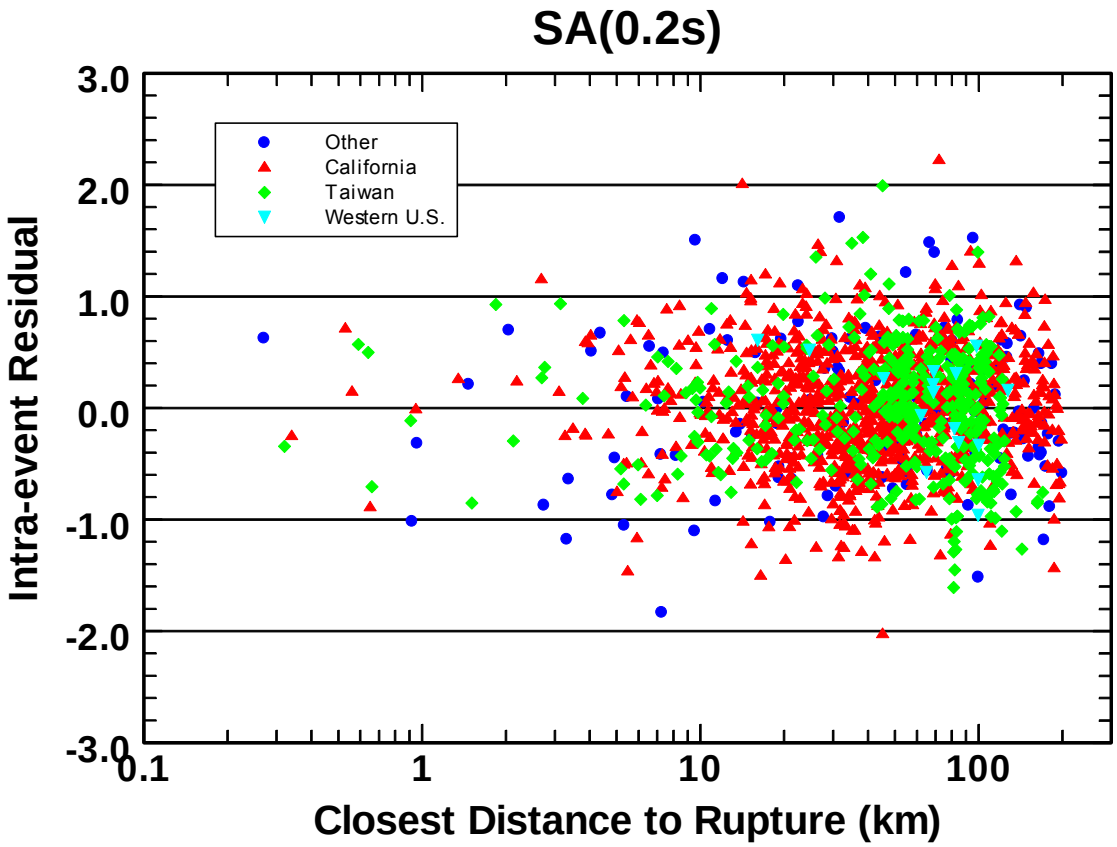

Figure 11: Plot of intra-event residuals for 0.2s spectral acceleration for the Campbell and Bozorgnia (CB06) NGA model showing their distribution with respect to distance.

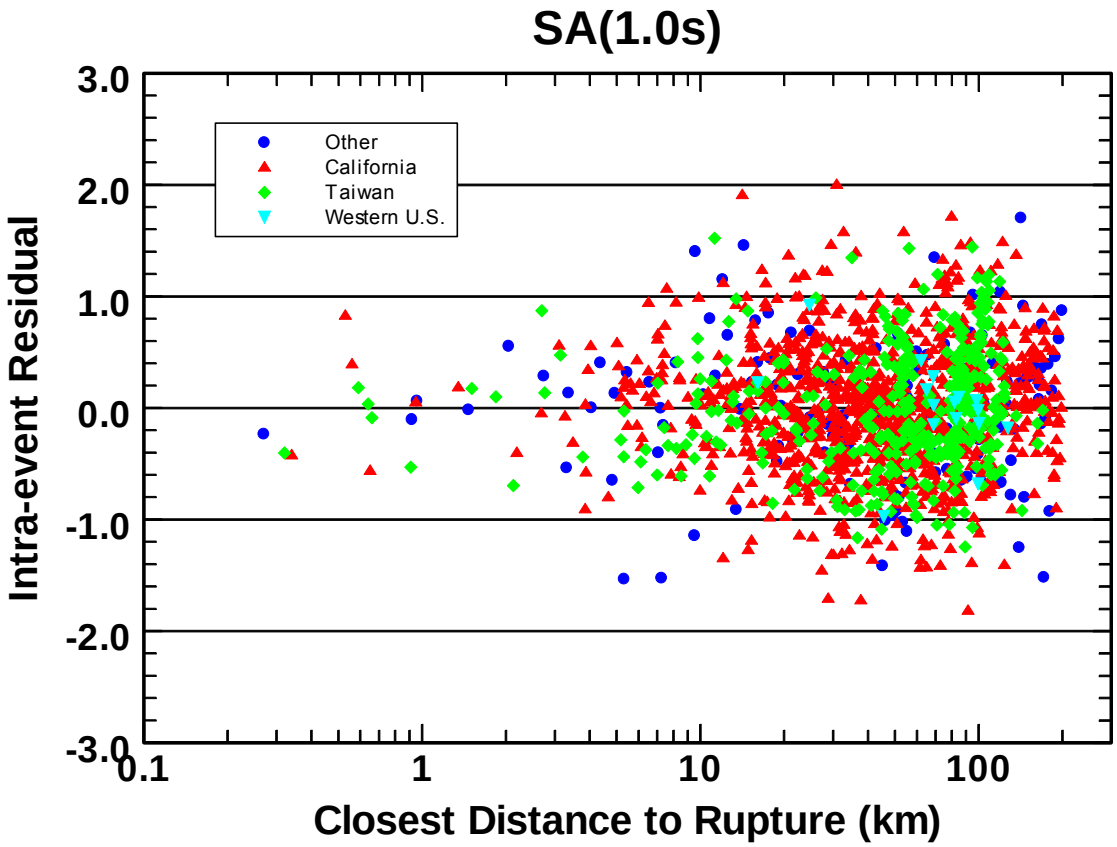

Figure 12: Plot of intra-event residuals for 1.0s spectral acceleration for the Campbell and Bozorgnia (CB06) NGA model showing their distribution with respect to distance.

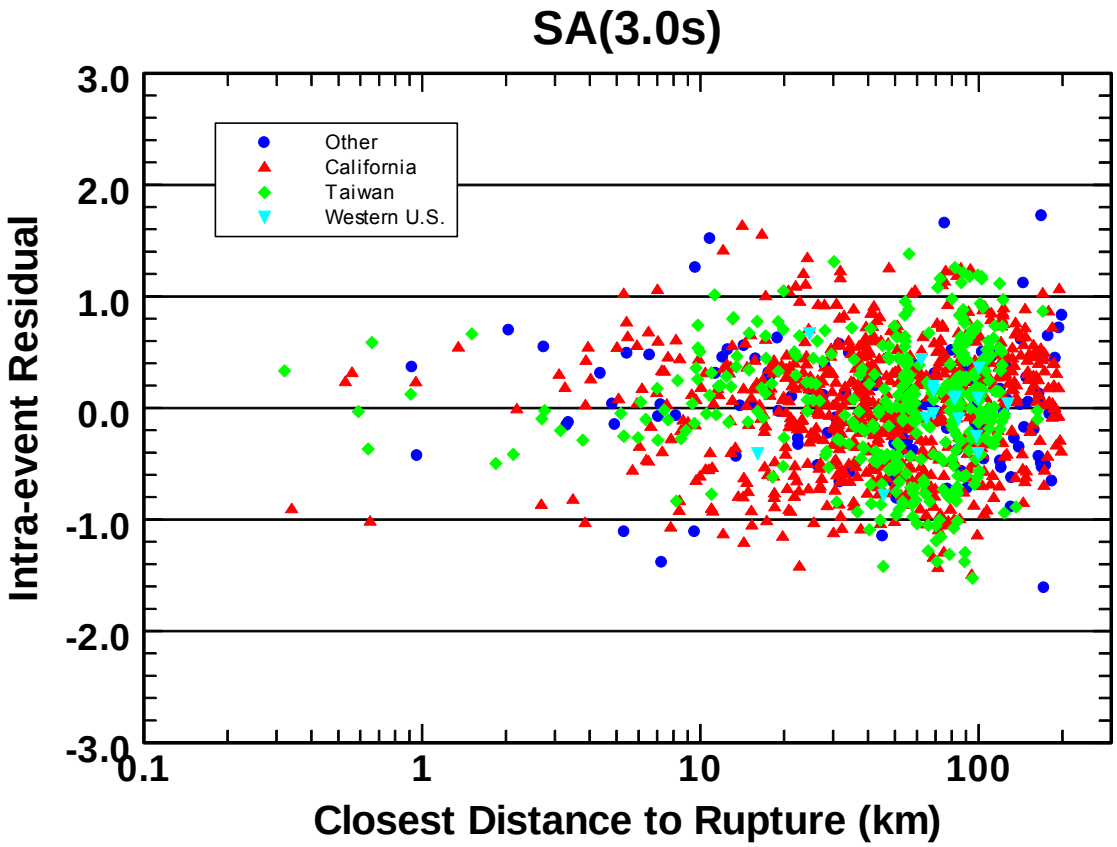

Figure 13: Plot of intra-event residuals for 3.0s spectral acceleration for the Campbell and Bozorgnia (CB06) NGA model showing their distribution with respect to distance.

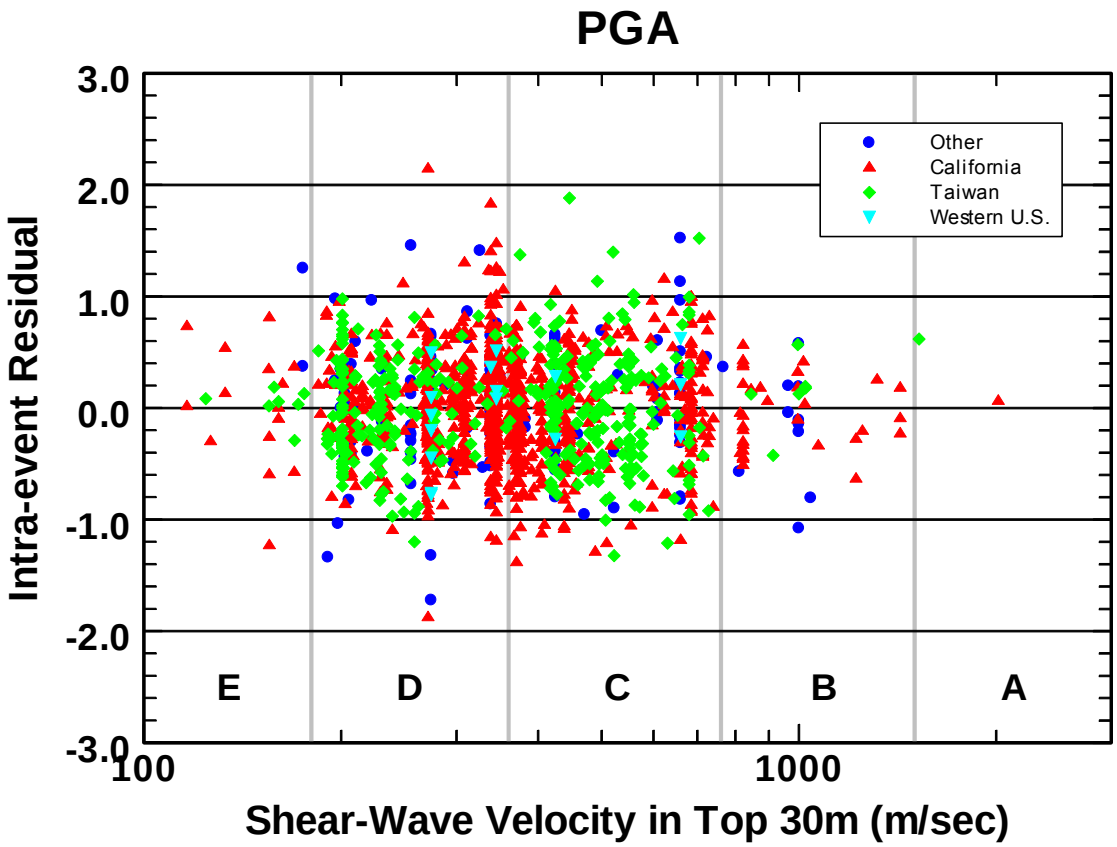

Figure 14: Plot of intra-event residuals for PGA for the Campbell and Bozorgnia (CB06) NGA model showing their distribution with respect to 30m shear-wave velocity. Also shown for reference are the ranges of V_{S30} corresponding to NEHRP site categories A–E.

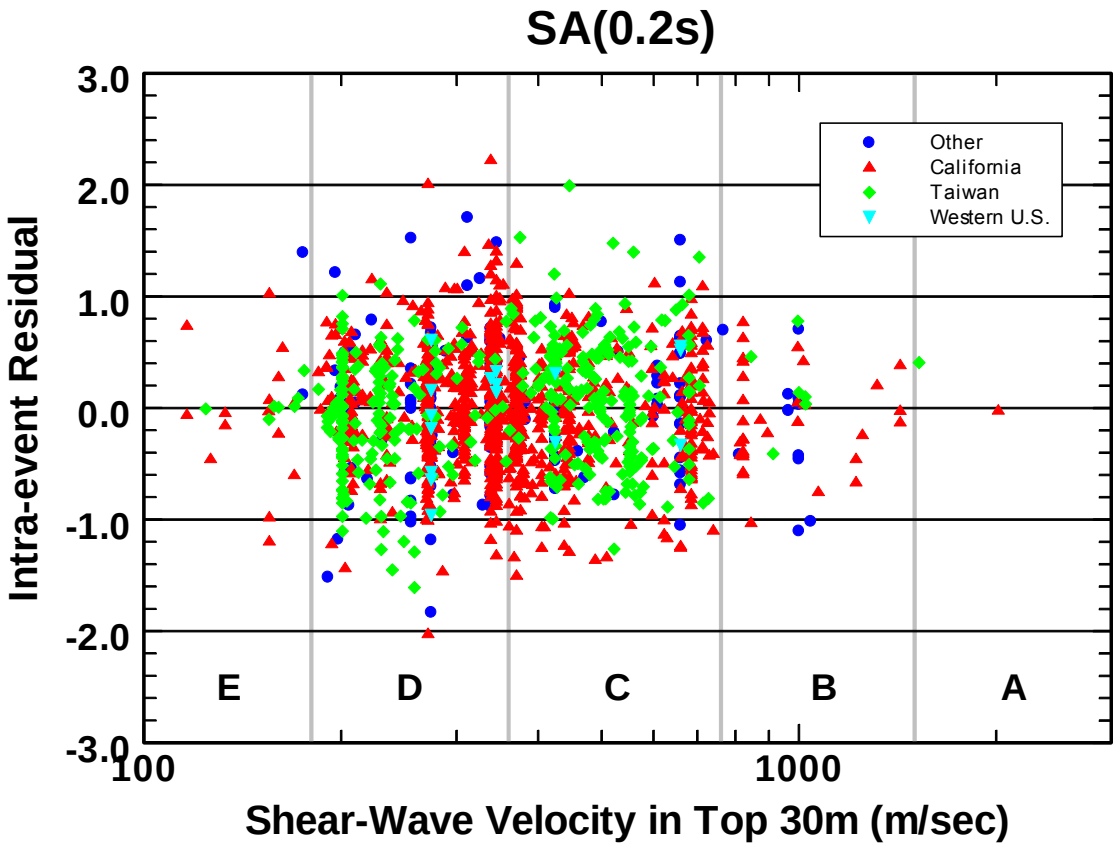

Figure 15: Plot of intra-event residuals for 0.2s spectral acceleration for the Campbell and Bozorgnia (CB06) NGA model showing their distribution with respect to 30m shear-wave velocity. Also shown for reference are the ranges of V_{S30} corresponding to NEHRP site categories A–E.

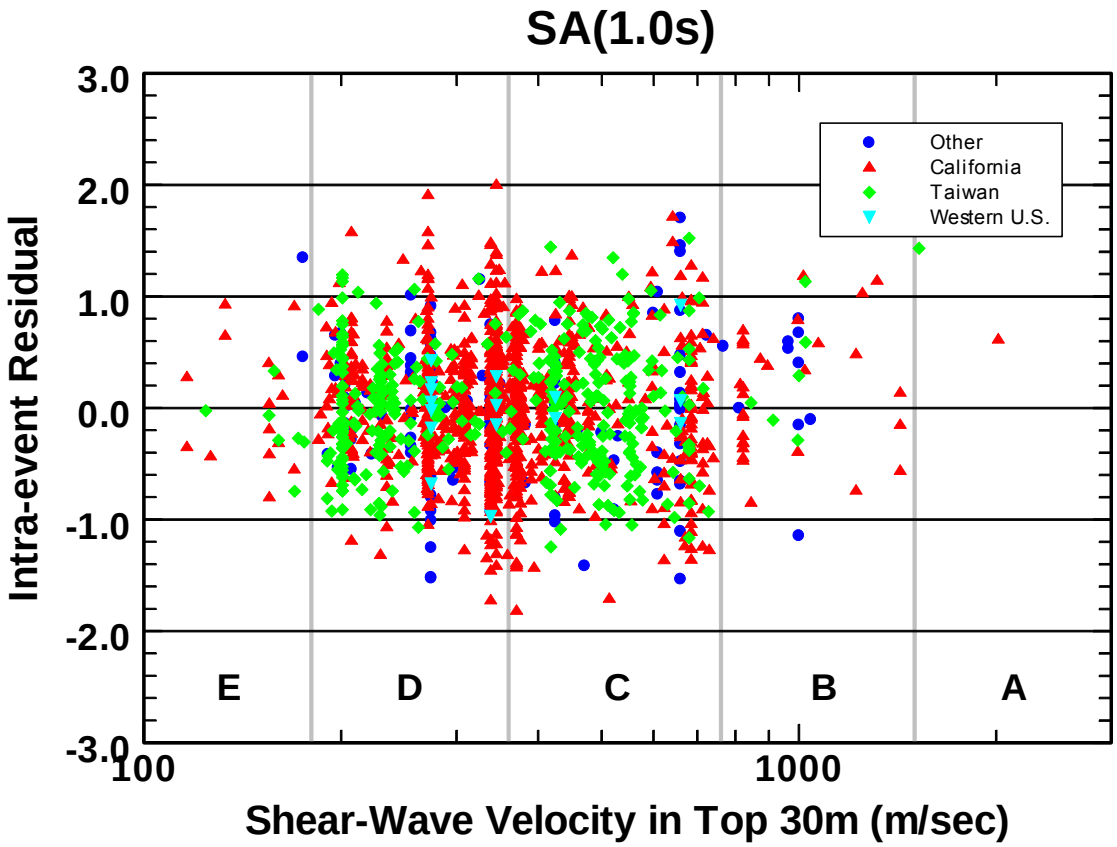

Figure 16: Plot of intra-event residuals for 1.0s spectral acceleration for the Campbell and Bozorgnia (CB06) NGA model showing their distribution with respect to 30m shear-wave velocity. Also shown for reference are the ranges of V_{S30} corresponding to NEHRP site categories A–E.

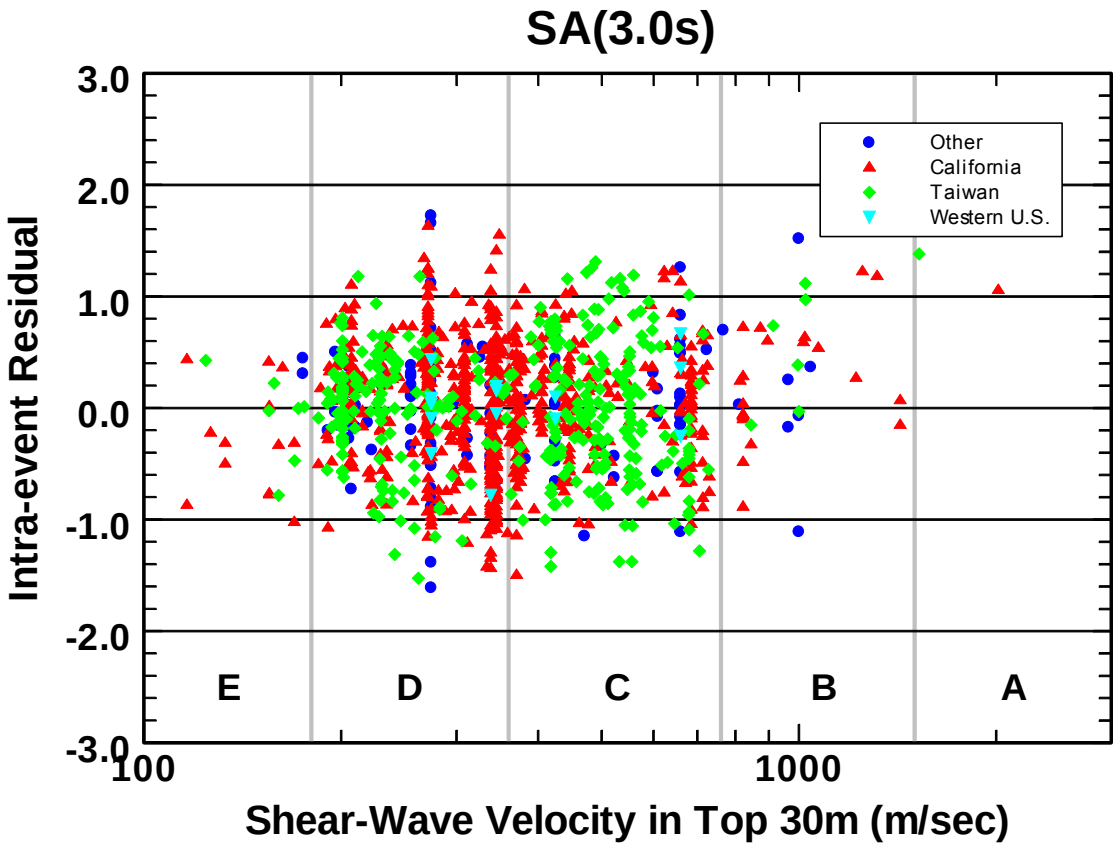

Figure 17: Plot of intra-event residuals for 3.0s spectral acceleration for the Campbell and Bozorgnia (CB06) NGA model showing their distribution with respect to 30m shear-wave velocity. Also shown for reference are the ranges of V_{S30} corresponding to NEHRP site categories A–E.

MARK PETERSEN'S QUESTION #1

Do you consider your ground motion prediction equations appropriate for seismic hazard assessments of California and throughout the western U.S.? Please explain. If you had left out international data and only used California data would you get a significantly different answer? Please explain.

CHIOU-YOUNGS RESPONSE

Response to the Question of Applicability to California

This question arises from the concern about undue influence of non-California data on the regression results. A good way to address this concern is to examine the residuals of California only data. We'll show that significant trends can not be detected in California residuals. Thus, the NGA models are not biased relative to California data and the concern of undue influence of non-California data is not justified.

Before the residual plots are presented, we need to point out several important factors that work in favor of reaching an attenuation model that is California-like. First, the majority of the data selected for use in NGA model development is from California. As an example, the magnitude-distance-region distribution of data used in the Chiou &Youngs model is shown in Figure 1. California data dominate the dataset at magnitude less than 7.2 and they play an important role in shaping the NGA model. Secondly, formulation of the NGA models and the constraints imposed on the model coefficients were mainly based on California data or on models derived from California data. For example, the Atkinson and Silva (1997, 2000) California-based seismic source models were used by Chiou and Youngs to generate synthetic motions, which were then used to formulate the form of magnitude scaling model. Another example is the use of California TriNet data by Boore & Atkinson and Chiou & Youngs to constrain the anelastic parameters. Thirdly, the developers were given the scope to develop models suitable for use in California. This goal strongly influenced developers' decisions and judgment made during model development.

Residuals plots for PGA, T=0.2, 1 and 3 seconds are provided to facilitate the examination of model applicability to California in terms of magnitude scaling, distance attenuation, and site effect. In the following, we'll use plots from Chiou & Youngs to demonstrate the appropriateness of NGA model for California.

Inter-event errors are shown in Figure 2 and there is no significant bias relative to California earthquakes. In fact, the magnitude scaling model fits both the California and non-California earthquakes well except in the cases of PGA and 0.2 seconds the low values of several non-California earthquakes with $M \geq 7.2$. The magnitude scaling model was not dragged down to fit the low values. The non-California earthquakes do not have a major influence on magnitude scaling because it was constrained to follow an earthquake source model derived from largely California data. One might argue that the low values could still drag down the intercept C_1 (and hence the overall level of median motion). This will be addressed later.

Intra-event residuals in six magnitude bins are plotted against distance on Figure 3. Intra-event residuals plotted against V_{S30} are shown on Figure 4. Fits to the California data are very good. It is difficult to argue there is significant bias relative to California data.

Based on the above observations, we conclude that, despite the use of some non-California earthquakes in the development of NGA models, the NGA models are appropriate for seismic hazard assessments of California.

Response to the Question of Applicability Throughout the Western U.S.

There are only a few data from the rest of western U.S. This makes it difficult to evaluate the applicability. Some developers warned that modifications of the NGA model may be needed in certain region. This applicability question is addressed in the Applicability Section of C&Y's report. Use of C&Y model in the rest of the WUS may require some modification if the anelastic attenuation (Q) is significantly different from California (e.g. in the Intermountain region).

Response to the Question of Using California Data Only

Given the good fits of C&Y model to California data, it is reasonable to state that if we were to develop a model using only California data the C & Y model would already be an excellent candidate. Some may suggest that the low values of several non-California earthquakes (Figure 2) could still have a significant influence on coefficient C_1 and therefore C_1 should be re-estimated. Responding to this suggestion, we rerun the regression analysis using only California data with C_1 being the only free fixed-effect coefficient. The differences between the resulting C_1 and C&Y's C_1 are shown on Figure 5. The consequences of removing the non-California data are: an increase of C_1 (and hence the predicted median motion) by 5% to 10% at high frequencies ($T<0.2$ sec), and a decrease of C_1 by less than 5% at long periods ($T>3$ sec). Such changes are not considered to be significant.

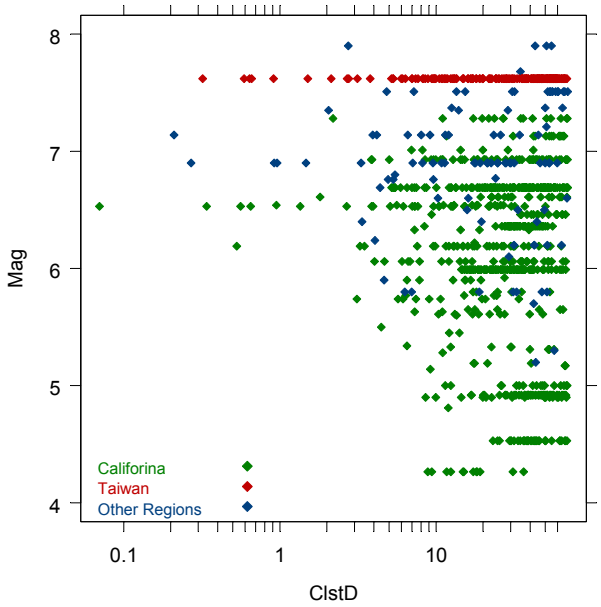

Figure 1: Magnitude-distance-region distribution of data used in the development of Chiou & Youngs model.

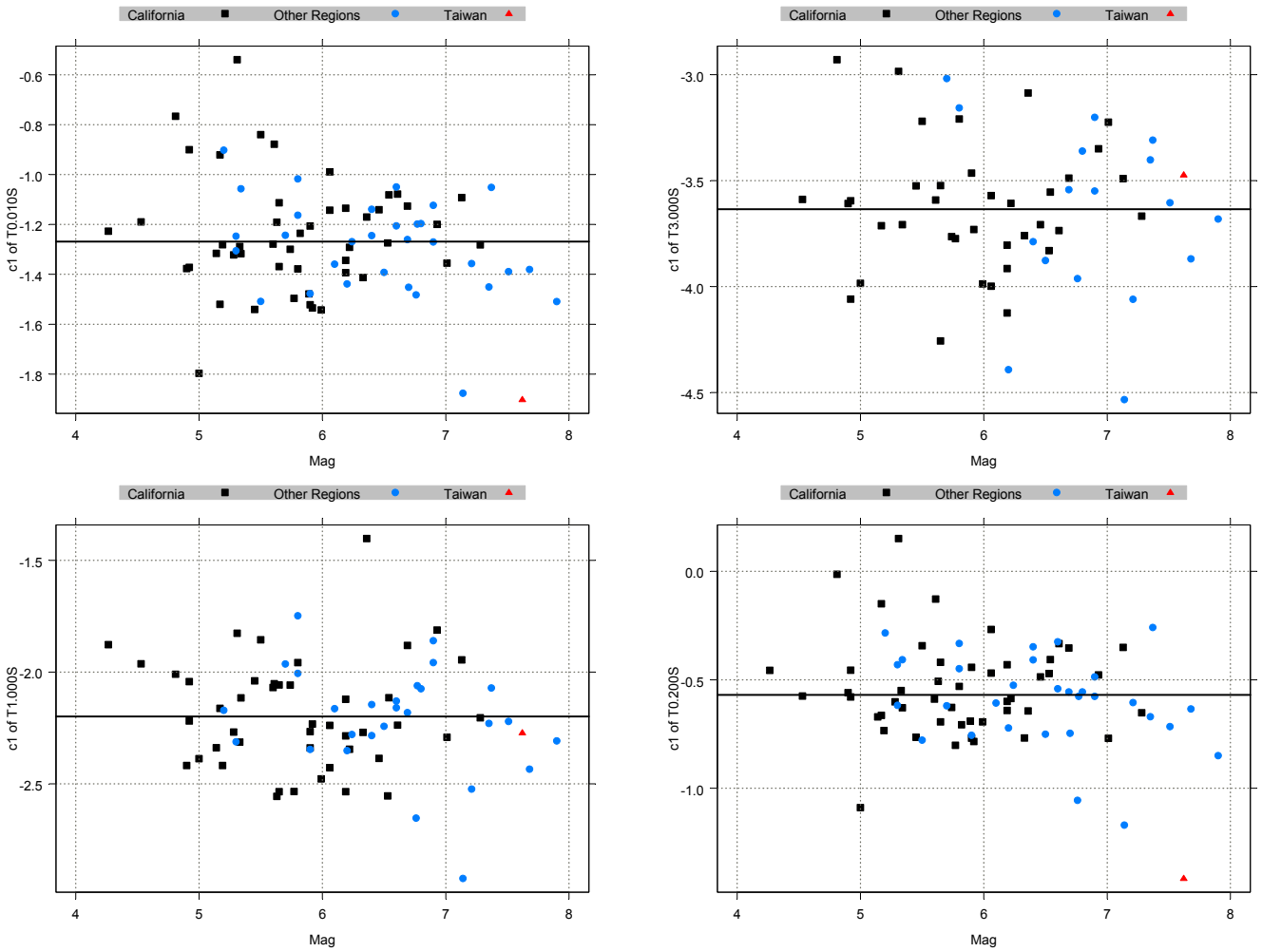

Figure 2: The random earthquake effects for PGA and the 0.2, 1, and 3 sec spectral periods of Chiou & Youngs. The horizontal line denotes coefficient C_1 (the population mean of random earthquake effects). Difference between population mean and individual value represents the random inter-event error.

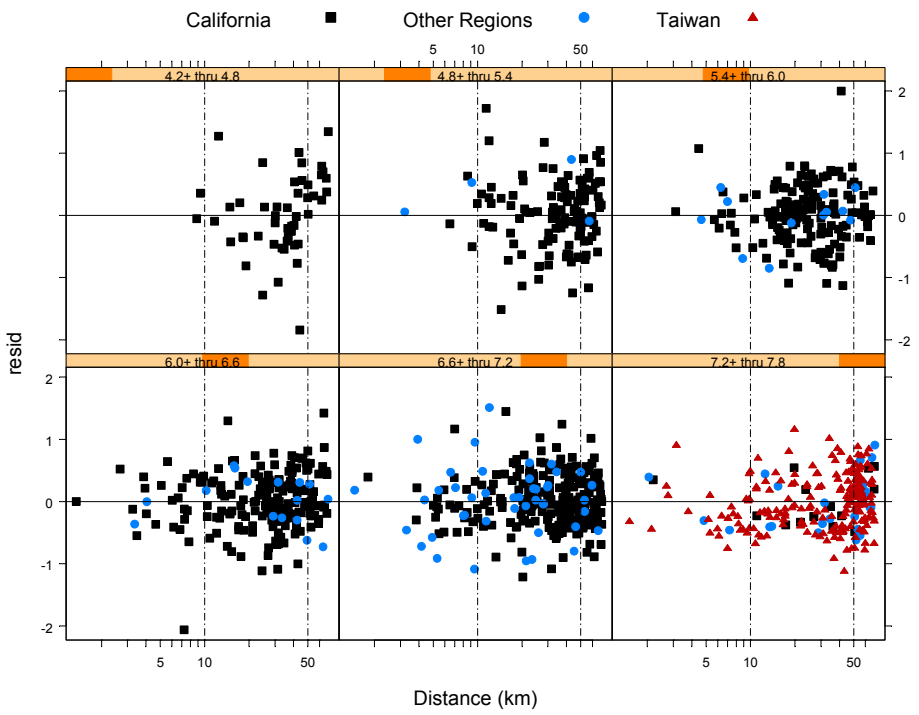

Figure 3a: Intra-event residuals from Chiou & Youngs for PGA are plotted against distance.

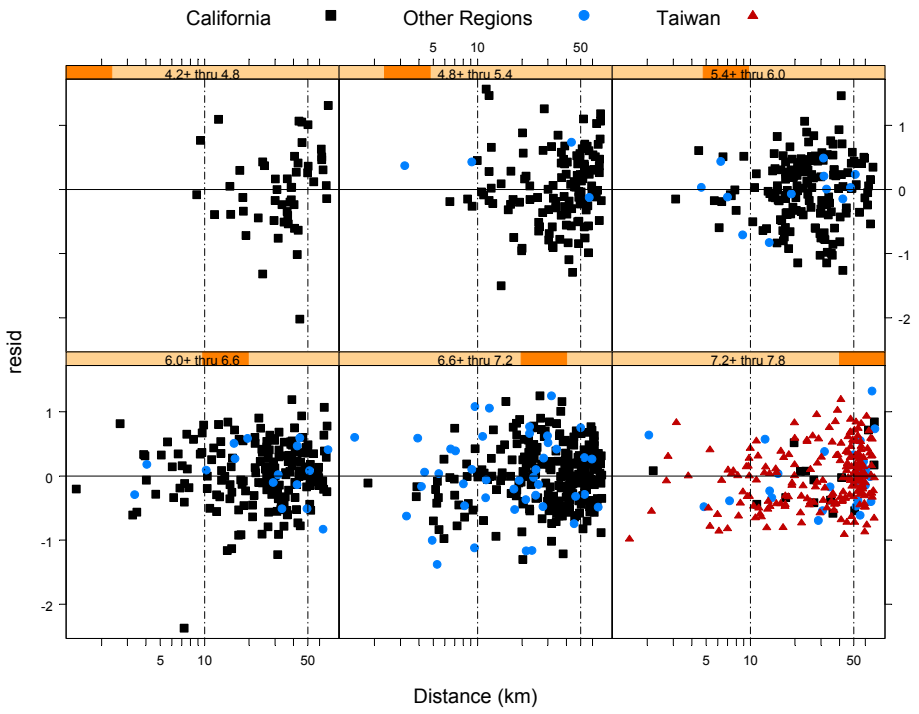

Figure 3b: Intra-event residuals from Chiou & Youngs for spectral period of 0.2 sec are plotted against distance.

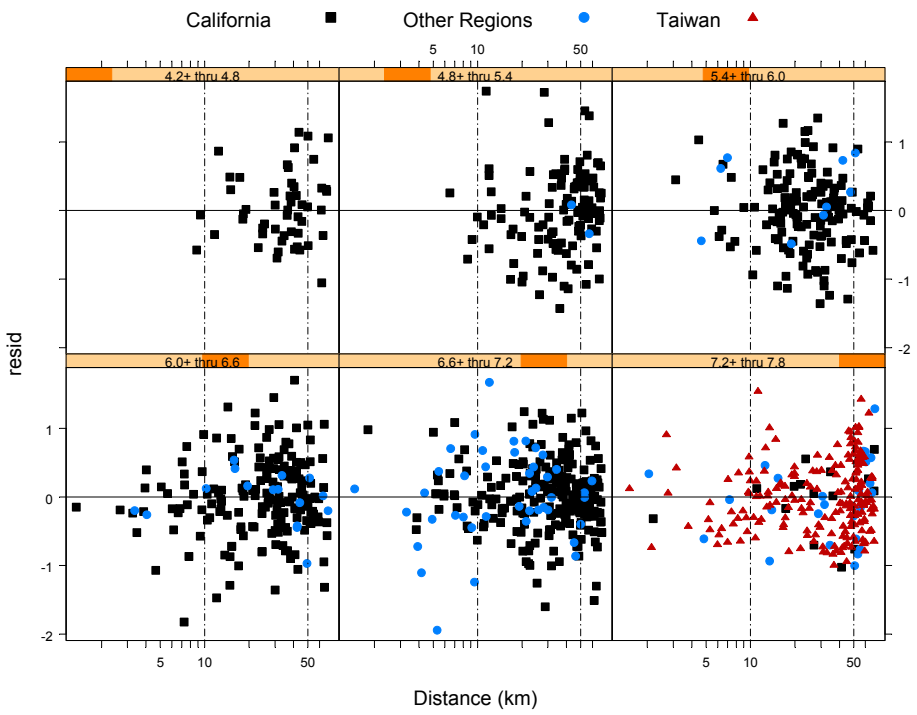

Figure 3c: Intra-event residuals from Chiou & Youngs for spectral period of 1 sec are plotted against distance.

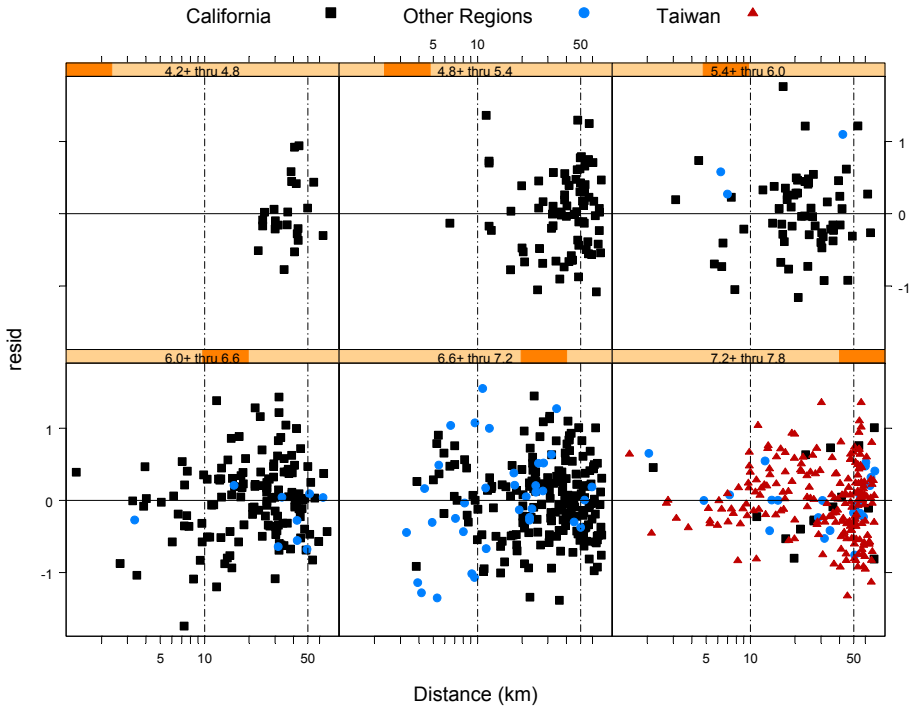

Figure 3d: Intra-event residuals from Chiou & Youngs for spectral period of 3 sec are plotted against distance.

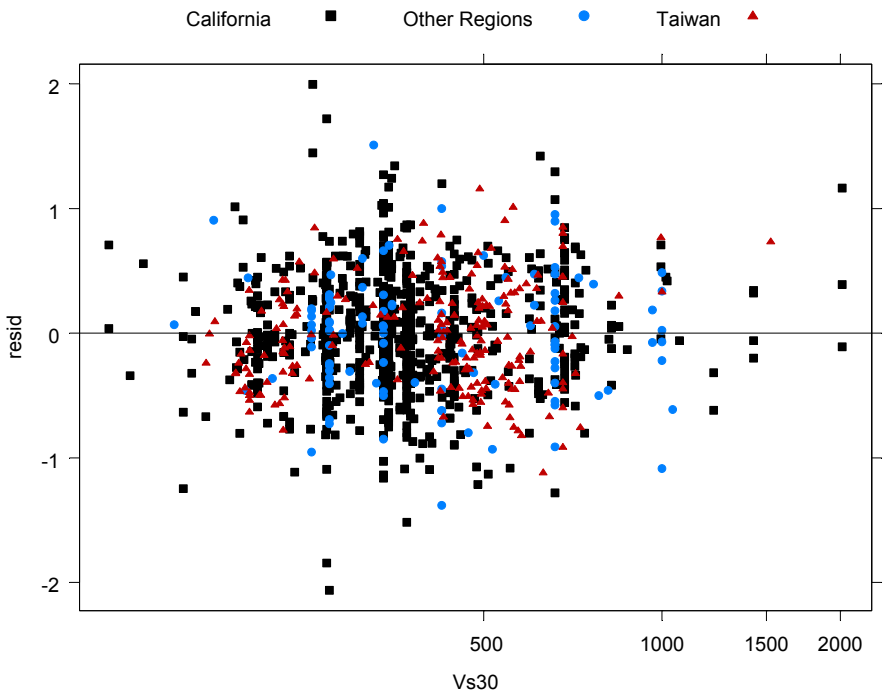

Figure 4a: Intra-event residuals from Chiou & Youngs for PGA are plotted against V_{S30} (m/sec).

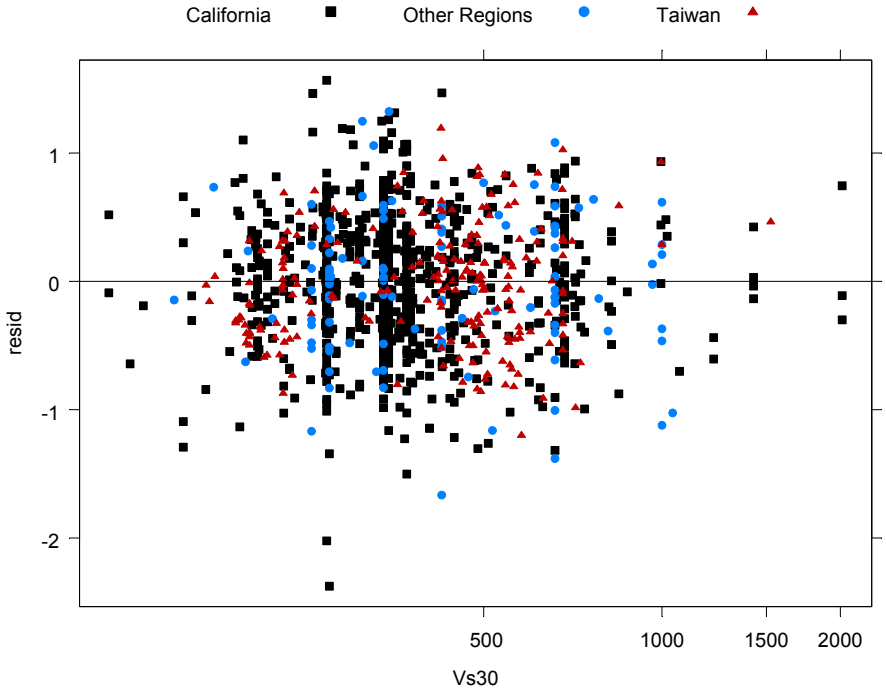

Figure 4b: Intra-event residuals from Chiou & Youngs for spectral period of 0.2 sec are plotted against V_{S30} (m/sec).

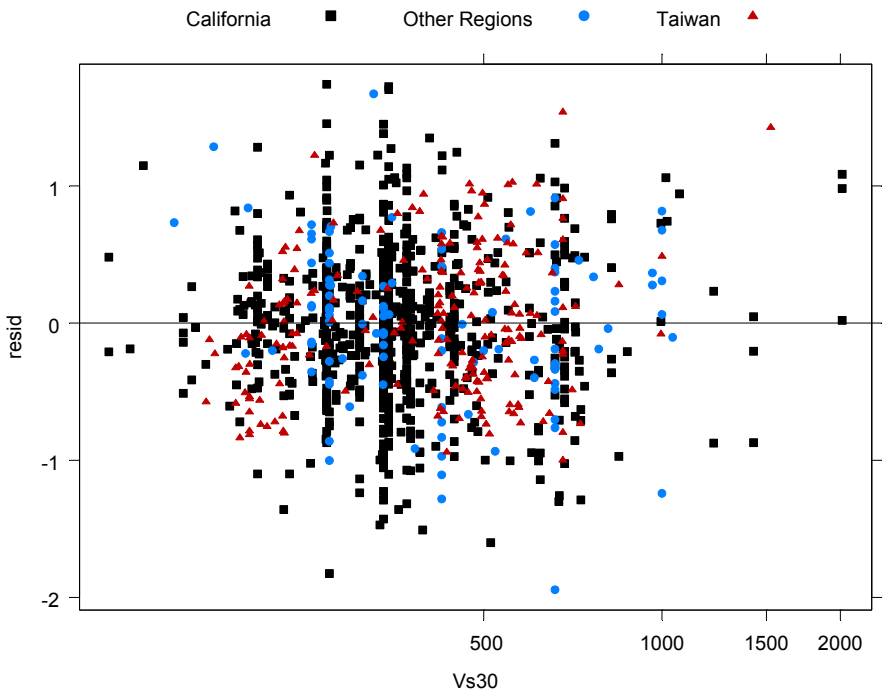

Figure 4c: Intra-event residuals from Chiou & Youngs for spectral period of 1 sec are plotted against V_{S30} (m/sec).

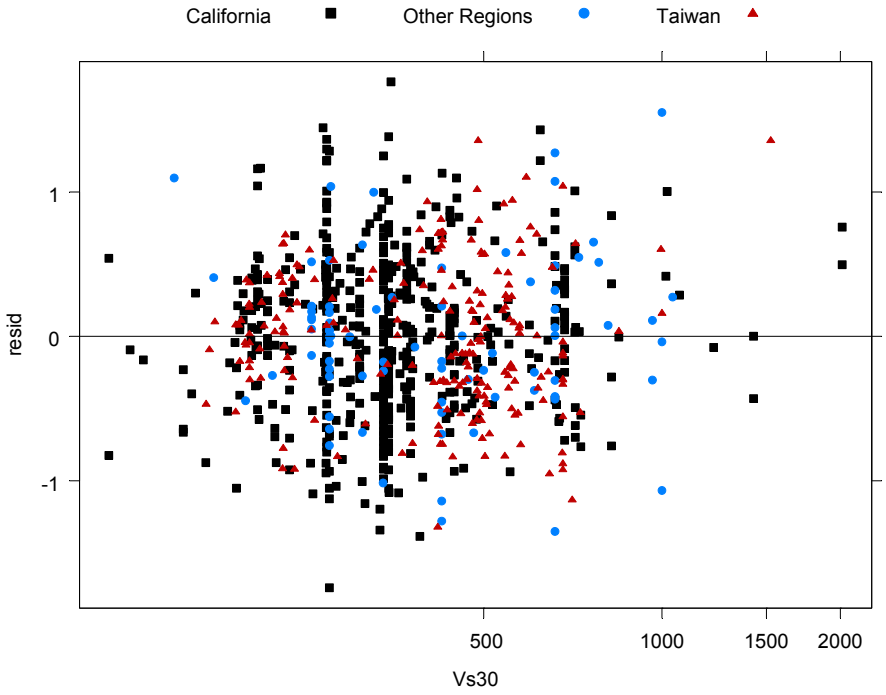

Figure 4d: Intra-event residuals from Chiou & Youngs for spectral period of 3 sec are plotted against V_{S30} (m/sec).

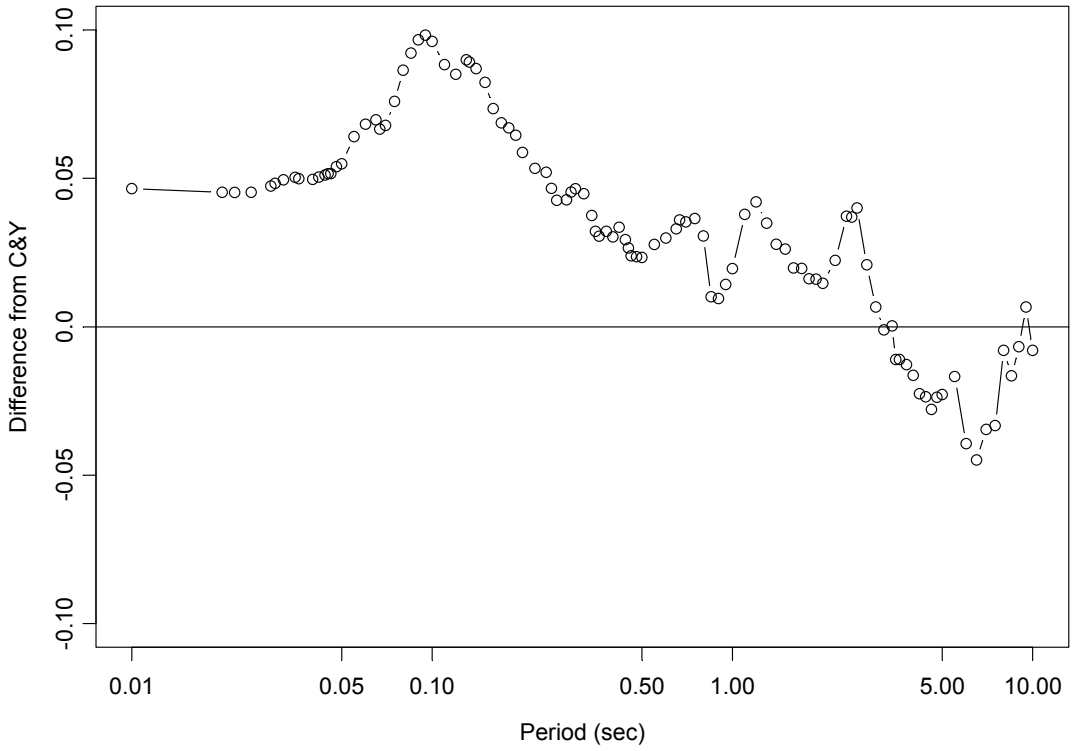

Figure 5: Differences between C_1 estimated from California data and the C_1 of Chiou & Youngs, which used also non-California earthquakes.

MARK PETERSEN'S QUESTION #2

Do you feel that your equations have adequately accounted for epistemic and aleatory uncertainties to be used for public policy? Please explain. How do you suggest that the USGS account for the epistemic uncertainties in the ground motion relations in the national maps?

CAMPBELL-BOZORGNIA RESPONSE

Because of the increase in the number of earthquakes and recording sites in the NGA database, we were able to apply stricter criteria to the selection of the data we used in the development of our NGA empirical ground motion model (see our report for a description of these criteria). One of the consequences of the larger number of events and recordings was to get a better estimate of the inter-event and intra-event aleatory uncertainties at both small and large magnitudes. These refined estimates of uncertainty led us to propose inter-event and intra-event standard deviations that are independent of magnitude. The result was to increase uncertainty at large magnitudes and decrease uncertainty at small magnitudes compared to our previous model (Campbell and Bozorgnia, 2003). The question, which we address below, is whether this change in aleatory uncertainty is warranted.

The NGA project also led to an increased degree of similarity in the new NGA models. This increased similarity is due mainly to the availability of a comprehensive database, supporting studies, and ample opportunity for developer interaction. There is still epistemic uncertainty in the actual subset of data used, in the functional forms (especially magnitude scaling and nonlinear site response), and in the use of supporting data to constrain the models (see each developer's report). In particular, the data selection criteria were quite different amongst the various developers in terms of, for example, whether only near-source recordings should be used and whether aftershocks should be included. Nevertheless, this uncertainty has been reduced from that implied by the previous models. The question, which will be addressed below, is whether the NGA models as a whole sufficiently represent the epistemic uncertainty in the median ground motions.

Aleatory Uncertainty

We believe that the better constrained magnitude-independent aleatory uncertainty predicted by our NGA model is appropriate and well-constrained, even at close distances. This latter conclusion has come under question because of the apparent increased scatter in near-fault ground motions from the 2004 Parkfield (**M** 6.0) earthquake. The large number of near-source recordings from this earthquake appears to show that intra-event uncertainty might increase very near the fault (e.g., see Figure 1). No other earthquake has provided such a large number of near-fault recordings with which to address this issue, except possibly the 1999 Chi-Chi (**M** 7.6) earthquake, which we address below. Scientifically, it makes sense that ground motions might become more variable as one approaches the causative fault do to such factors as rupture complexity (e.g., asperities), fault zone effects (e.g., wave guides and focusing), directivity effects, and more variable site response. However, the question is whether it is larger than that calculated for a large number of earthquakes and a large range of distances, as done for our NGA model

There is very little data with which to address this issue in our database, but some does exist (Figure 2). To estimate what the impacts of these effects might be on near-fault aleatory uncertainty, we first looked at the variability of the ground motions from the 2004 Parkfield earthquake for PGA and SA at periods of 0.2, 1.0 and 3.0s. We found that variability in ground motions did seem to increase within about 10 km of the rupture (e.g., see Figure 1), but only by a relatively modest amount (around 10%). However, our intra-event residuals within this same distance range (Figure 2) for all earthquakes as a whole and for the Chi-Chi earthquake in particular do not show this same effect, as shown by our intra-event residuals plotted in terms of linear distance for $R_{RUP} < 50$ (Figures 3–6). The intra-event residuals for the Taiwan region in these figures are from the Chi-Chi earthquake.

One possible explanation for the discrepancy between the near-fault variability in the Parkfield earthquake and that in the Chi-Chi earthquake and the database as a whole is the treatment of site effects. The Parkfield earthquake was evaluated without accounting for site effects, since site characteristics such as V_{S30} are not generally known, whereas site effects have been removed from the intra-event residuals of the Chi-Chi earthquake and the database as a whole. The complexity of the geological conditions in the vicinity of the Parkfield earthquake could easily explain the larger degree of variability that was observed. Until the cause of the increased near-fault variability in the 2004 Parkfield earthquake is better understood, we do not recommend altering our aleatory uncertainty model based on this one earthquake, when the Chi-Chi earthquake and our database as a whole do not show increased ground-motion variability near the fault.

Epistemic Uncertainty

The intent of the NGA project was to obtain a better estimate of modeling uncertainty by providing all of the developers with a common comprehensive database. Although we believe that this goal was achieved, we also believe that the decreased variability in the median predictions from the NGA models that resulted from this process does not necessarily provide an appropriate characterization of the actual epistemic uncertainty in these models. As a result, we recommend that a separate epistemic uncertainty model should be developed and used in conjunction with our model. Norm Abrahamson has proposed a simplified statistical method for estimating such an epistemic model based on the number of earthquakes and recordings in a set of magnitude-distance bins; see Equation 2 of Chiou-Youngs response to this question. The following table shows the application of Equation 2 to the C-B data set. The Tau and Sigma used for this calculation are 0.219 and 0.478, respectively.

Application of Equation (2) to the C-B data set.

M and R_{RUP} Range	Average **M**	Median R_{RUP}	n_{Eq}	n_{Sites}	$\sigma_{\overline{\ln[PGA(m,r)]}}$
$\mathbf{M} < 5$ $R_{RUP} < 10$			0	0	
$\mathbf{M} < 5$ $10 \le R_{RUP} < 30$	4.71	20.1	5	28	0.133
$\mathbf{M} < 5$ $R_{RUP} \ge 30$	4.71	61.2	5	169	0.105
$5 \le \mathbf{M} < 6$ $R_{RUP} < 10$	5.83	6.4	4	9	0.193
$5 \le \mathbf{M} < 6$ $10 \le R_{RUP} < 30$	5.60	20.0	15	110	0.073
$5 \le \mathbf{M} < 6$ $R_{RUP} \ge 30$	5.56	54.7	14	121	0.073
$6 \le \mathbf{M} < 7$ $R_{RUP} < 10$	6.49	4.1	19	67	0.077
$6 \le \mathbf{M} < 7$ $10 \le R_{RUP} < 30$	6.45	19.6	20	152	0.062
$6 \le \mathbf{M} < 7$ $R_{RUP} \ge 30$	6.54	55.5	18	309	0.058
$\mathbf{M} \ge 7$ $R_{RUP} < 10$	7.40	4.2	7	41	0.111
$\mathbf{M} \ge 7$ $10 \le R_{RUP} < 30$	7.33	18.0	9	70	0.093
$\mathbf{M} \ge 7$ $R_{RUP} \ge 30$	7.39	83.7	13	485	0.065

Although this table provides a rough idea of what the epistemic uncertainty related to the selection of the data set is, it can't be evaluated when there are no data. Also, the degree of calculated uncertainty is strongly dependent on the bin sizes. We can probably use these results for something very simple, but the bootstrap and jackknife methods that Bob Youngs has reviewed are the best means of assessing epistemic uncertainty.

Conclusion

Based on the above discussion, we conclude that our aleatory model is sufficient but that epistemic uncertainty as represented by the suite of NGA models is insufficient for determining ground motions to be used for engineering applications or for public policy (e.g., for developing national seismic hazard maps).

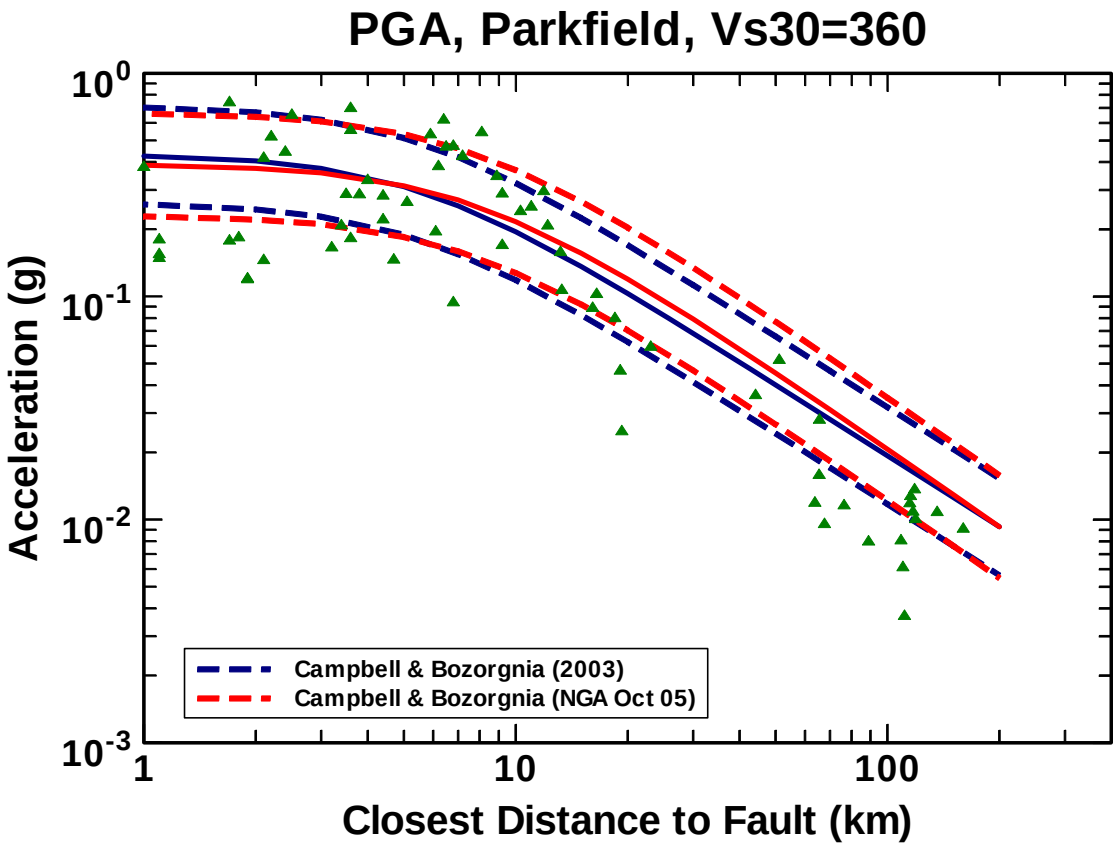

Figure 1: Plot of PGA from the 2004 Parkfield earthquake (Dave Boore, written communication) compared to ground-motion predictions from the Campbell-Bozorgnia NGA (CB06) and 2003 (CB03) empirical ground motion models.

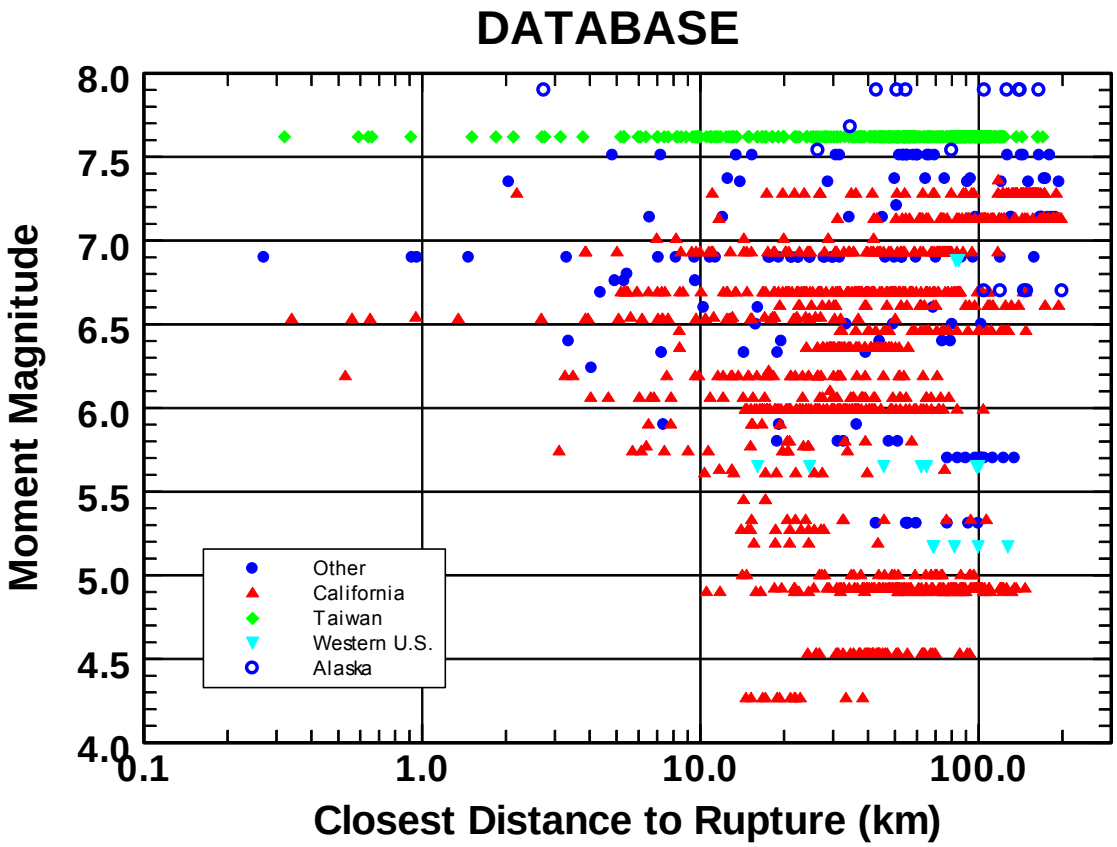

Figure 2: Plot of the distribution of recordings with respect to magnitude, distance and geographic region for the Campbell-Bozorgnia (CB06) NGA database. The regions identified in the legend include: California, the western United States outside of California, Alaska, Taiwan, and all other regions.

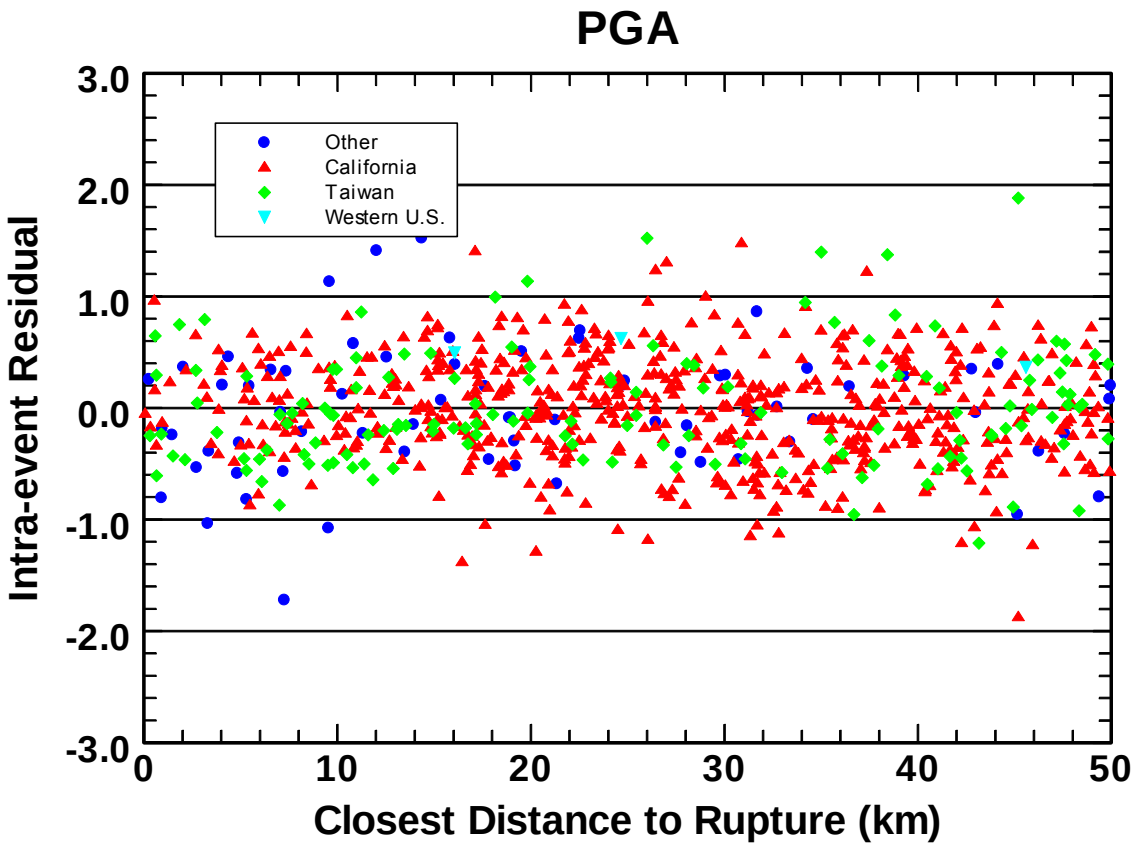

Figure 3: Plot of intra-event residuals for PGA for the Campbell and Bozorgnia (CB06) NGA model showing their distribution with respect to geographic region at near-fault distances.

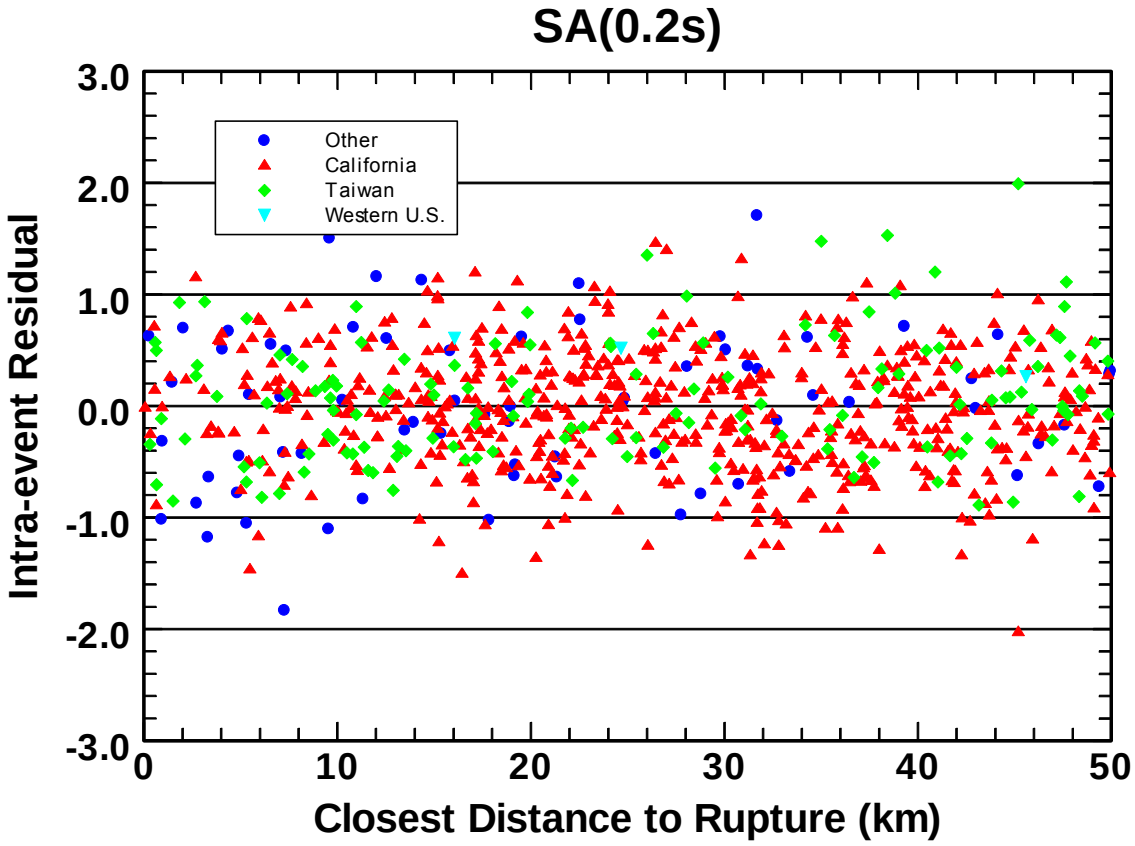

Figure 4: Plot of intra-event residuals for 0.2s spectral acceleration for the Campbell and Bozorgnia (CB06) NGA model showing their distribution with respect to geographic region at near-fault distances.

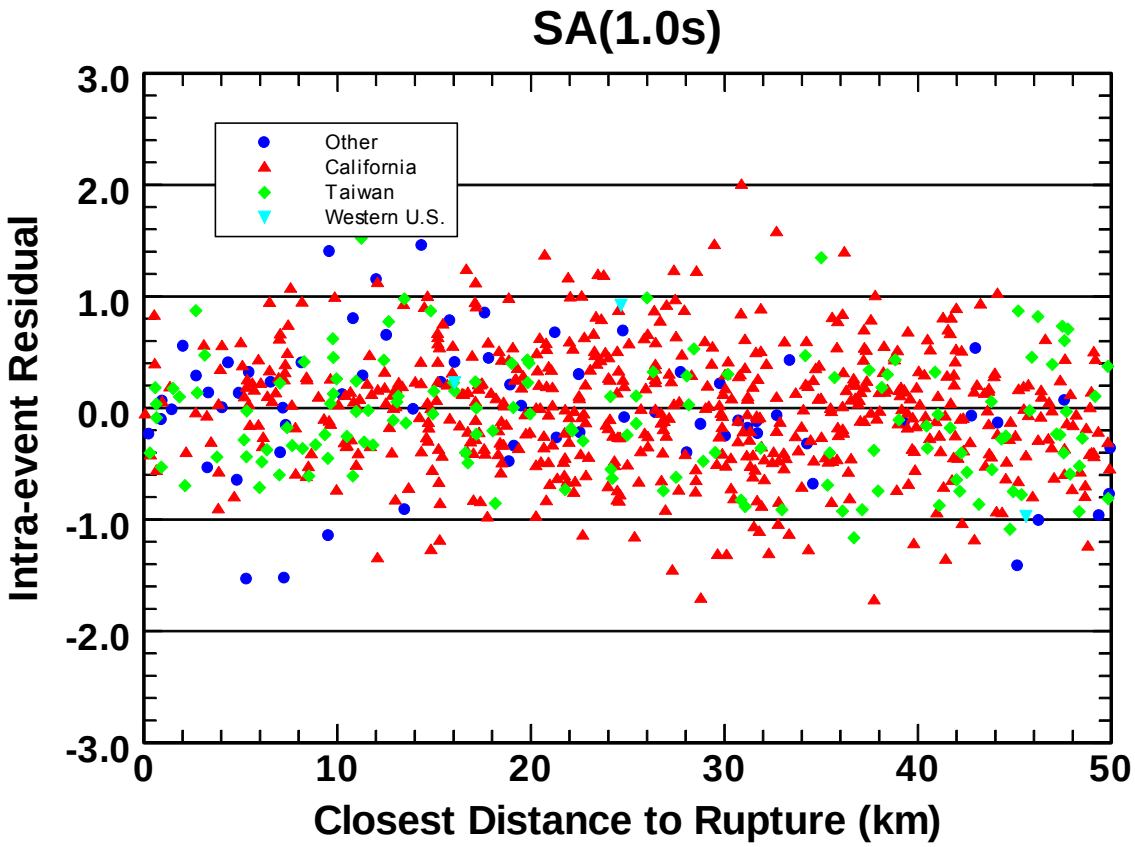

Figure 5: Plot of intra-event residuals for 1.0s spectral acceleration for the Campbell and Bozorgnia (CB06) NGA model showing their distribution with respect to geographic region at near-fault distances.

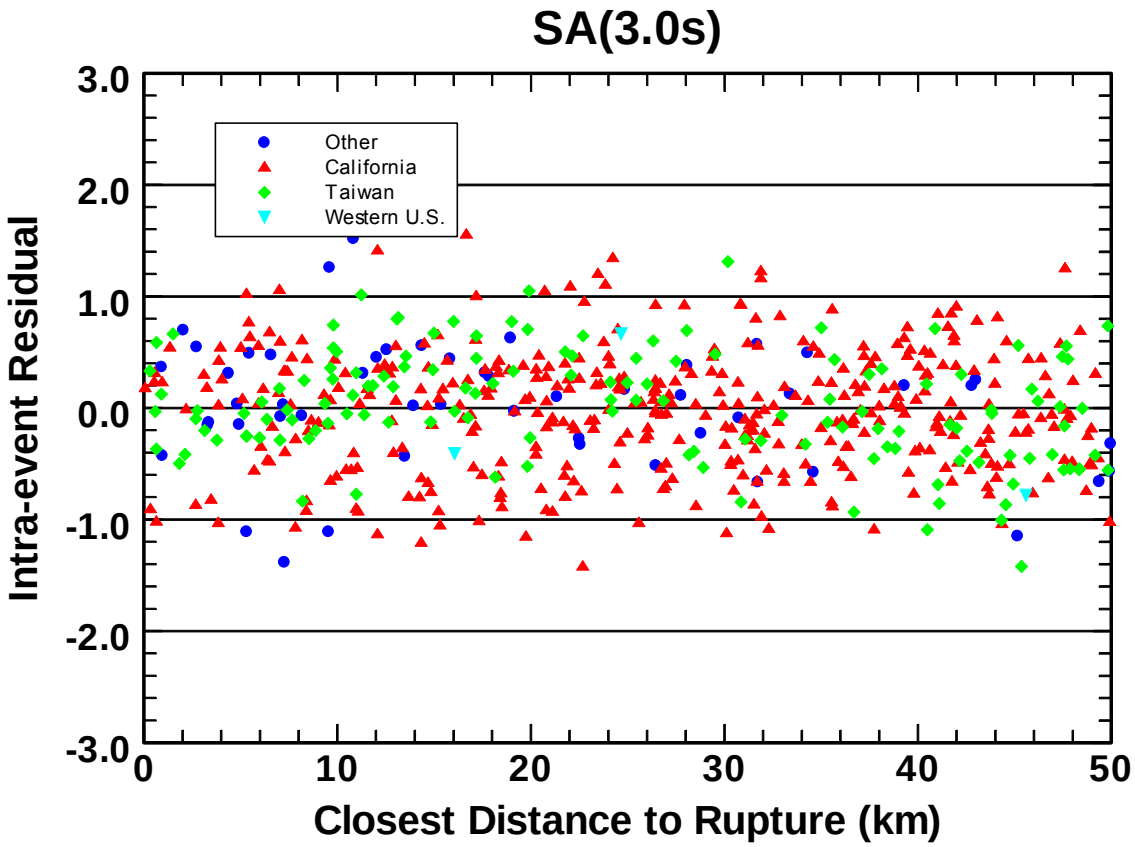

Figure 6: Plot of intra-event residuals for 3.0s spectral acceleration for the Campbell and Bozorgnia (CB06) NGA model showing their distribution with respect to geographic region at near-fault distances.

MARK PETERSEN'S QUESTION #2

Do you feel that your equations have adequately accounted for epistemic and aleatory uncertainties to be used for public policy? Please explain. How do you suggest that the USGS account for the epistemic uncertainties in the ground motion relations in the national maps?

CHIOU-YOUNGS RESPONSE

Preliminary Epistemic Uncertainty Model

The epistemic uncertainty in the median ground motions has a number of components, including:

- Uncertainty in selecting the appropriate database
- Uncertainty in selecting the appropriate model formulation
- Uncertainty in estimating the population mean with a finite data set
- Uncertainty in estimating the population mean due to uncertainty in the predictor variables in the dataset (magnitude, distance, V_{S30}, etc.)

The first two items are addressed (to some degree) by the alternative model forms and databases use by the five development teams. Presented below is an assessment of the uncertainty in the Chiou and Youngs (C&Y) model due to the second two items.

Uncertainty in estimation of model from finite data set

A simple first order estimate of the uncertainty in the median (mean log) estimates of ground motion for an individual model can be made using the standard statistical estimate of the uncertainty in the mean, $\bar{x}$, of a sample of size n :

$$\sigma_{\bar{x}} = \sqrt{\frac{\sigma_x^2}{n}} \qquad (1)$$

where σ_x^2 is the sample variance.

The parameters of the PEER-NGA ground motion models are defined by mixed effects regression (or equivalently two-stage regression) such that the total variance in the log of ground motion amplitude is partitioned into an inter-event component τ^2 and an intra-event component σ^2. For this case, an equivalent form of Equation (1) is

$$\sigma_{\overline{\ln[PGA]}} = \sqrt{\frac{\tau^2}{n_{Eq}} + \frac{\sigma^2}{n_{Sites}}} \qquad (2)$$

where n_{Eq} is the number of earthquakes and n_{Sites} is the number of recordings. Equation (2) can be used to qualitatively assess the estimation uncertainty in ground motion for different magnitude and distance intervals.

Figure 1 shows the magnitude-distance distribution of the data used to develop the C&Y model. The magnitude range was divided into four intervals, $\mathbf{M} < 5$, $5 \le \mathbf{M} < 6$, $6 \le \mathbf{M} < 7$, and $\mathbf{M} \ge 7$ and the distance range was divided into three intervals, $R_{RUP} < 10$, $10 \le R_{RUP} < 30$, and $R_{RUP} \ge 30$. Table 1 lists the values of n_{Eq} and n_{Sites} for the C&Y data set and values of $\sigma_{\overline{\ln[PGA(m,r)]}}$ computed using $\tau = 0.288$ and $\sigma = 0.515$. Table 2 lists the corresponding values for the Campbell and Bozorgnia (C&B) model.

Table 1: Application of Equation (2) to the C&Y data set.

M and R_{RUP} Range	Average **M**	Median RRUP	n_{Eq}	n_{Sites}	$\sigma_{\overline{\ln[PGA(m,r)]}}$
M < 5 R_{RUP} < 10	4.7	7.3	6	25	0.156
M < 5 10 ≤ R_{RUP} < 30	4.7	15.7	12	47	0.112
M < 5 R_{RUP} ≥ 30	4.8	45.4	5	98	0.139
5 ≤ **M** < 6 R_{RUP} < 10	5.6	7.0	23	32	0.109
5 ≤ **M** < 6 10 ≤ R_{RUP} < 30	5.5	16.9	50	263	0.052
5 ≤ **M** < 6 R_{RUP} ≥ 30	5.7	46.5	26	241	0.065
6 ≤ **M** < 7 R_{RUP} < 10	6.5	4.4	24	78	0.083
6 ≤ **M** < 7 10 ≤ R_{RUP} < 30	6.5	20.1	26	210	0.067
6 ≤ **M** < 7 R_{RUP} ≥ 30	6.3	48.8	23	670	0.063
M ≥ 7 R_{RUP} < 10	7.5	4.1	7	45	0.133
M ≥ 7 10 ≤ R_{RUP} < 30	7.5	17.9	8	71	0.119
M ≥ 7 R_{RUP} ≥ 30	7.5	50.3	10	170	0.099

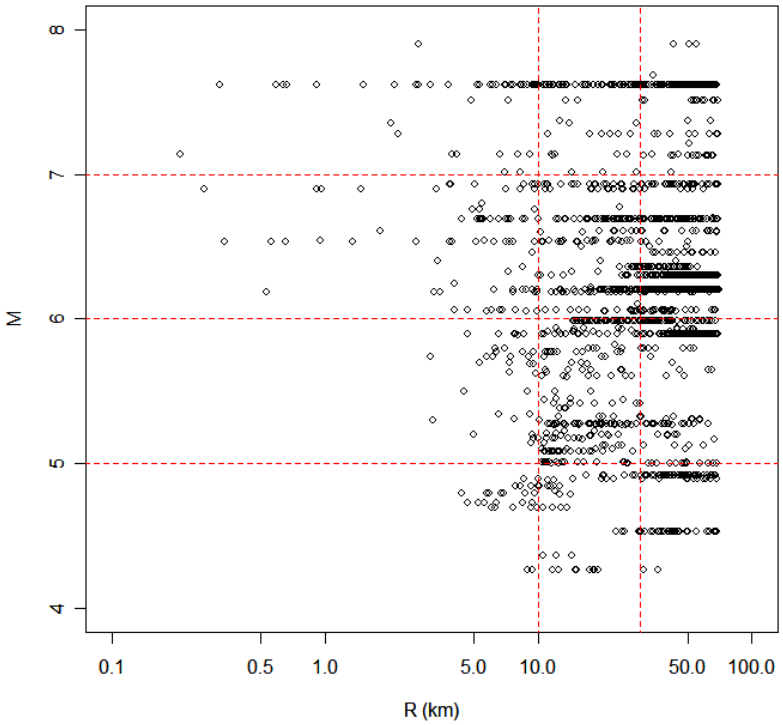

Figure 1: Magnitude-distance distribution of C&Y data set for PGA.

Table 2: Application of Equation (2) to the C&B data set.

M and R_{RUP} Range	Average **M**	Median R_{RUP}	n_{Eq}	n_{Sites}	$\sigma_{\overline{\ln[PGA(m,r)]}}$
M < 5 R_{RUP} < 10			0	0	
M < 5 10 ≤ R_{RUP} < 30	4.71	20.1	5	28	0.133
M < 5 R_{RUP} ≥ 30	4.71	61.2	5	169	0.105
5 ≤ **M** < 6 R_{RUP} < 10	5.83	6.4	4	9	0.193
5 ≤ **M** < 6 10 ≤ R_{RUP} < 30	5.60	20.0	15	110	0.073
5 ≤ **M** < 6 R_{RUP} ≥ 30	5.56	54.7	14	121	0.073
6 ≤ **M** < 7 R_{RUP} < 10	6.49	4.1	19	67	0.077
6 ≤ **M** < 7 10 ≤ R_{RUP} < 30	6.45	19.6	20	152	0.062
6 ≤ **M** < 7 R_{RUP} ≥ 30	6.54	55.5	18	309	0.058
M ≥ 7 R_{RUP} < 10	7.40	4.2	7	41	0.111
M ≥ 7 10 ≤ R_{RUP} < 30	7.33	18.0	9	70	0.093
M ≥ 7 R_{RUP} ≥ 30	7.39	83.7	13	485	0.065

The magnitude and distance ranges selected above are arbitrary but they provide an indication of the variation of uncertainty in the estimate of $\overline{\ln[PGA(m,r)]}$ as a function the amount of data.

The uncertainty estimates illustrated above do not incorporate the structure of the regression model and any external constraints imposed in the fitting. For linear regression models there are standard formulations for the uncertainty in the mean estimate as a function of the location of the estimation point with respect to the mean of the predictor variables. The uncertainty is smallest near the mean of the predictors and grows as the estimation point moves to the edges of the data used to fit the model. For non-linear, mixed effect regression models, explicit formulation of the uncertainty becomes much more difficult.

An alternative is to use non-parametric methods to estimate the uncertainty in the median prediction. One method that is widely employed is the bootstrap (Efron and Tibshirana, 1993). In the standard bootstrap, repeated random samples of size n_{Total} are drawn with replacement from the original data set. Each bootstrap sample is fit and the resulting model used to estimate $\overline{\ln[PGA(m,r)]}$ for a range of magnitudes and distances. The process is repeated multiple times and the resulting variability in $\overline{\ln[PGA(m,r)]}$ provides an estimate of uncertainty. The bootstrap process draws repeated samples from the unknown true distribution of the data using the empirical distribution as a substitute.

Unfortunately, application of the bootstrap to a mixed effects regression model is not straight forward because of the assumed nested nature of the data (correlation of ground motions from the same earthquake) and there is very little in the literature on how to proceed. As a first step, bootstrapping of the intra-event data was performed. This involved sampling with replacement from the recordings for each earthquake to build a data set of the same size as the original. Figures 2 and 3 show the resulting range and 90% interval in $\overline{\ln[PGA(m,r)]}$ for 100 bootstrap samples. It should be noted that Efron and Tibshirani (1993) recommend on the order of 1000 samples for confidence intervals. However, the results presented on Figure 2 and 3 indicate the magnitude of the estimation uncertainty for $\overline{\ln[PGA(m,r)]}$.

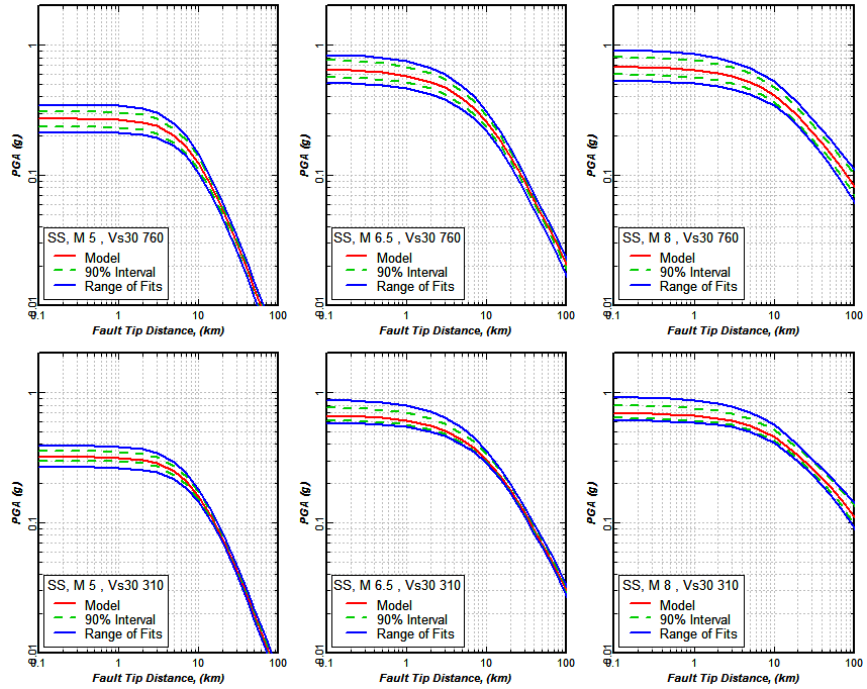

Figure 2: Bootstrap 90% intervals for $\overline{\ln[PGA(m,r)]}$ for strike-slip earthquake ground motions. Bootstrapping restricted to intra-event samples. (Z_{TOR} = 5, 0, 0; dip = 90º)

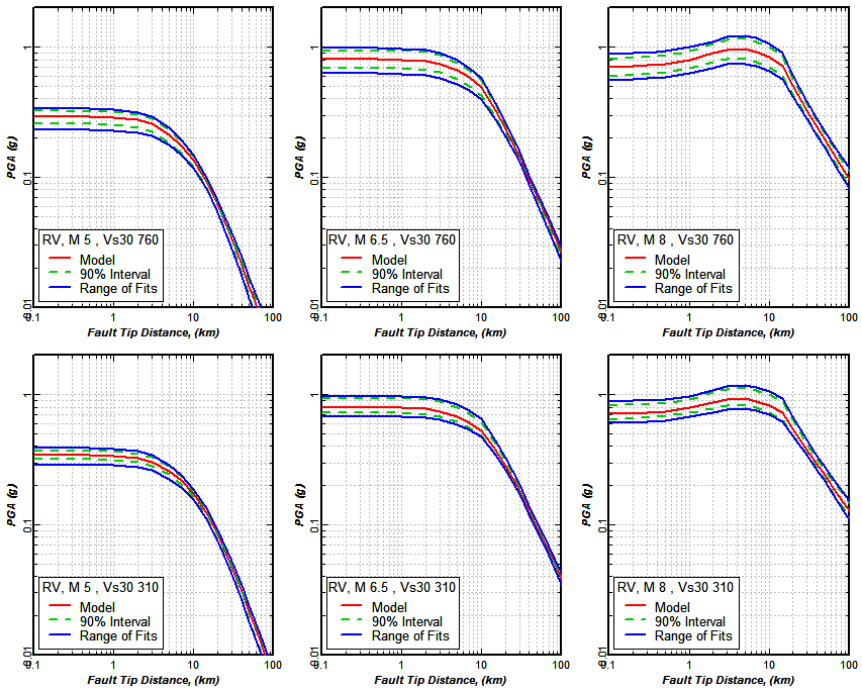

Figure 3: Bootstrap 90% intervals for $\overline{\ln[PGA(m,r)]}$ for reverse earthquake ground motions. Bootstrapping restricted to intra-event samples. (Z_{TOR} = 5, 2, 0; dip = 45º; widths 3, 15, 21.21 km)

The examples presented above provide an estimate of uncertainty by sampling from the empirical distribution of the intra-event terms. An estimate of uncertainty from sampling from the inter-event terms can be provided by employing another non-parametric technique, the jackknife. The standard jackknife technique uses repeated samples in which one data point is left out each time. For a data set of size *n*, *n* samples are created leaving out each data point in turn. We adapted this concept by creating 125 data sets for the C&Y model, each set has one of the 125 earthquakes removed. Figures 4 and 5 show the resulting range of values for $\overline{\ln[PGA(m,r)]}$. Ninety percent of the estimates lie very close to the model prediction and the 90% interval is not shown.

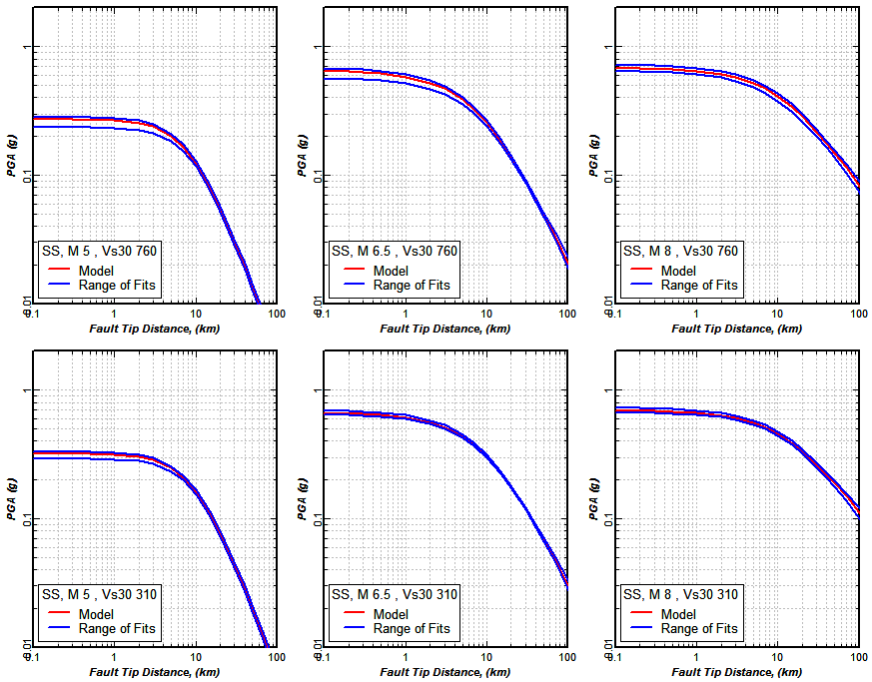

Figure 4: Range of $\overline{\ln[PGA(m,r)]}$ for strike-slip faulting from jack knife (on earthquakes) fits to C&Y database (Z_{TOR} = 5, 0, 0; dip = 90º)

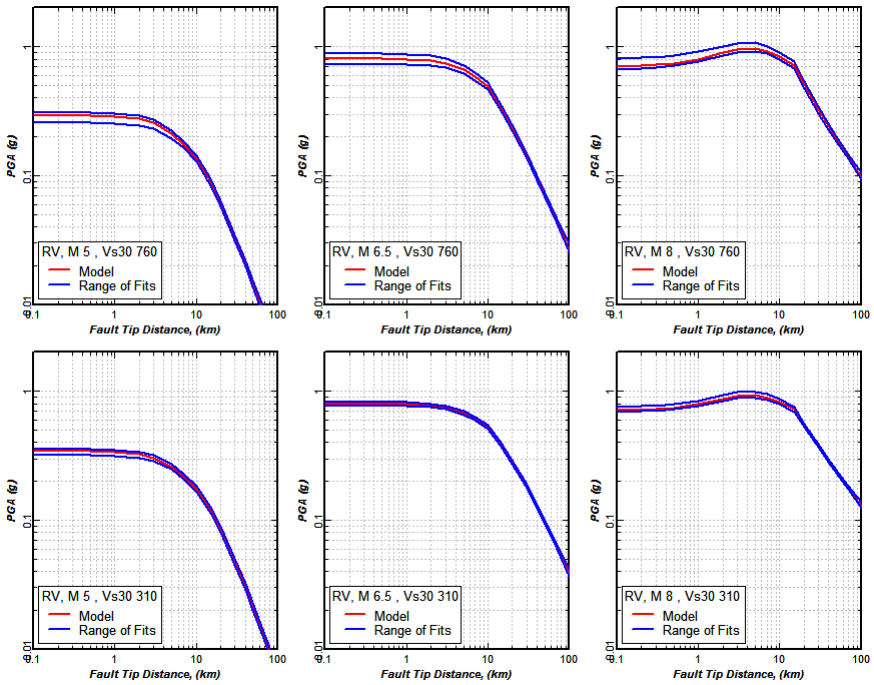

Figure 5: Range of $\overline{\ln[PGA(m,r)]}$ for reverse faulting from jack knife (on earthquakes) fits to C&Y database (Z_{TOR} = 5, 2, 0; dip = 45º; widths 3, 15, 21.21 km).

We believe that some combination of the uncertainties shown on Figure 2 and 3 with that shown on Figures 4 and 5 provides a reasonable estimate of the uncertainty in $\overline{\ln[PGA(m,r)]}$ derived from fitting the ground motion model to the selected data base.

Effect of uncertainty in predictor variables

The fourth contribution to uncertainty in $\overline{\ln[PGA(m,r)]}$ is from uncertainty in the predictor variables (**M**, R, Z_{TOR}, V_{S30}). We estimate this using simulation. One hundred data sets are simulated with random errors added to the predictor variables. The standard deviations for the individual values of **M** and V_{S30} given in the flat file were used for these variables. Approximate errors for R and Z_{TOR} were included based on judgment (these will need to be refined). Figures 6 and 7 show the resulting uncertainties in $\overline{\ln[PGA(m,r)]}$.

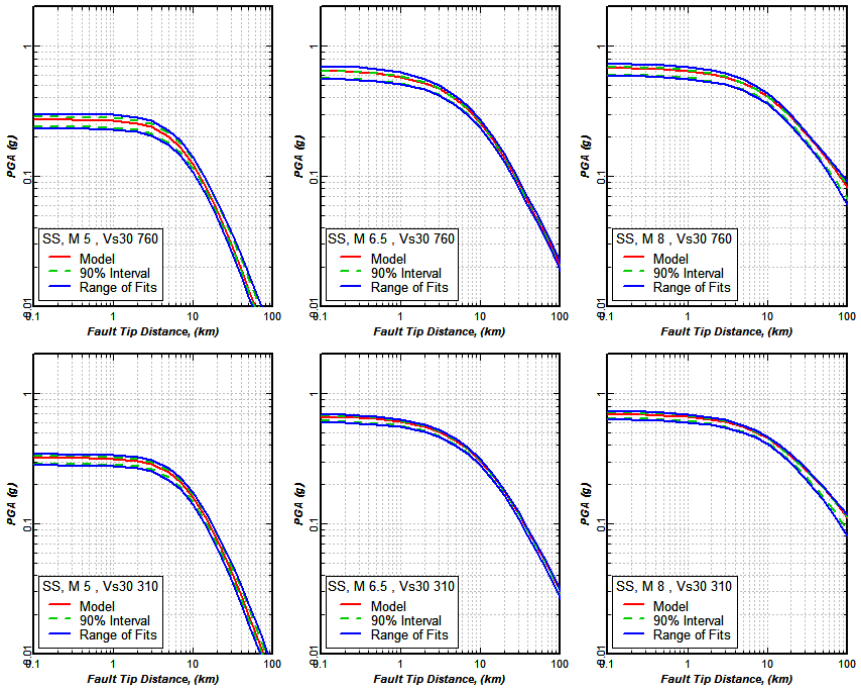

Figure 6: Uncertainty in $\overline{\ln[PGA(m,r)]}$ for strike-slip earthquake ground motions due to uncertainty in predictor variables.

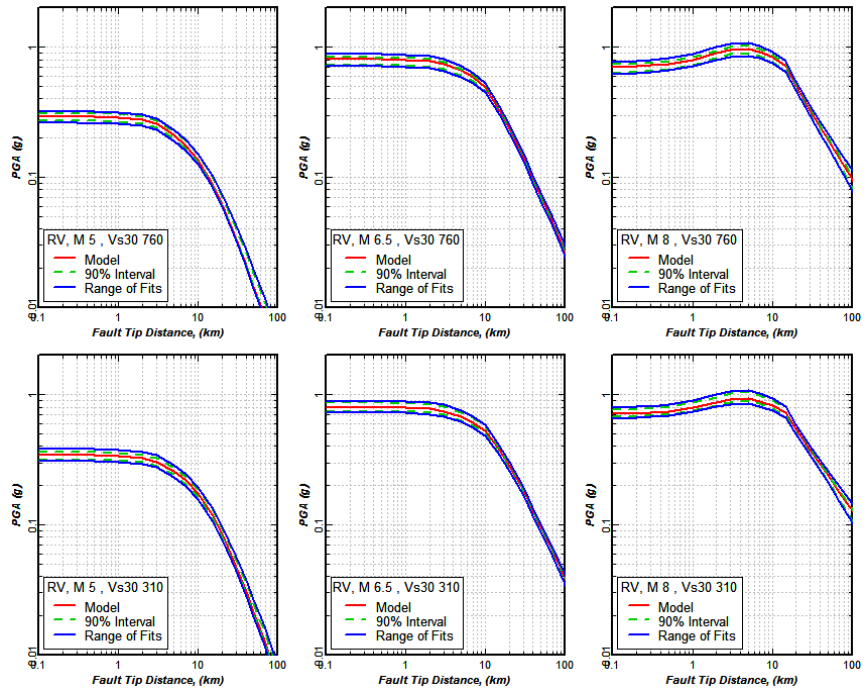

Figure 7: Uncertainty in $\overline{\ln[PGA(m,r)]}$ for reverse earthquake ground motions due to uncertainty in predictor variables.

Suggested Uncertainty Model

We understand that the USGS has implemented inclusion of an additional "sigma" term to incorporate additional uncertainties. We propose that epistemic uncertainty in individual NGA models can be addressed in this manner for the computation of a mean hazard map. We will develop a table/relationship that defines the uncertainty in the median ground motions as a function of magnitude and distance for each of the NGA models. These tables/relationships will be built from assessments like those presented in Figures 2 through 7. These are combined by adding the variances from each assessment. Additional modeling uncertainty may be added based on judgment. Tables similar to 1 and 2 will provide a basis for evaluating potential differences in the epistemic uncertainty in the median for the different NGA models. We will provide initial estimates of these values for PGA at the Sept 25th meeting.

Efron, B., and R.J. Tibshirani, 1993, *An Introduction to the Bootstrap*, Monographs on Statistics and Applied Probability 57, Chapman Hall, 436 p.

MARK PETERSEN'S QUESTION #3

When will you be able to provide the other spectral accelerations that were planned early in the process?

RESPONSE FOR ALL DEVELOPERS

Abrahamson-Silva: The current report addresses PGA and spectral accelerations for 0.2, 1.0, and 3.0 seconds. It is planned that PGA, PGV, and spectral accelerations for the full minimum set of periods for NGA models (see Campbell-Bozorgnia below) or more will be provided by October 16.

Boore-Atkinson: The current report addresses PGA, PGV, and spectral accelerations for 0.1, 0.2, 1.0, 2.0, and 3.0 seconds. It is planned that the full minimum set of periods for NGA models will be provided by October 16.

Campbell-Bozorgnia: The current report addresses PGA, PGV, and spectral accelerations for the full minimum set of periods for NGA models from zero to 10 seconds: 0.01, 0.02, 0.03, 0.05, 0.075, 0.1, 0.15, 0.2, 0.25, 0.3, 0.4, 0.5, 0.75, 1.0, 1.5, 2.0, 3.0, 4.0, 5.0, 7.5, and 10.0 seconds.

Chiou-Youngs: The current report addresses PGA and spectral accelerations for more than 100 periods in the range 0 to 10 seconds.

Idriss: The current report addresses PGA and spectral accelerations for 0.2, 1.0, and 3.0 seconds. A date has not yet been set for the full minimum set of periods for NGA models.

MARK PETERSEN'S QUESTION #4

Do you feel that the USGS could use your prediction equations with distance dependent uncertainties to account for directivity effects? Please explain. When will you provide these uncertainties?

RESPONSE FOR ALL DEVELOPERS

As you know, the currently-developed NGA models do not incorporate directivity parameters. Studies in progress are evaluating effects of directivity on the average horizontal component and the fault-strike-normal and fault-strike-parallel components of spectral accelerations. Paul Spudich is working with the NGA Developers using a directivity parameterization developed by Spudich et al. (2004)[2] based on isochrone theory as well as the directivity parameterization developed by Somerville et al. (1997)[3]. Jennie Watson-Lamprey has begun a separate study to evaluate directivity effects on the average horizontal component in terms of a distance-dependent sigma using a hypocenter-independent directivity parameterization. The studies of directivity effects has had to receive a lower priority than completing the basic NGA models for the average horizontal component.

We recognize the need for a simple representation of directivity effects that can be applied in national ground motion mapping and hope that the studies in progress will result in or can be approximated by a simple representation for use in mapping. However, the studies to date have not established the magnitude of the directivity effects and we are not far enough long to estimate the future schedule. We hope to have a better indication of the magnitude of the effects and the schedule by the time of the September 25 review meeting and will be happy to provide a status report at the meeting.

[2] Spudich, P., B.S. J. Chiou, R. Graves, N. Collins, and P. Sommerville, 2004. A formulation of directivity for earthquake sources using isochrone theory, *U.S. Geological Survey Open File Report 2004-1263*, available at http://pubs.usgs.gov/of/2004/1268/

[3] Sommerville, P.G., N.F. Smith, R.W. Graves, and N.A. Abrahamson, 1997. Modification of empirical strong ground motion attenuation relations to include the amplitude and duration effects of rupture directivity, *Seismological Research Letters* 68 (1), 199-222.

RESPONSES TO ART FRANKEL'S QUESTIONS

ART FRANKEL'S QUESTION #1

Buried rupture versus surface rupture. Somerville and Pitarka (2006) find no significant difference in source terms, on average, between surface and buried ruptures for periods of 0.2 sec and shorter. Yet the NGA relations that do include terms for depth to top of rupture, predict significant differences between surface faulting and buried faulting at all periods. This discrepancy should be explained. It appears to me that the difference in surface and buried ruptures cited in Somerville and Pitarka (2006) may be at least partly due to the differences in the period of the forward directivity pulses. The buried ruptures used in their paper have magnitudes between 6.4 and 7.0, whereas the surface rupture events have magnitudes between 6.5 and 7.6 and produce forward directivity pulses with longer periods, on average.

ABRAHAMSON-SILVA RESPONSE

As another example of the dependence of short period ($\leq$ 1 to 2 sec) motions on shallow slip dominated earthquakes verses deep slip dominated earthquakes, the table below shows Brune stress drops (parameters) computed for large **M** (**M** > 6) crustal earthquakes in active regions. Over all earthquakes the median stress drop is about 50 bars with a $\sigma_{ln} \approx 0.5$. Separating deep and shallow slip dominated earthquakes (shallow defined as more than 20% moment released over the top 5 km of the crust) shows a clear difference with the shallow slip near 30 bars and the deep slip near 60 bars. This stress drop difference reflects stable differences in short period Fourier amplitude spectra computed from recordings; deep slip dominated earthquakes result in significantly larger short period motions compared to shallow slip dominated earthquakes. Evidence for stability lies in the corresponding reduction in the respective variability, from about 0.5 for the combined set to about 0.4 for each set, suggesting the presence of two populations: epistemic variability was masquerading as aleatory variability when all earthquakes are pooled.

WNA Stress Parameters		
Set	**Stress Drop (bars)**	σ_{ln}
All	46.9	0.47
Shallow Slip	30.6	0.37
Deep Slip	56.6	0.38

Somerville, P., and A. Pitarka. (2006). Differences in earthquake source and ground motion characteristic between surface and buried earthquakes. In *Proceedings, Eighth National Conference on Earthquake Engineering*, Proceedings CD-ROM, Paper No. 977, Oakland, California: Earthquake Engineering Research Institute.

ART FRANKEL'S QUESTION #1

Buried rupture versus surface rupture. Somerville and Pitarka (2006) find no significant difference in source terms, on average, between surface and buried ruptures for periods of 0.2 sec and shorter. Yet the NGA relations that do include terms for depth to top of rupture, predict significant differences between surface faulting and buried faulting at all periods. This discrepancy should be explained. It appears to me that the difference in surface and buried ruptures cited in Somerville and Pitarka (2006) may be at least partly due to the differences in the period of the forward directivity pulses. The buried ruptures used in their paper have magnitudes between 6.4 and 7.0, whereas the surface rupture events have magnitudes between 6.5 and 7.6 and produce forward directivity pulses with longer periods, on average.

CAMPBELL-BOZORGNIA RESPONSE

In response to this question, we first summarize how each of the NGA models treats the depth to top of rupture (Z_{TOR}) parameter in their model. This is followed by some general comments regarding the Somerville and Pitarka (2006) paper.

Treatment of Buried Rupture in NGA Models

The Campbell and Bozorgnia (CB06) model uses Z_{TOR} to distinguish between buried and surface faulting for reverse-faulting events only, with buried faulting resulting in higher ground motions. The effect is constant for source depths greater than 1 km and phases out for source depths less than 1 km and for mid-to-long periods. In essence, this term replaces the reverse and thrust faulting factor used in the Campbell and Bozorgnia (2003) model, except that surface-faulting events are now excluded from this effect. This is tantamount to phasing out the source-depth effect for large magnitude earthquakes, which are more likely to have surface rupture.

The Chiou and Youngs (CY06) model uses Z_{TOR} to increase the amplitude of ground motion with source depth for all depths, with depths below 4 km having a negative source-depth factor. The negative factor at shallow depth simply reflects an arbitrary reference value for the source depth of 4 km. For purposes of comparison, the factor has been normalized to have a value of 1.0 at $Z_{TOR} = 0$ (surface faulting) so that all of the models can be compared with the same reference value of source depth. The effect is the same for all styles of faulting and phases out for mid-to-long periods. This is tantamount to phasing out the effect for large magnitude earthquakes, which are more likely to have surface faulting.

The Abrahamson and Silva (AS06) model also uses Z_{TOR} to increase the amplitude of ground motion with source depth for all depths, with depths below 5 km having a negative source-depth factor. The negative factor at shallow depth simply reflects an arbitrary reference value for the source depth of 5 km. The effect phases out between magnitudes of 6.0 and 6.5 and vanishes for **M** > 6.5. Since this model is still under development, the magnitude of the effect is not known other than it is smaller for strike-slip events than for reverse-faulting events. The Boore and Atkinson (BA06) model does not include Z_{TOR} as a parameter.

Plots comparing the source-depth factors predicted by the NGA models are shown in Figures 1–4 for PGA and SA at periods of 0.2, 1.0 and 3.0s. These plots will need to be revised once the final model of AS06 is available. Until then, this model is shown as having no effect, consistent with the last version of their model. Note that there is a considerable degree of epistemic uncertainty in how depth to top of rupture is treated in the NGA models, which appears to be commensurate with the level of understanding of this effect within the scientific community. Note also that the average affect (calculated as the geometric mean of the source-depth factor assuming equal weighting) over all the models is strongly influenced by the CY06 model that predicts the strongest effects. At the 0–10 km depths to top of rupture of greatest of greatest interest to seismic hazard assessment in the western United States, the average effect is less than about 22% and 14% for PGA and 0.2s spectral acceleration, less than about 16% and 9% for 1.0s spectral acceleration, and less than about 3% for 3.0s spectral acceleration for reverse-faulting and strike-slip faulting, respectively.

Comments on Somerville and Pitarka (2006) Paper

Somerville and Pitarka (2006) provide both empirical and theoretical evidence to support their conclusion that ground motions from earthquakes that break the ground surface are weaker than ground motions from buried faulting events. Granted, the empirical evidence shown in their Figure 2 is weak at short periods, but as you point out, the comparison depends on only a few earthquakes with different magnitude ranges. The NGA results, for those models that include source depth as a parameter, are based on a larger number of earthquakes that include events with magnitudes less than those used by Somerville and Pitarka and, as a result, are statistically more robust.

The most compelling evidence of weaker ground motions from surface faulting events comes from their dynamic simulations and from similar modeling results by others. These simulations show that, if a weak zone exists at shallow depths, rupture of the shallow part of the fault will be controlled by velocity strengthening, with larger slip weakening distance, larger fracture energy, larger energy absorption from the crack tip, lower rupture velocity, and lower slip velocity than at greater depths on the fault. These properties lead to lower ground motions for surface faulting than for buried faulting events. If a weak shallow zone does not exist, then similar short-period ground motions would be expected for surface and buried faulting, as indicated in the top two panels of their Figure 6. The weaker the shallow zone, the greater the expected difference between surface and buried faulting. One possible reason for a shallow weak zone is the presence of thick fault gauge, which has been shown from rock mechanics experiments to cause velocity strengthening, similar to the ground motion simulations.

Conclusion

The issue of whether buried faulting events have stronger ground motions than surface faulting events is currently a topic of intense study by the scientific community and cannot be considered resolved at this time. However, considering the empirical, theoretical and laboratory results summarized by Somerville and Pitarka (2006), it is plausible that this effect exists, but that its effects are subject to large epistemic uncertainty. This uncertainty is reflected in the diverse treatment of this effect in the NGA models, which would appear to be consistent with the state of knowledge within the scientific community at this time.

We didn't find a strong relationship between ground motion and depth to top of rupture (Z_{TOR}) in the data that we used to develop our model, except for reverse-faulting events. In order to demonstrate this, we plot our inter-event residuals versus depth to top of rupture in Figures 5–8 for PGA and spectral acceleration at periods of 0.2, 1.0 and 3.0s, respectively. This depth is taken to be hypocentral depth for earthquakes with magnitudes less than about 6.0, since no direct estimate of Z_{TOR} was available. There is some indication in Figures 5 and 6 that events with $Z_{TOR} > 10-12$ km are systematically under-predicted at short periods. The four deepest events that control this observation are the two Whittier Narrows earthquakes and two events from Anza. All four of these events use hypocentral depth as a proxy for depth to top of rupture. Actual values of Z_{TOR} would be smaller and might reduce the observed trend.

The possible bias seen in the inter-event residuals at short periods appears to phase out at long periods (Figures 7 and 8). So if the depth effect is real, it seems to be limited to short periods. Although it is tempting to add a factor to increase short-period ground motions for $Z_{TOR} > 10-12$ km, we believe that it is premature to include it at this time, at least based on our database, since the effect is controlled by only four earthquakes of $M < 6.0$ from two specific regions in southern California for which we do not have a direct estimate of Z_{TOR}. That is not to say that we wouldn't expect higher ground motions at depth, only that its importance for moderate-to-large earthquakes is not sufficiently resolved at this time, except for reverse faults.

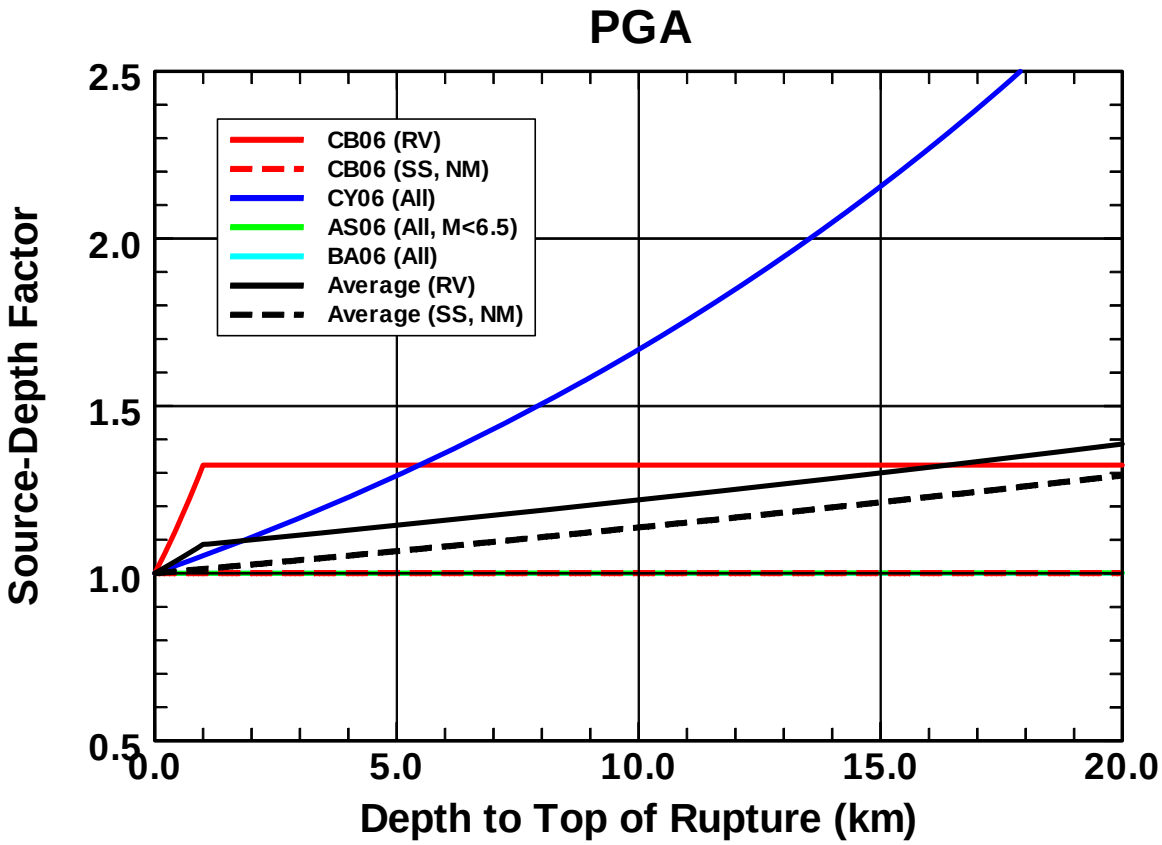

Figure 1: Comparison of depth to top of rupture factor for PGA amongst four NGA models: Campbell and Bozorgnia (CB06), Chiou and Youngs (CY06), Abrahamson and Silva (AS06), and Boore and Atkinson (BA06). All of the factors have been normalized to have a value of 1.0 for $Z_{TOR} = 0$ (surface faulting).

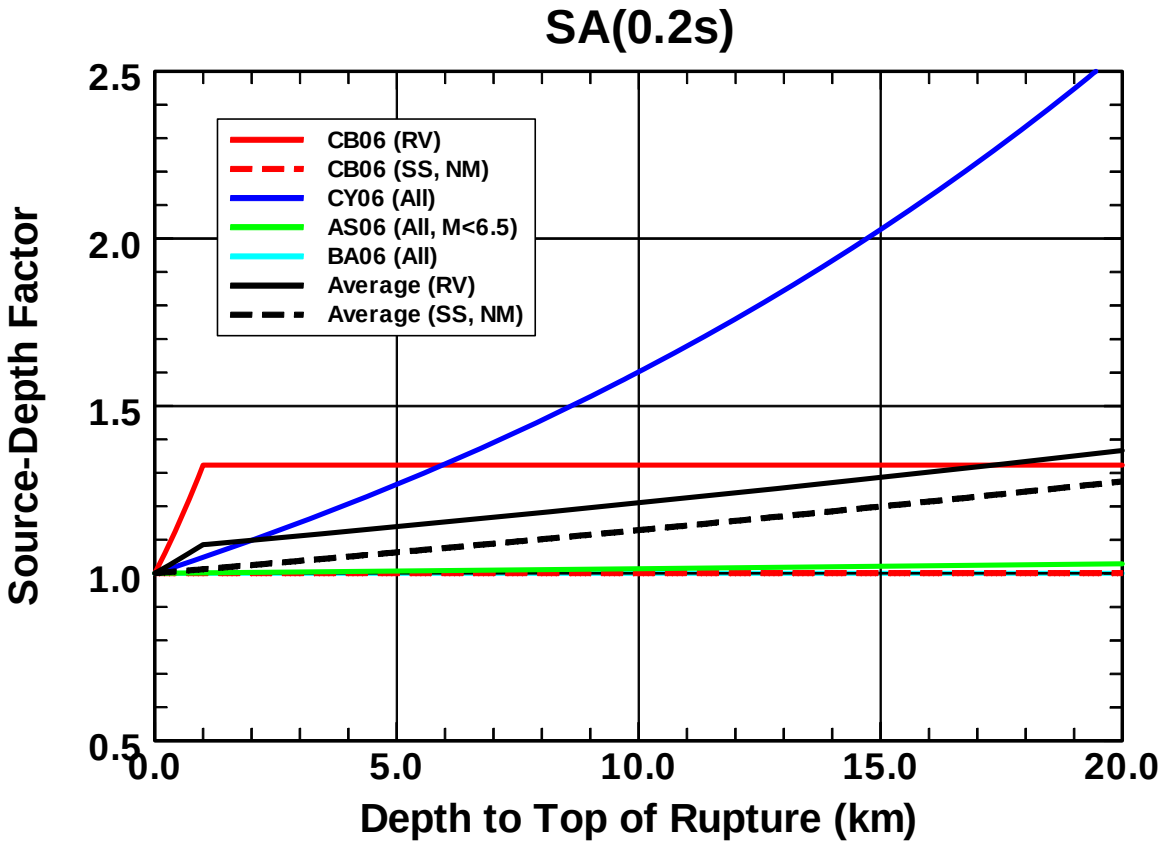

Figure 2: Comparison of depth to top of rupture factor for 0.2s spectral acceleration amongst four NGA models: Campbell and Bozorgnia (CB06), Chiou and Youngs (CY06), Abrahamson and Silva (AS06), and Boore and Atkinson (BA06). All of the factors have been normalized to have a value of 1.0 for $Z_{TOR} = 0$ (surface faulting).

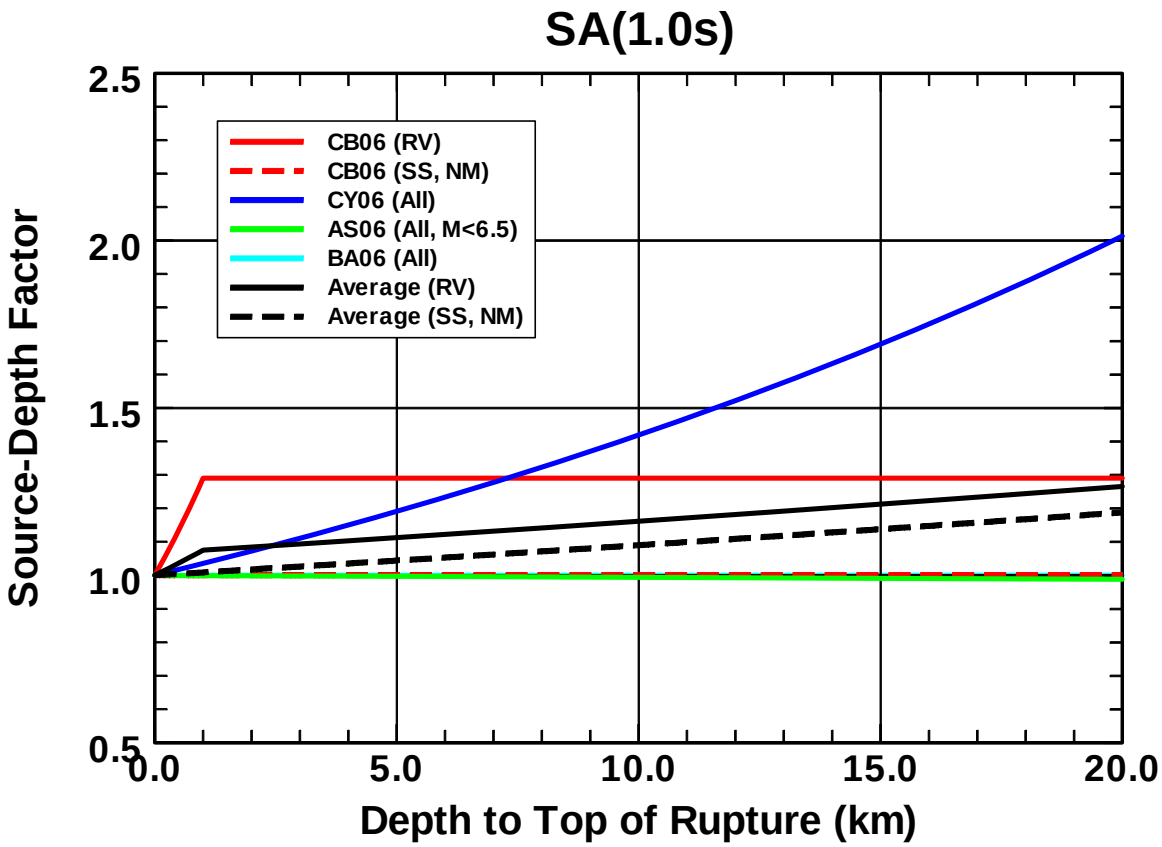

Figure 3: Comparison of depth to top of rupture factor for 1.0s spectral acceleration amongst four NGA models: Campbell and Bozorgnia (CB06), Chiou and Youngs (CY06), Abrahamson and Silva (AS06), and Boore and Atkinson (BA06). All of the factors have been normalized to have a value of 1.0 for $Z_{TOR} = 0$ (surface faulting).

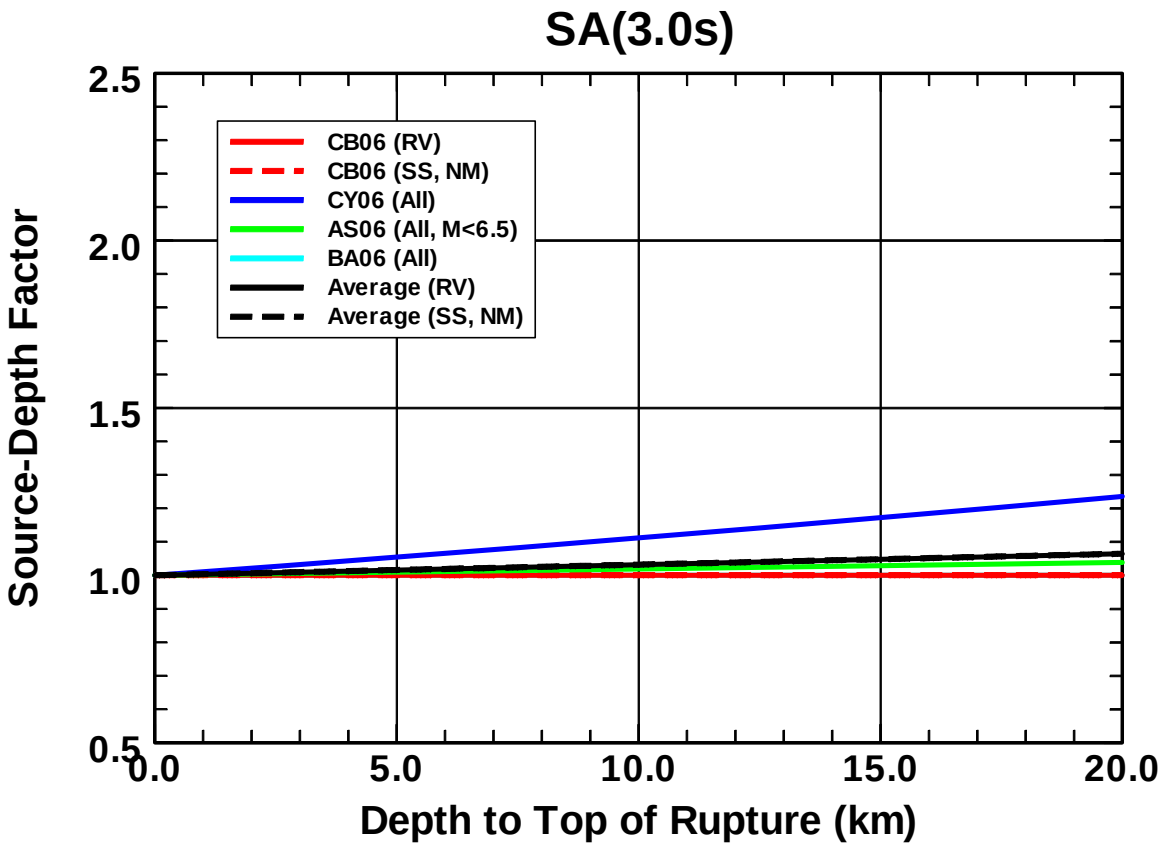

Figure 4: Comparison of depth to top of rupture factor for 3.0s spectral acceleration amongst four NGA models: Campbell and Bozorgnia (CB06), Chiou and Youngs (CY06), Abrahamson and Silva (AS06), and Boore and Atkinson (BA06). All of the factors have been normalized to have a value of 1.0 for $Z_{TOR} = 0$ (surface faulting).

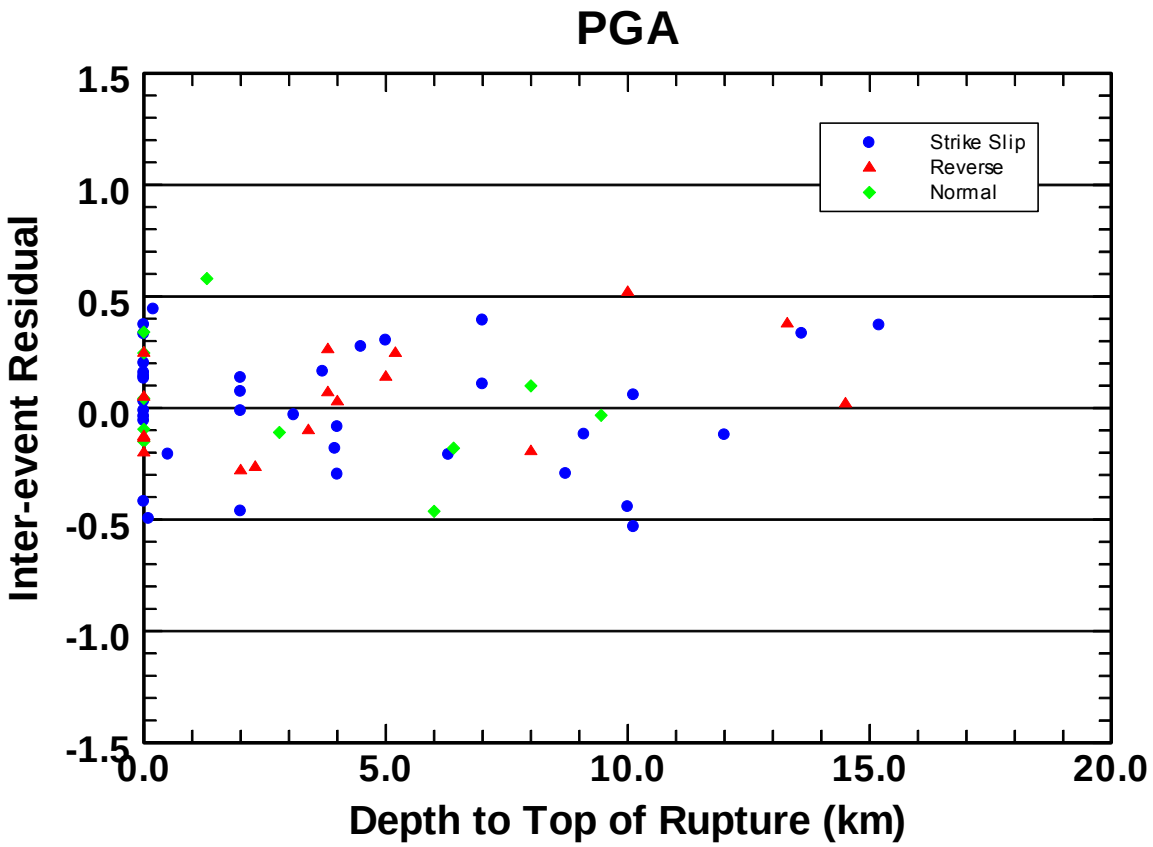

Figure 5: Plot of inter-event residuals for PGA versus depth to top of rupture for the Campbell and Bozorgnia (CB06) NGA model. The symbols represent different styles of faulting as indicated in the legend.

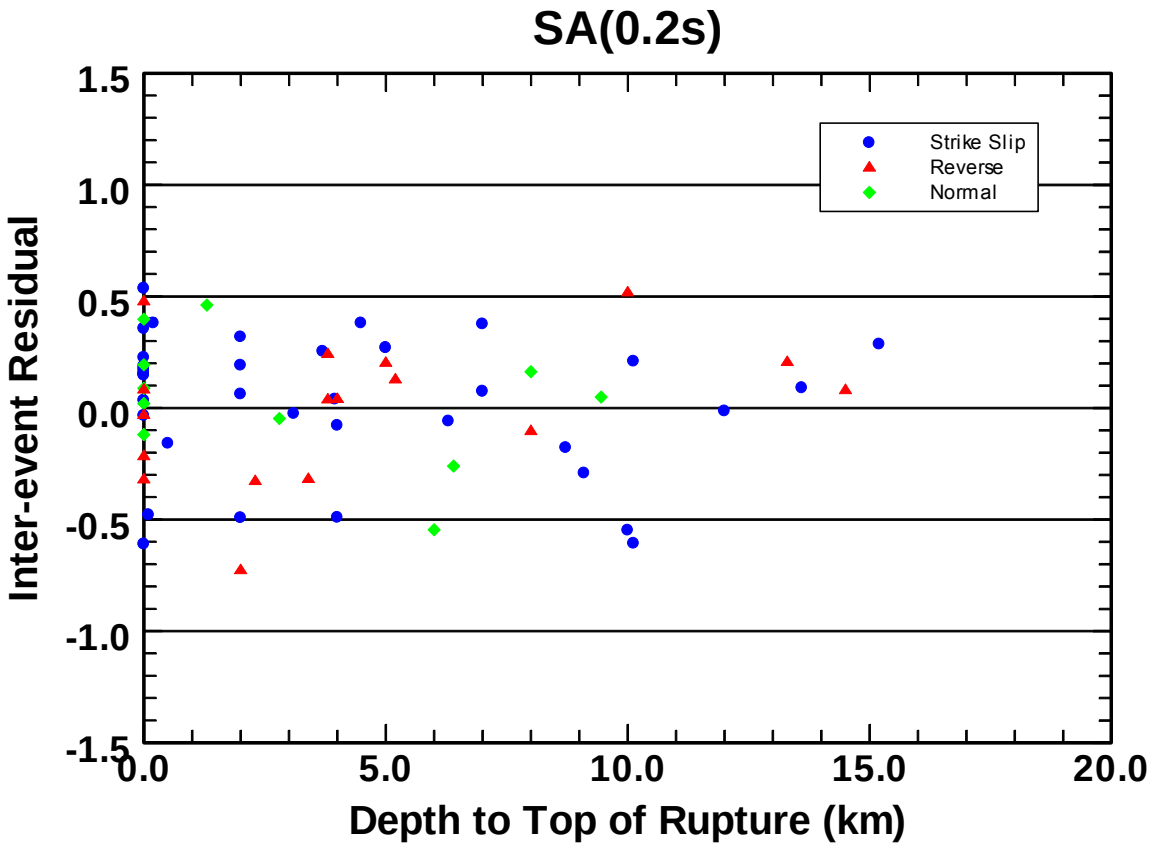

Figure 6: Plot of inter-event residuals for 0.2s spectral acceleration versus depth to top of rupture for the Campbell and Bozorgnia (CB06) NGA model. The symbols represent different styles of faulting as indicated in the legend.

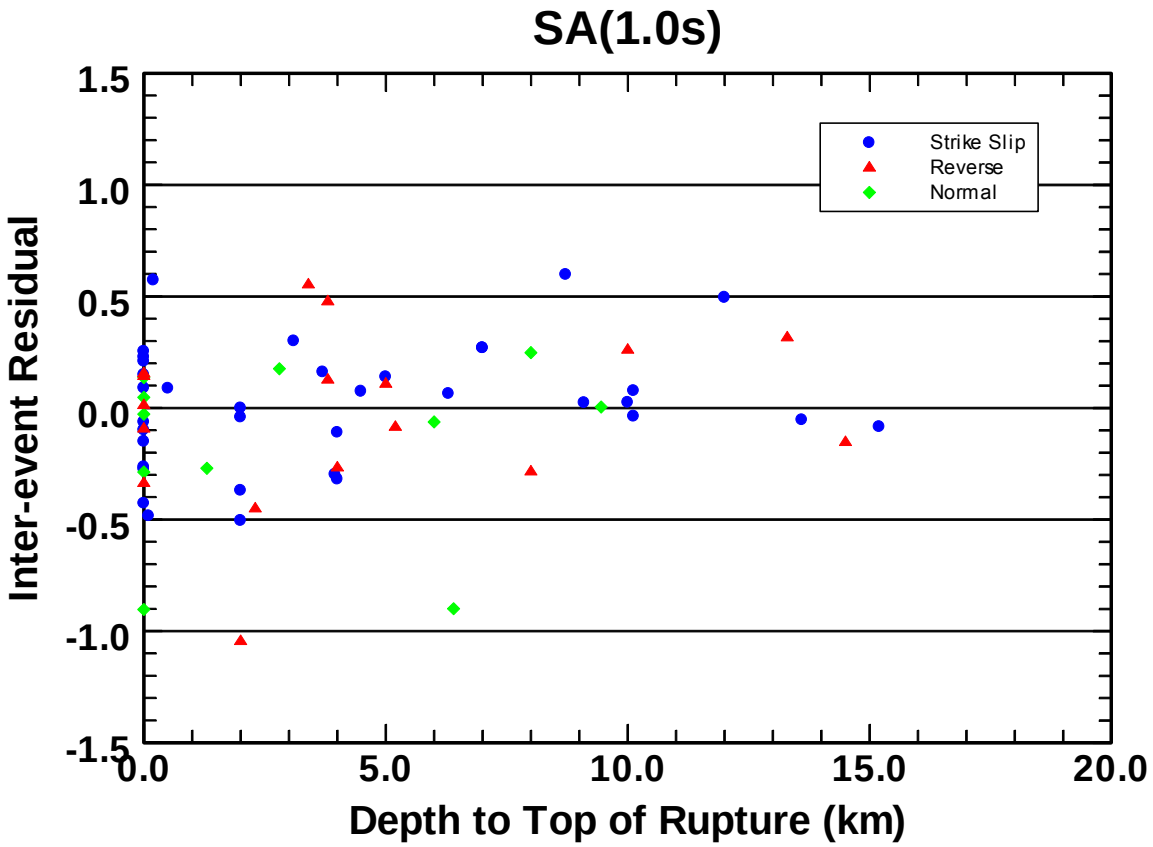

Figure 7: Plot of inter-event residuals for 1.0s spectral acceleration versus depth to top of rupture for the Campbell and Bozorgnia (CB06) NGA model. The symbols represent different styles of faulting as indicated in the legend.

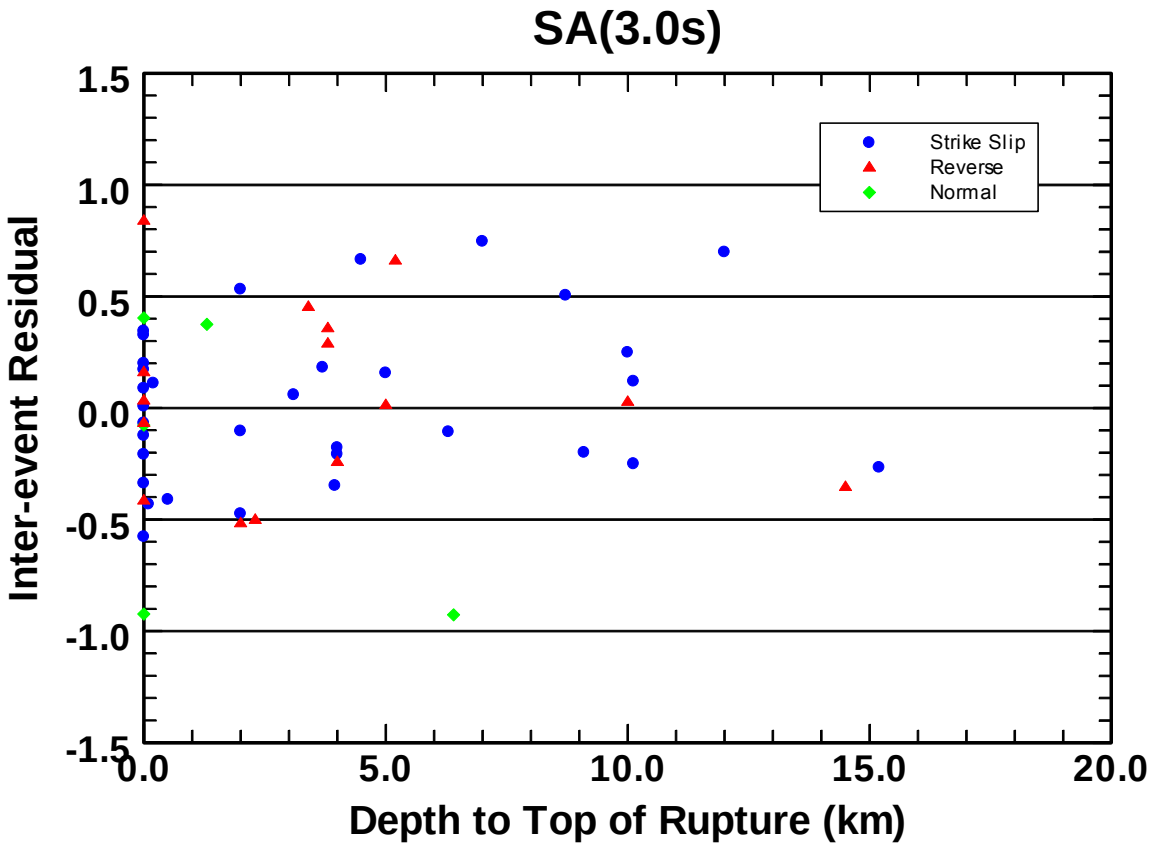

Figure 8: Plot of inter-event residuals for 3.0s spectral acceleration versus depth to top of rupture for the Campbell and Bozorgnia (CB06) NGA model. The symbols represent different styles of faulting as indicated in the legend.

ART FRANKEL'S QUESTION #1

Buried rupture versus surface rupture. Somerville and Pitarka (2006) find no significant difference in source terms, on average, between surface and buried ruptures for periods of 0.2 sec and shorter. Yet the NGA relations that do include terms for depth to top of rupture, predict significant differences between surface faulting and buried faulting at all periods. This discrepancy should be explained. It appears to me that the difference in surface and buried ruptures cited in Somerville and Pitarka (2006) may be at least partly due to the differences in the period of the forward directivity pulses. The buried ruptures used in their paper have magnitudes between 6.4 and 7.0, whereas the surface rupture events have magnitudes between 6.5 and 7.6 and produce forward directivity pulses with longer periods, on average.

CHIOU-YOUNGS RESPONSE

It is not clear whether Somerville and Pitarka intend to use their Figure 2 as an authoritative estimate of the difference in ground motion between surface and buried ruptures. They may merely use it as a compelling evidence of the existence of such difference.

We believe the Z_{TOR} (depth to top of rupture) effects in the CY2006 model are consistent with the NGA mainshock data. Below, we present plots of earthquake terms from the CY2006 model with the Z_{TOR} effect turned off to verify our claim. We'll also show that the Z_{TOR} effect is responsible for a 15% to 20% reduction of the inter-event standard error (τ) at high frequencies. The large variance reduction highlights the importance of including Z_{TOR} effort in the CY2006 model.

Earthquake terms as a function of Z_{TOR}

To obtain earthquake terms with the Z_{TOR} effect turned off, we take the CY2006 model, set coefficient c_7 (the coefficient of the Z_{TOR} term) to zero, and rerun the regression. The new earthquake terms, grouped into three magnitude bins, are plotted against Z_{TOR} on Figure 1. We use the pseudo-standard error $\sigma/\sqrt{n_i}$ [1] of each earthquake term as an approximation for estimation uncertainty. The red (long dashed) line is the predicted Z_{TOR} effect from the CY2006 model.

Figure 1 indicates a clear Z_{TOR} dependence in the earthquake terms, with some indication that the linear trend for earthquakes with $M \leq 5.5$ is weaker than that for earthquakes with $M > 5.5$. We tested the significance of magnitude dependence in the early stage of our model development and found it to be not statistically significant. We conducted the test against our final model again and also found the dependence to be not significant. Moreover, we cannot think of a physical basis for an increase in the Z_{TOR} effect with increasing magnitude. Based on these two reasons, we feel that we can't justify including magnitude dependence in Z_{TOR} effort in our model.

[1] n_i is the number of records in an earthquake.

Is the CY2006 model inconsistent with Somerville and Pitarka (2006) at high frequency?

The average Z_{TOR} is 0.2 km for the 6 surface rupture events used by Somerville and Pitarka, and 3 km for the 4 buried rupture events. Note that Kobe earthquake was treated by Somerville and Pitarka as having a buried rupture, but its Z_{TOR} is 0.0 km. Using the CY2006 model, the expected difference between these two groups of earthquakes is about 0.15, not very different from the difference shown by Somerville and Pitarka[1].

In fact, it's the depth effects at long periods that are quite different between the two studies. At 1-second period, the difference between the two types of rupture is about 0.6 in Somerville and Pitarka, but only 0.12 is predicted by CY2006. To understand this striking difference, earthquake terms of 1-sec spectral acceleration is plotted on Figure 2. It turns out the 4 buried earthquakes picked by Somerville and Pitarka happen to have much larger event terms than other buried earthquakes with similar Z_{TOR}. The CY2006 model has a weaker depth effect because it was fit to all the earthquakes in the NGA dataset.

Reduction of inter-event standard error due to ZTOR

As another confirmation of the importance of Z_{TOR} effect at high frequency, we compute the amount of reduction of the inter-event standard error due to including the Z_{TOR} effect. The results are shown on Figure 3 for every period in the CY2006 model. The reduction of inter-event standard error is large (by about 15% to 20%) at high frequency. It diminishes as the Z_{TOR} effect becomes smaller toward longer periods.

Future refinement of the ZTOR term

The recent paper by Shearer et al (2006) indicates that the stress drops of southern California earthquakes show an increase with increasing depth up to a depth of ~8 km, and no trend below this depth. In our model development, we did not find that a change in the slope of the depth trend at large depths was statistically significant. However, we have very limited data for Z_{TOR} > 8 km. Our data cannot reject the trends seen by Shearer et al (2006). Based on their results we plan to change the depth trend to level off at a depth of about 8 to 10 km. We will have this adjustment by the time of the meeting on the 25th.

[1] The average curve for shallow crustal earthquakes plotted on Figure 2 of Somerville and Pitarka may be in error. For example, at 0.1 sec period, the average of the 6 earthquake terms is more negative than what is indicated by the plotted curve.

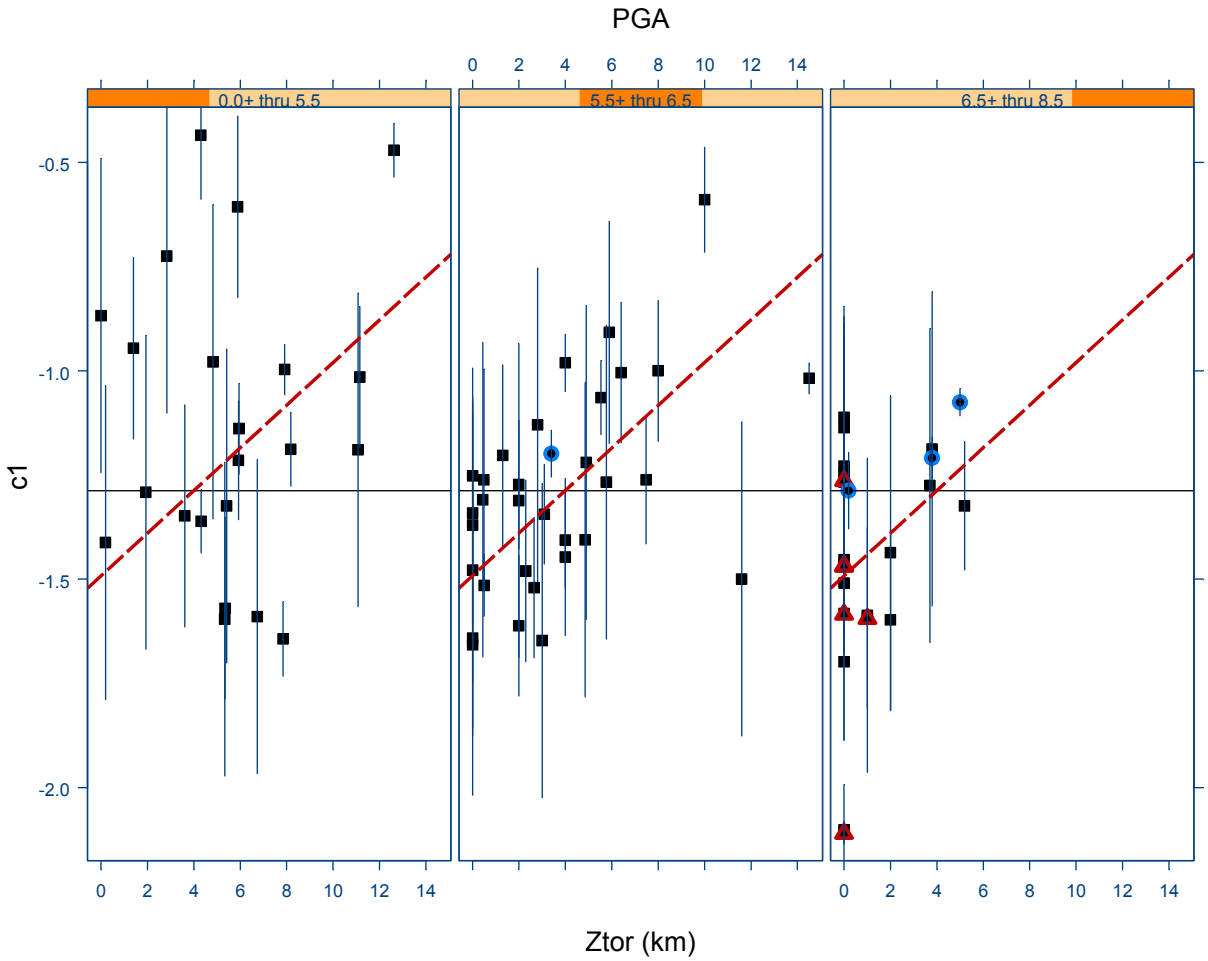

Figure 1a: Earthquake event terms of PGA from CY2006 with the effect of Z_{TOR} turned off. The red line is the predicted effect of Z_{TOR} from CY2006. Earthquakes used by Somerville and Pitarka are the red triangles (shallow rupture) and the blue circles (buried rupture).

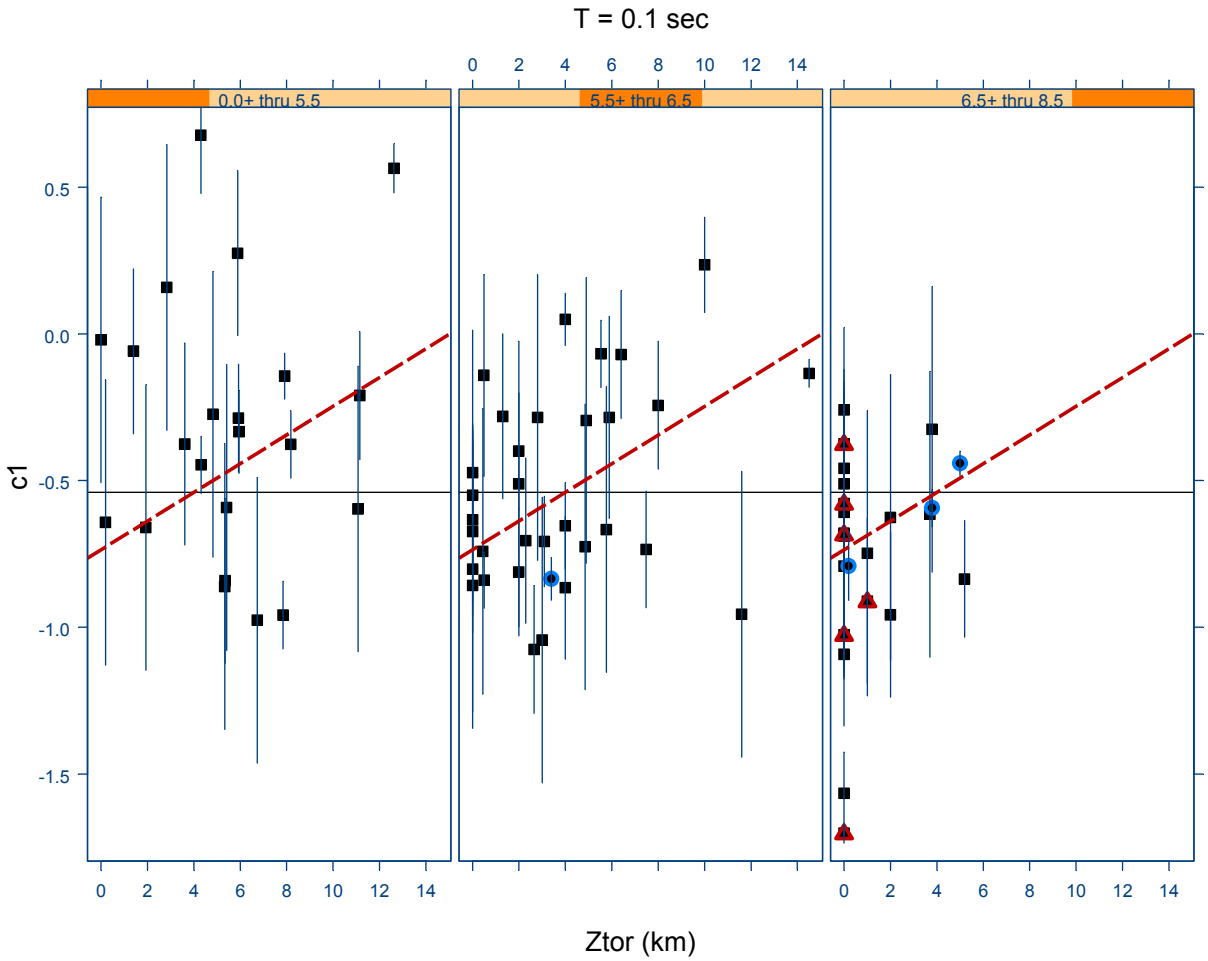

Figure 1b: Same as Figure 1a, but for 0.1-sec period.

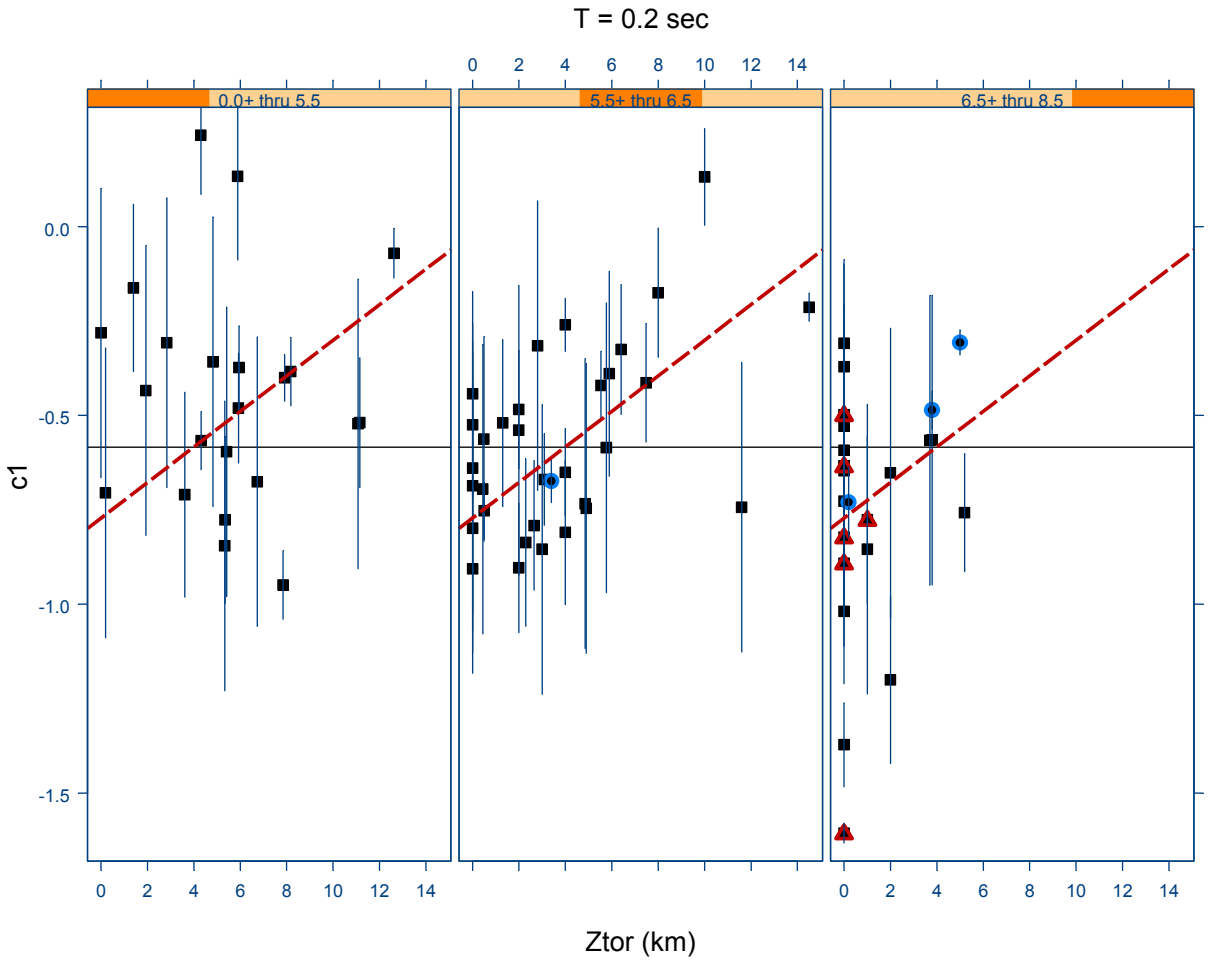

Figure 1c: Sam as Figure 1a, but for 0.2-sec period.

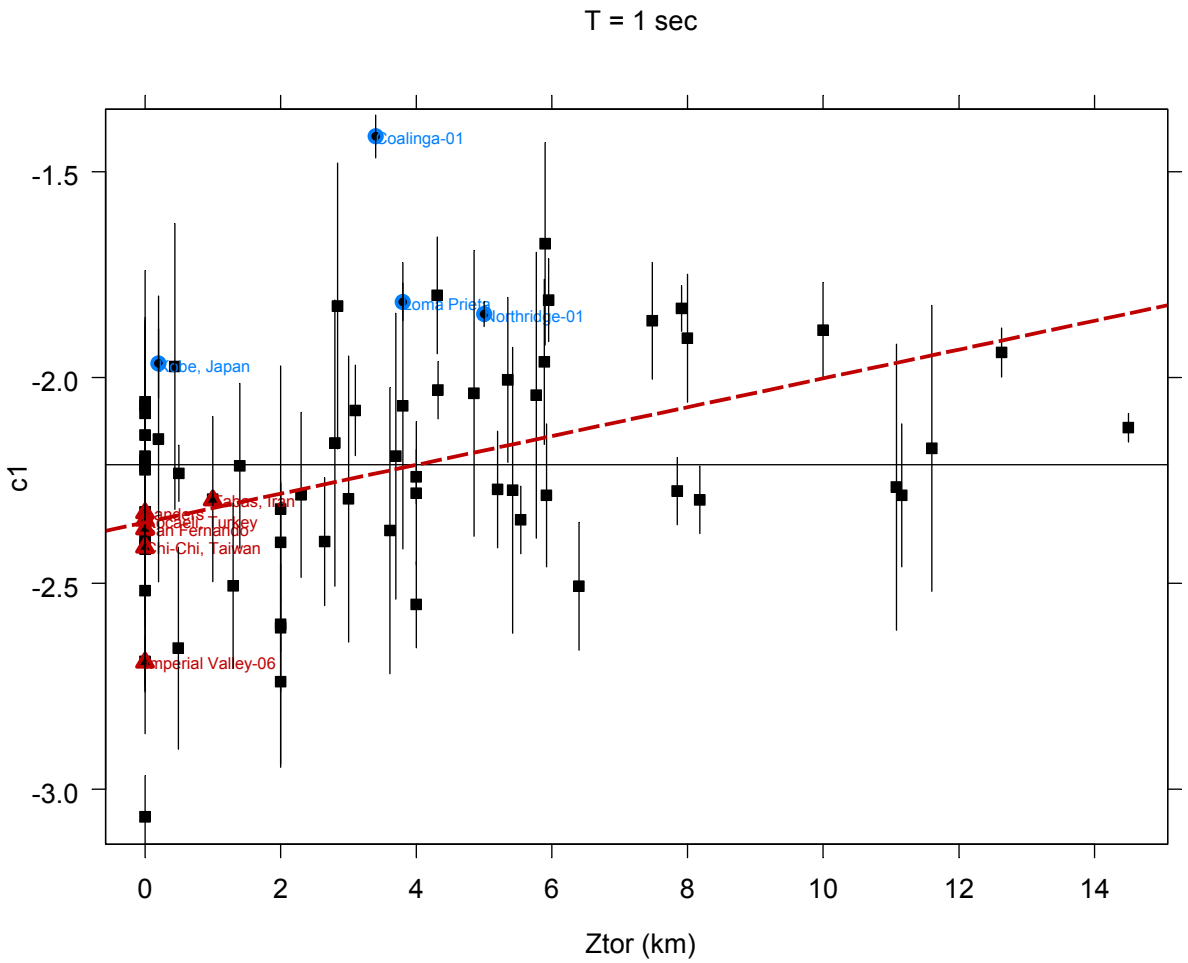

Figure 2: Same as Figure 1, but for 1-sec period.

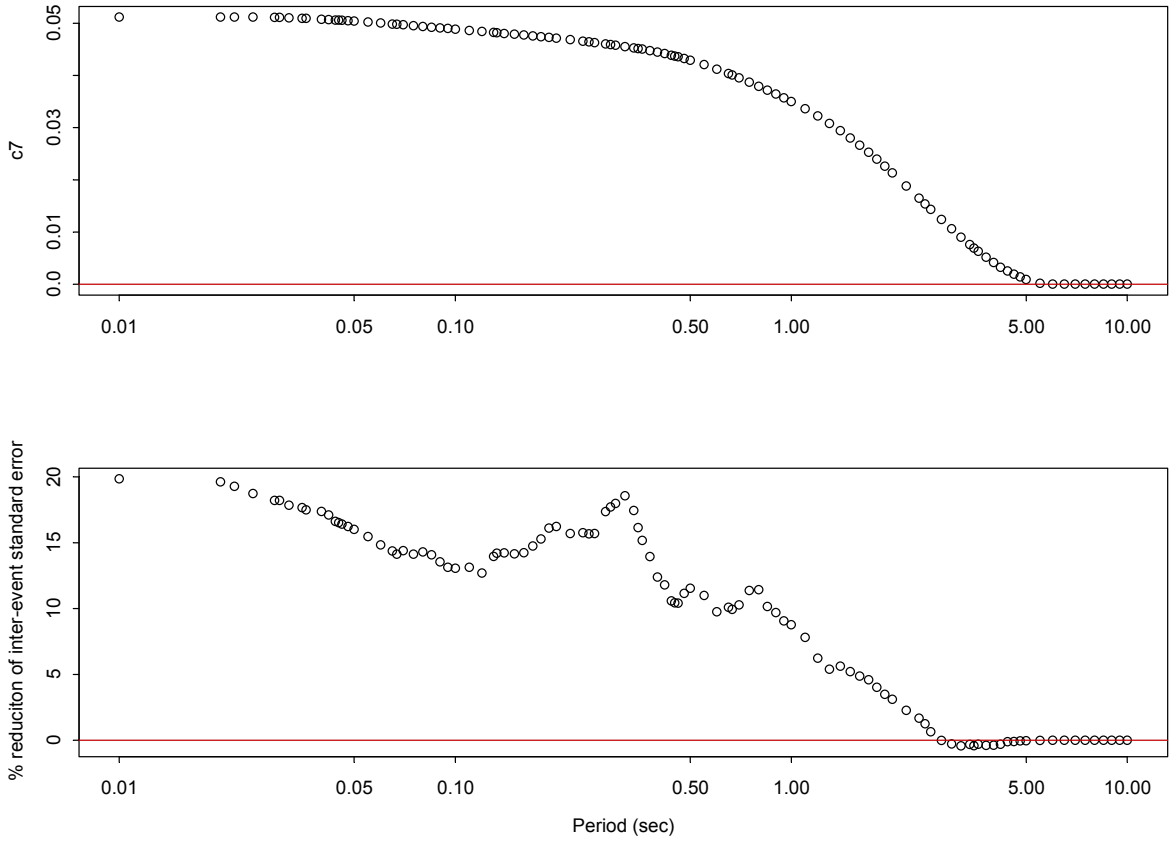

Figure 3: (a) Coefficient c_7 (estimated effect of Z_{TOR}) as a function of period. (b) Percentage of reduction of τ (standard error of inter-event error) due to the Z_{TOR} effect.

ART FRANKEL'S QUESTION #2

Too many predictive variables. The above paragraph points out the danger of using too many predictive variables. For example, magnitude-dependent effects may be confused with a depth to top of faulting effect. Larger events are more likely to rupture the surface. Also, rupture aspect ratio is correlated with magnitude, so it is not obvious these two effects can be separated using the available data.

CAMPBELL-BOZORGNIA REPONSE

Finding the Right Balance of Predictive Variables

There is a trade-off between using too few and too many predictive variables in an empirical ground motion model. Using too few predictive variables will lead to models that have higher aleatory uncertainty and that are less useful in many engineering applications. Using too many predictive variables can lead to models that also have higher aleatory uncertainty and that are less reliable (e.g., because of potential correlation between variables and poorly constrained coefficients). Both of these situations should be avoided and each NGA model did so in its own way. Our method for avoiding these two situations is described below.

We used a two-stage regression analysis to develop an appropriate functional form for the terms in our model before we applied the more comprehensive, but less transparent, random effects analysis to develop the final results (see our NGA report). This allowed us to evaluate the statistical significance of each term (a combination of coefficients, predictive variables, and functional forms) as we added it to the model as well as to evaluate its correlation with other terms in the model. We used an analysis of residuals to determine which terms should be included in the model in order not to exclude any important effects. Aside from a few exceptions, we only included coefficients that provided a reasonable degree of confidence (around 16% or better) and that were not strongly correlated with other coefficients in the model. Exceptions to this rule were made when a coefficient was statistically significant for some oscillator periods but not for others or when seismologists and engineers queried at USGS workshops and other scientific meetings over the course of the last few years believed that a modeled effect should be included even though there was insufficient data to constrain it. In the former case, the term was allowed to smoothly phase out with period, even though it was not statistically significant for many of the phase-out periods. In the second case, the coefficient was assigned a value based on an analogous parameter or on theoretical considerations.

Coefficients for those terms that were constrained in the model included: (1) hanging-wall effects for strike-slip and normal faults, (2) nonlinear soil effects, and (3) deep sediment-depth (basin) effects. For hanging-wall effects, the limited hanging-wall data from normal faults confirmed that these effects were similar on average to those empirically derived for reverse faults, as suggested by Jim Brune from foam rubber modeling. There was insufficient data to confirm these effects for dipping strike-slip faults, but Jim Brune could provide no seismological reason why such faults should not also be subject to hanging-wall effects. Nonlinear soil effects are well documented by observations and nonlinear site-response analyses and accepted by both seismologists and geotechnical engineers. Model residuals, when plotted against PGA, definitely showed behavior consistent with nonlinear soil effects,

but the data were insufficient to develop a functional form. Therefore, theoretical site-response analyses were used to constrain this term. Deep sediment-depth effects were also visible in the data, but like the nonlinear soil effects, the data were insufficient to develop a functional form. Therefore, theoretical 3-D basin response analyses were used to constrain this term. More details and references regarding this topic can be found in our NGA report.

Although we were reasonably successful at avoiding strong correlations between coefficients and predictive variables, there were two important variables for which this correlation could not be avoided, as discussed in our NGA report. These two variables were sediment depth ($Z_{2.5}$) and 30m shear-wave velocity (V_{S30}). The two variables were found to be strongly correlated for $Z_{2.5} < 3$ km, which meant that only one of these parameters were needed to model local site conditions. Since we selected V_{S30} as the primary site-response variable (for consistency with engineering applications), we used it to model site-response and allowed $Z_{2.5}$ to enter the model for sediment depths greater than 3 km, where the model residuals indicated that this effect was significant at moderate-to-long periods. The residuals also indicated that an additional sediment-depth term was needed for $Z_{2.5} < 1$ km. Therefore, the sediment-depth terms were used only to provide an additional site effect when V_{S30} was found to be insufficient to model local soil conditions. More details and references regarding this topic can be found in our NGA report.

Discussion of Specific Cited Examples

You provide three examples where having too many predictive variables might make the model unreliable: (1) the potential correlation between magnitude scaling and the effects of depth to top of rupture, (2) the fact that larger earthquakes are more likely to rupture to the surface, and (3) the correlation between magnitude scaling and aspect ratio.

In our NGA model, the depth to top of rupture is used only to distinguish between reverse-faulting effects for earthquakes that rupture to the surface and those that do not. In essence, it allows large surface-rupturing reverse events to scale with magnitude similar to strike-slip and normal events. An analysis of residuals indicated that if this distinction was not made, either reverse-faulting effects would have been under-estimated for the majority of the reverse earthquakes in the database or the magnitude-scaling for large strike-slip and normal events would have lead to an under-estimation of ground motion for these events. Even at that, because of our decision to constrain the model to saturate when the analysis predicted over-saturation at large magnitudes and close distances, our model over-estimates, on average, the short-period ground motions from the large surface-rupturing reverse earthquakes. Therefore, we believe that by allowing ground motions to be different between surface-rupturing and buried reverse earthquakes we have avoided biasing the reverse-faulting term and the magnitude-scaling effects for strike-slip and normal events.

We agree that larger earthquakes are more likely to rupture to the surface than smaller earthquakes, so there is indeed a correlation between magnitude scaling at large magnitudes and surface rupture. However, as noted above, we included a surface-faulting term only to determine when we applied an additional reverse-faulting factor to the predicted ground

motions. We did not use it to change the magnitude-scaling term. As indicated above, our buried vs. surface-faulting term impacted the magnitude scaling for large earthquakes only to the extent that, had we not allowed this difference, the model would have predicted even a greater degree of over-saturation than it did. As it stands, the over-saturation predicted by the model (before constraining it to saturate) was reasonably small and not statistically significant, giving us a stronger justification for forcing saturation in our model.

The Abrahamson-Silva NGA model was the only one that included aspect ratio as a predictive variable.[1] As indicated in our report, we considered using it in our model (in fact, we were the ones who first introduced it), but we decided not to when we discovered a discrepancy between the magnitude-dependence of the aspect ratios in the NGA database and those in the 2002 source model developed by the USGS and CGS. However, this is a separate issue than the one that you have raised regarding the correlation between surface rupture and aspect ratio. Granted, surface-rupturing events are the ones with the largest aspect ratios. This simply means that one has to be careful not to adversely bias the magnitude-scaling term when aspect ratio is included in the model. We found that we could have just as easily accounted for the reduced magnitude-scaling at large magnitudes included in our model (for all styles of faulting) by not reducing the magnitude scaling at large magnitudes, but instead adding aspect ratio as a variable. In other words, either one modeling approach or the other could be used. We chose to change the magnitude scaling rather than include aspect ratio as a predictive variable in our model for the reason specified above. Abrahamson and Silva chose not to change the magnitude scaling but, instead, include aspect ratio as a parameter.

Conclusion

We believe that we avoided the pitfall of including too few or too many predictive variables in our NGA model by carefully reviewing each added term (coefficient) for its statistical significance and its lack of correlation with other terms (coefficients) in the model. We only included a predictive variable in the model when it was statistically significant or when it was supported by theoretical modeling or recommended by seismologists or engineers. Even in such cases, the model residuals were reviewed to see that they were consistent with the added term or, at least, did not violate it. Many predictive variables were reviewed through an analysis of residuals to ensure that no important variable was excluded. Therefore, we believe that we have not included too few or too many predictive variables in our NGA model.

[1] Subsequently, Abrahamson-Silva eliminated aspect-ratio as a predictor variable in their model.

ART FRANKEL'S QUESTION #2:

Too many predictive variables: The above paragraph points out the danger of using too many predictive variables. For example, magnitude-dependent effects may be confused with a depth to top of faulting effect. Larger events are more likely to rupture the surface. Also, rupture aspect ratio is correlated with magnitude, so it is not obvious these two effects can be separated using the available data.

CHIOU-YOUNGS RESPONSE

Question of confusing magnitude-dependent effects with Z_{TOR} effect

Our response to this question is already in the response to Frankel's Question #1, in which we demonstrated that, given the magnitude scaling of Chiou and Youngs, there is a clear and significant effect of Z_{TOR}.

Too many predictors in the Chiou and Youngs model?

We include in our model terms to address six basic trends in residuals: magnitude, distance (including magnitude effects), style of faulting, hanging wall, depth to top of rupture (addressed in our response to 1), and site condition effects. We believe that all of these trends are observed in the data and should be included in the model. Our formulation attempts to model these trends with smooth functions to avoid sharp "corners", rather than magnitude and distance ramps. This leads to somewhat complicated model equations, but not necessarily more parameters.

ART FRANKEL'S QUESTION #3

Foot wall term. Chang et al. (BSSA Dec. 2004) shows that there is a dip in residuals of the Chi-Chi footwall motions (at distances less than 15 km) when they are plotted as a function of nearest distance to rupture. This is caused by the fact that the distance to the center of the rupture is farther than the nearest distance for footwall sites. Is this relative dip of footwall ground motions accommodated in the functional forms used in NGA? If not, this could artificially lower ground motions in the distance ranges greater than 15 km. The dip in Chi Chi ground motions is also observed when using RJB. This dip does not appear to be present in the Northridge data. This calls into question the utility of the Chi Chi records for predicting ground motions for large events in other regions (see below).

CAMPBELL-BOZORGNIA RESPONSE

Comments on Chang et al. (2004) Paper

Chang et al. (2004) developed an empirical ground motion model for the 1999 Chi-Chi earthquake using only hanging-wall and footwall stations in order to evaluate the impact of hanging-wall effects during this earthquake. They did this by fitting simultaneously a single relationship to both sets of data, then plotting the residuals from the relationship versus distance to look for hanging-wall effects. No adjustment for site effects was made. The bias in their residuals, suggesting over-prediction of ground motions on the footwall at short distances, is visible in their Figures 4–6. We believe that this apparent bias does not necessarily represent a bias in the footwall ground motions for distances less than 15 km. Rather, it is likely caused by the requirement that the relationship must fit simultaneously the close-in hanging-wall and footwall recordings; thereby, over-predicting the footwall ground motions and under-predicting the hanging-wall ground motions. Had an appropriate hanging-wall term been included in the relationship, this apparent bias would have been reduced, if not completely eliminated. To demonstrate that this bias does not appear in our model, we show our residuals for the Chi-Chi earthquake below.

Residuals for Chi-Chi Earthquake

We plot the intra-event residuals from our NGA model for the Chi-Chi earthquake in Figures 1-4 for PGA and SA at periods of 0.2, 1.0 and 3.0s, respectively. The data are identified as being on the hanging-wall, the footwall, off the edge of the fault to the north in the direction of rupture, and off the edge of the fault to the south in the opposite direction of rupture. The horizontal dashed line shows the adjusted baseline after taking into account the inter-event (source) term and the over-prediction resulting from constraining our model to saturate (as opposed to over-saturate) at short periods (see our NGA report). A positive value for this adjusted baseline indicates an over-prediction by the model (i.e., most of the points fall below this line). All of the figures show that overall the intra-event residuals are relatively unbiased with respect to distance, except for a few large-distant stations to the south. However, there is an interesting trend at large distances that will become evident below.

In order to understand how the residuals are impacted by azimuth, we plot only those residuals for stations located on the hanging-wall and the footwall in Figures 5-8 for PGA and SA at periods of 0.2, 1.0 and 3.0s, respectively. The distance range in these plots is more restricted

than in the previous plots because of the limitation in the physical dimensions of Taiwan in the east-west direction. The bias noted by Chang et al. (2004) is not evident in these figures, although there is a tendency to over-estimate the ground motion for footwall sites at distances greater than about 10–15 km, except for the 3.0s period, where the opposite trend is observed. This bias is particularly strong at short periods when the residuals are compared to the adjusted baseline. There is no noticeable bias in the hanging-wall sites except for a slight over-prediction at short periods and at 3.0s with respect to the adjusted baseline.

Similar plots for stations located off the edge of the rupture to the north and to the south are shown in Figures 9-12 for PGA and SA at periods of 0.2, 1.0 and 3.0s, respectively. These figures indicate that the residuals are relatively unbiased out to distances of around 40–50 km, but display an interesting trend at larger distances. In particular, the residuals to the north (in the direction of rupture) beyond this distance show a decreased rate of attenuation and an under-prediction of ground motion; whereas, the residuals to the south (in the opposite direction of rupture) show a increased rate of attenuation compared to the average trend. This could be caused by either anisotropic crustal properties or source directivity effects or both. We are not aware of any study that has addressed this issue. For PGA and the 0.2s spectral acceleration, the source term compensates completely for the under-prediction of ground motions to the north at the expense of grossly over-predicting ground motions to the south. For the longer periods, the source term biases the predictions towards the northern stations, almost completely compensating for any potential under-prediction to the north, at the expense of over-predicting ground motions to the south.

Conclusion

Our intra-event residual plots for the Chi-Chi earthquake do not show the biases in the footwall and hanging-wall residuals at short distances that were observed in the Chang et al. (2004) residual plots. As noted above, this bias was likely caused by these authors not including a hanging-wall term in their ground motion model. In fact, we find no bias with distance overall out to a distance of at least 100 km and no significant bias in the hanging-wall residuals out to the 60-km limit of the data, except at 3.0s period where the more distant hanging-wall ground motions are over-predicted. Footwall sites are over-predicted beyond a distance of 10–15 km, except at 3.0s period where they are under-predicted. We do find a bias in the rate of attenuation between stations located to the north and to the south for distances greater than about 40–50 km, which will need additional study to explain. Forcing saturation in our model generally causes it to over-predict ground motion at short periods, even for hanging wall sites. At longer periods, the predictions are biased towards the relatively higher ground motions to the north. In conclusion, we believe that our results confirm the utility in using the Chi-Chi recordings for predicting ground motion from large events in regions outside of Taiwan.

Chang, T.Y., Cotton, F., Tsai, Y.B., and Angelier, J. (2004). Quantification of hanging-wall effects on ground motion: some insights from the 1999 Chi-Chi earthquake. *Bull. Seism. Soc. Am*. **94**, 2186-2197.

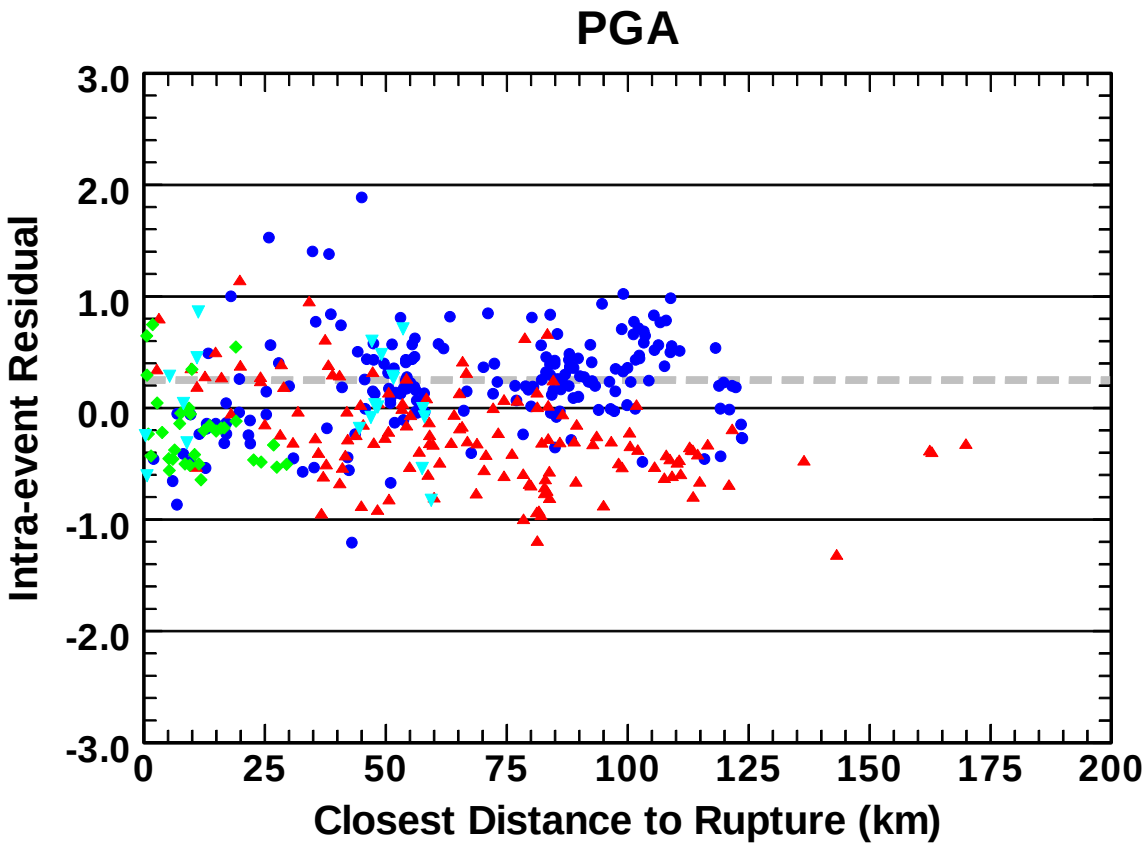

Figure1: Plot of the PGA intra-event residuals from the Campbell-Bozorgnia NGA model for the Chi-Chi mainshock. Recordings are identified as being on the hanging-wall (cyan inverted triangles), on the footwall (green diamonds), off the edge of the fault to the north in the direction of rupture (blue circles), and off the edge of the fault to the south in the opposite direction of rupture (red triangles). The horizontal dashed grey line represents the adjusted baseline after accounting for the source term and the additional bias caused by disallowing over-saturation, where a positive value represents an over-prediction by the model (in this case a significant over-prediction).

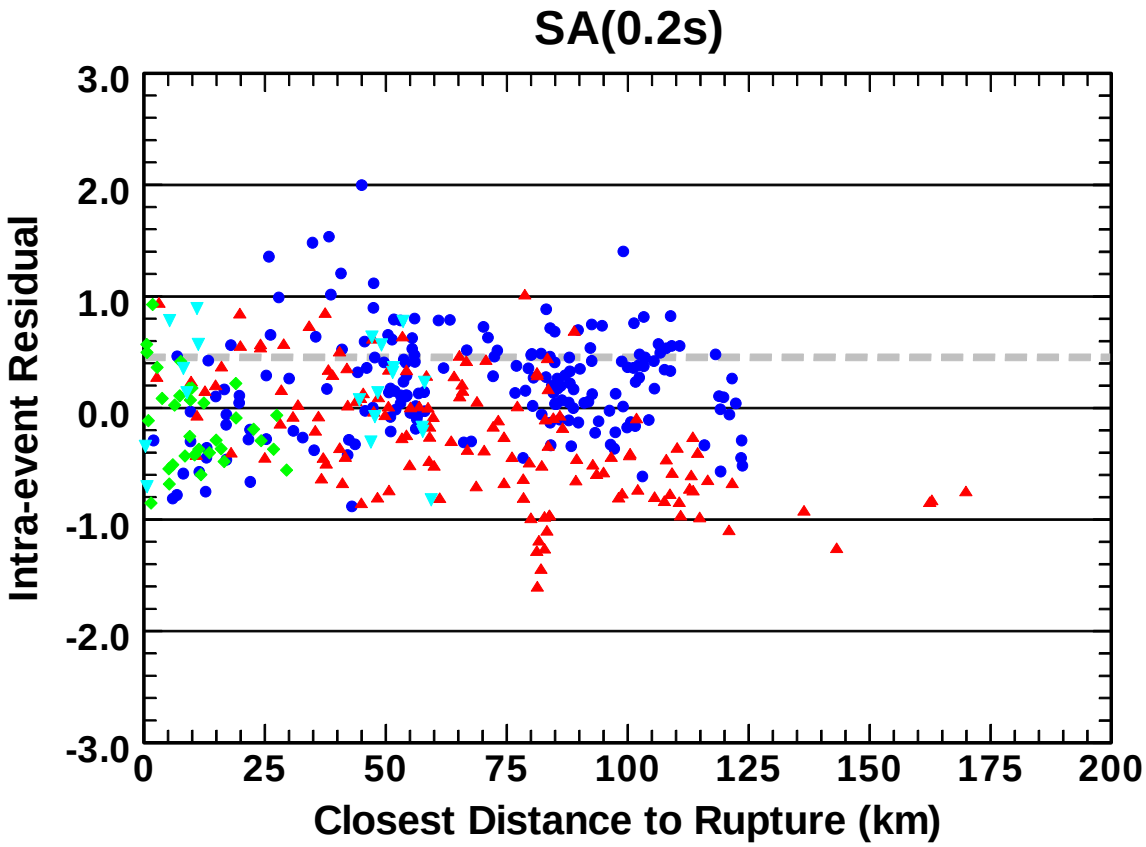

Figure2: Plot of the 0.2s spectral acceleration intra-event residuals from the Campbell-Bozorgnia NGA model for the Chi-Chi mainshock. The symbols and dashed grey line are the same as in Figure1.

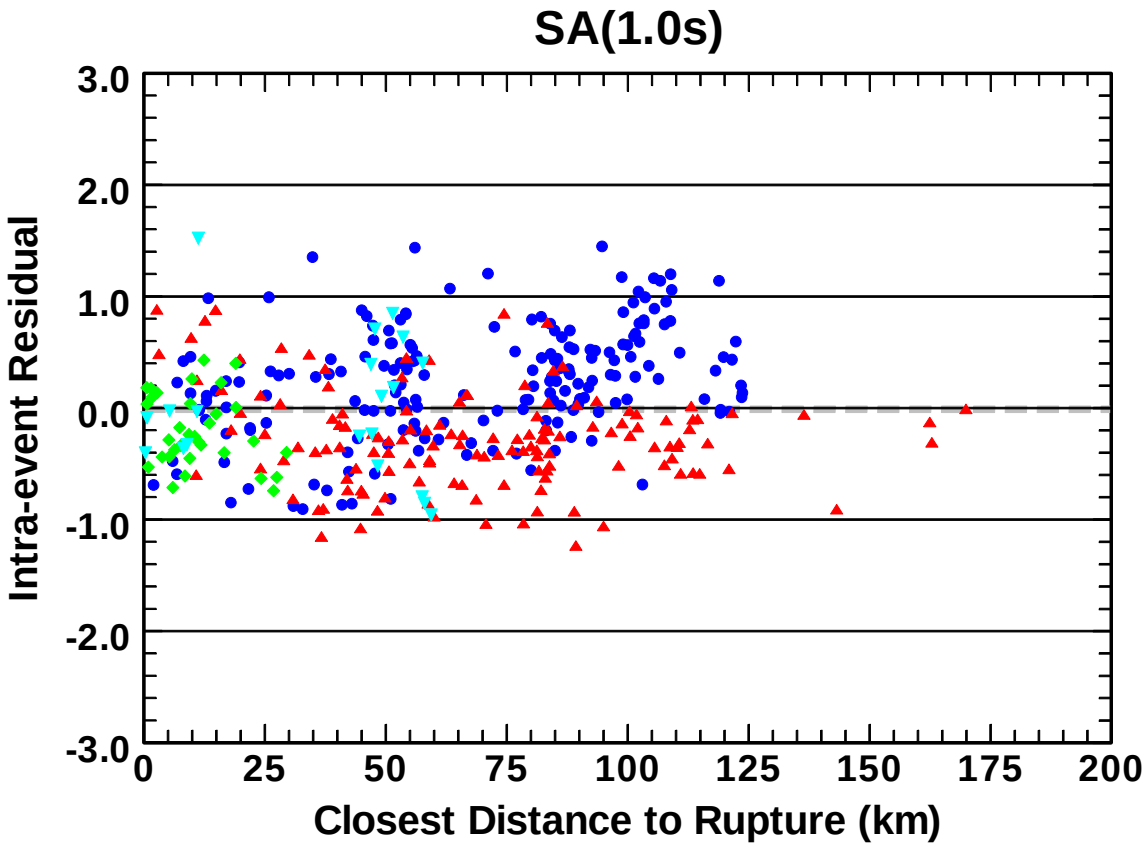

Figure3: Plot of the 1.0s spectral acceleration intra-event residuals from the Campbell-Bozorgnia NGA model for the Chi-Chi mainshock. The symbols and dashed grey line are the same as in Figure1.

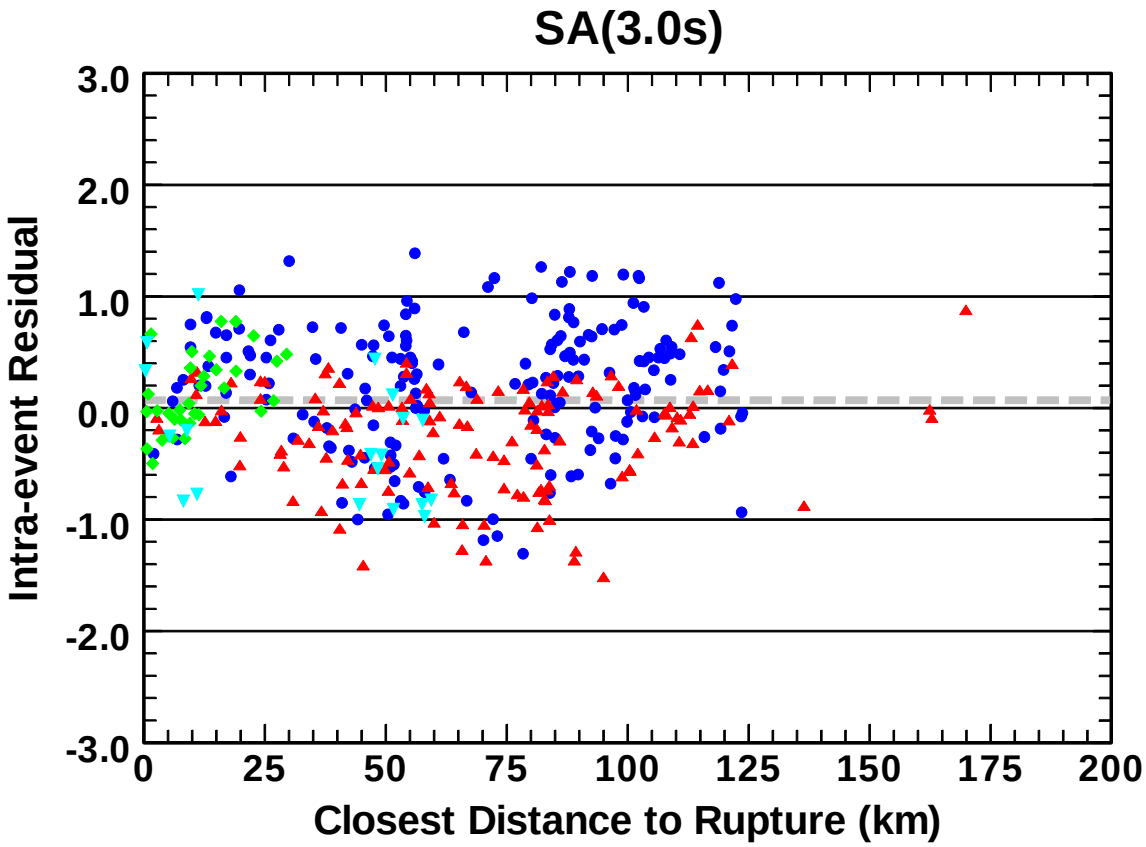

Figure4: Plot of the 3.0s spectral acceleration intra-event residuals from the Campbell-Bozorgnia NGA model for the Chi-Chi mainshock. The symbols and dashed grey line are the same as in Figure1.

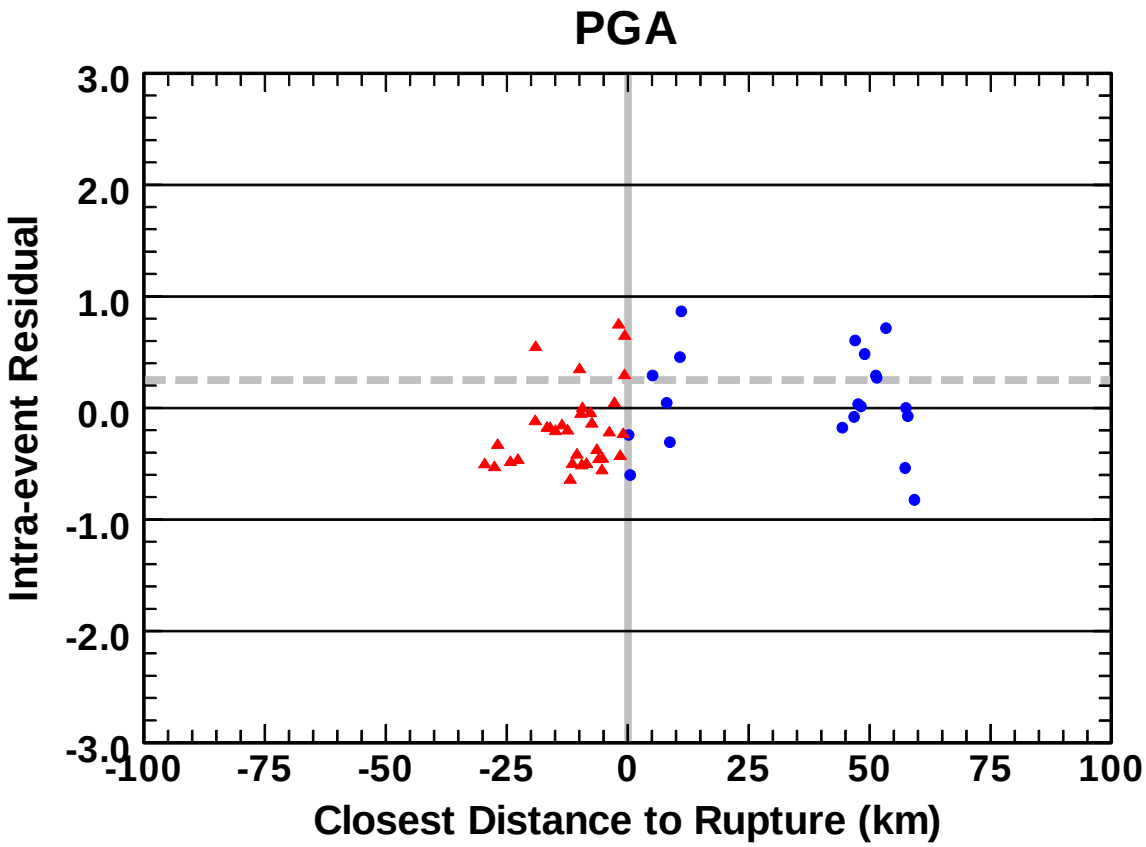

Figure5: Plot of the PGA intra-event residuals from the Campbell-Bozorgnia NGA model for the Chi-Chi mainshock. Recordings are identified as being on the hanging-wall (blue circles) or on the footwall (red triangles). Footwall distances are plotted as negative values for clarity. The vertical solid grey line demarks the transition from the hanging wall to the footwall. The horizontal dashed grey line represents the adjusted baseline after accounting for the source term and the additional bias caused by disallowing over-saturation, where a positive value represents an over-prediction by the model (in this case a significant over-prediction).

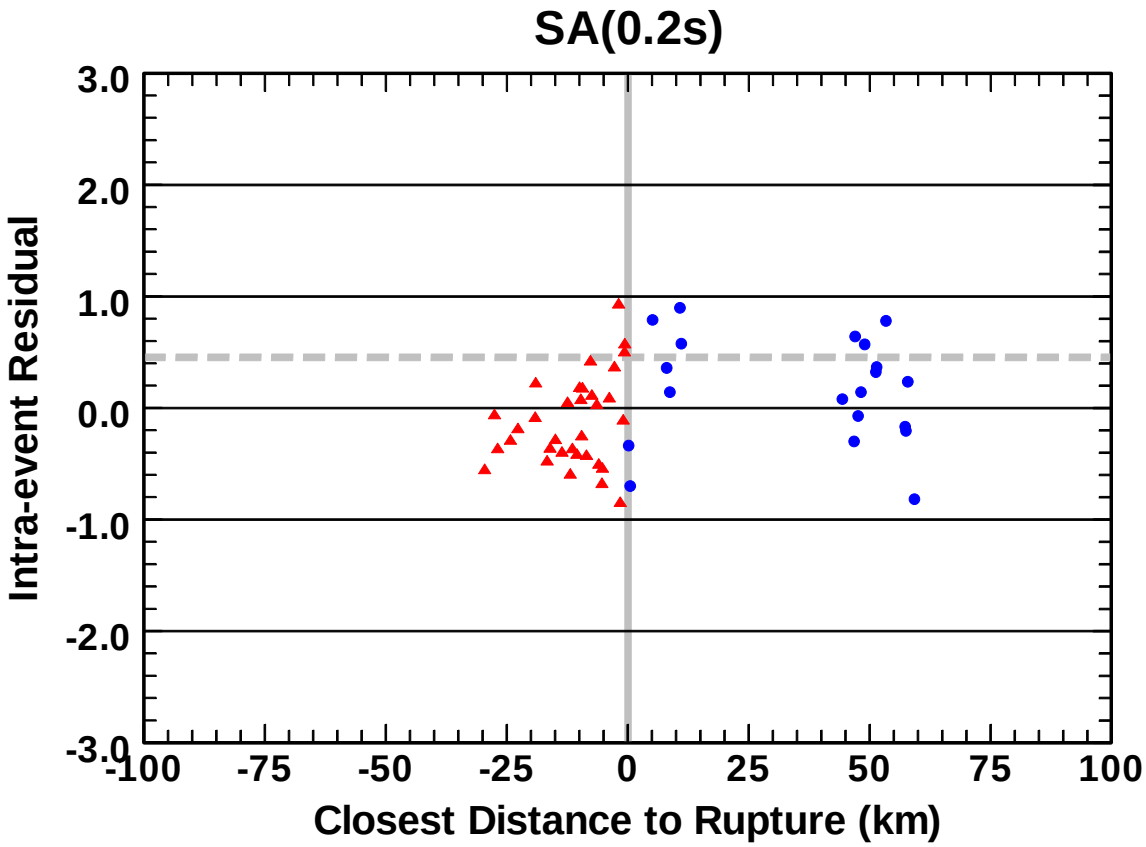

Figure6: Plot of the 0.2s spectral acceleration intra-event residuals from the Campbell-Bozorgnia NGA model for the Chi-Chi mainshock. Recordings are identified as being on the hanging-wall (blue circles) or on the footwall (red triangles). The symbols and solid and dashed grey lines are the same as in Figure5.

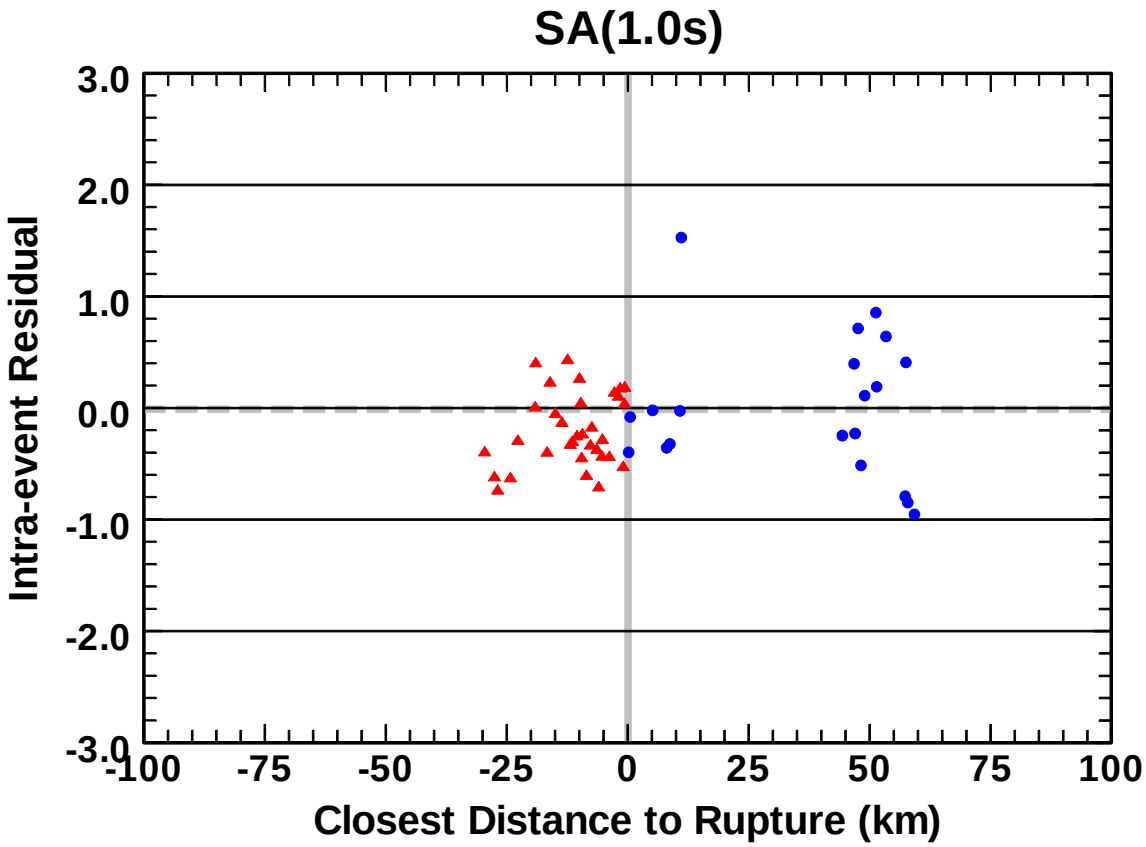

Figure7: Plot of the 1.0s spectral acceleration intra-event residuals from the Campbell-Bozorgnia NGA model for the Chi-Chi mainshock. Recordings are identified as being on the hanging-wall (blue circles) or on the footwall (red triangles). The symbols and solid and dashed grey lines are the same as in Figure5.

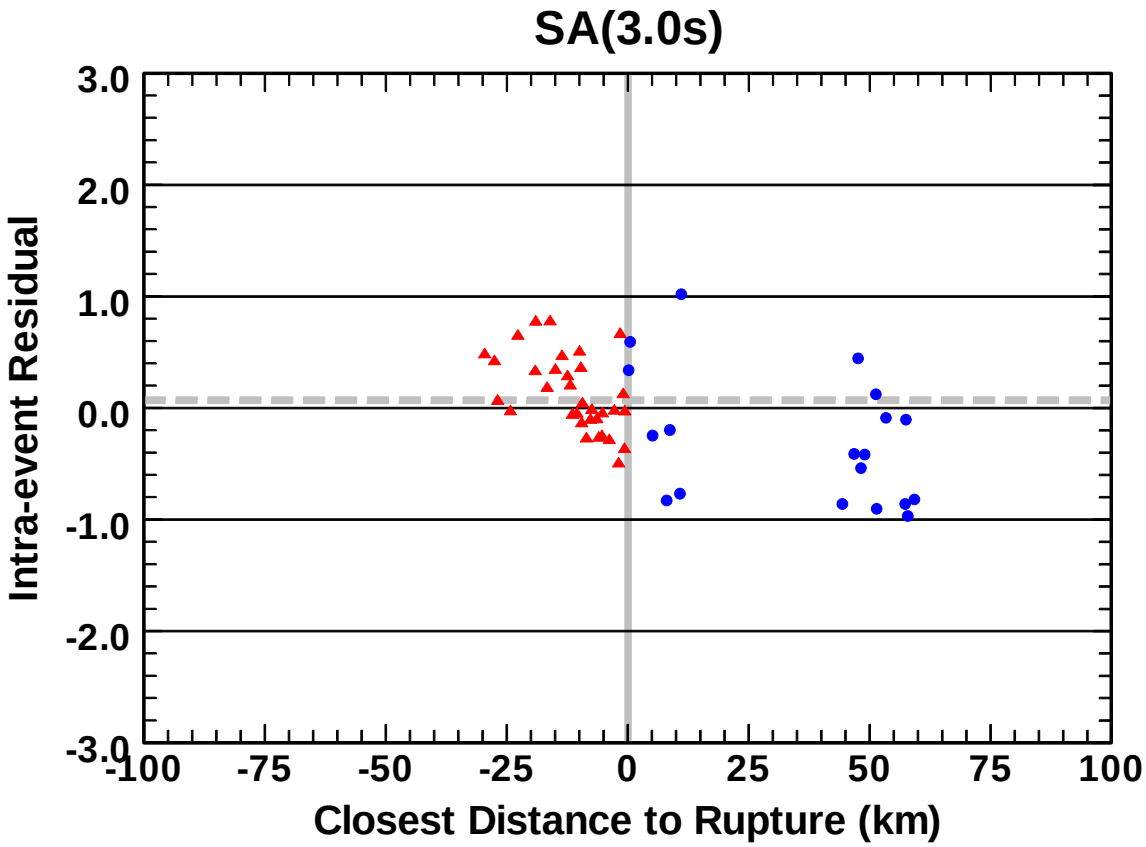

Figure8: Plot of the 3.0s spectral acceleration intra-event residuals from the Campbell-Bozorgnia NGA model for the Chi-Chi mainshock. Recordings are identified as being on the hanging-wall (blue circles) or on the footwall (red triangles). The symbols and solid and dashed grey lines are the same as in Figure5.

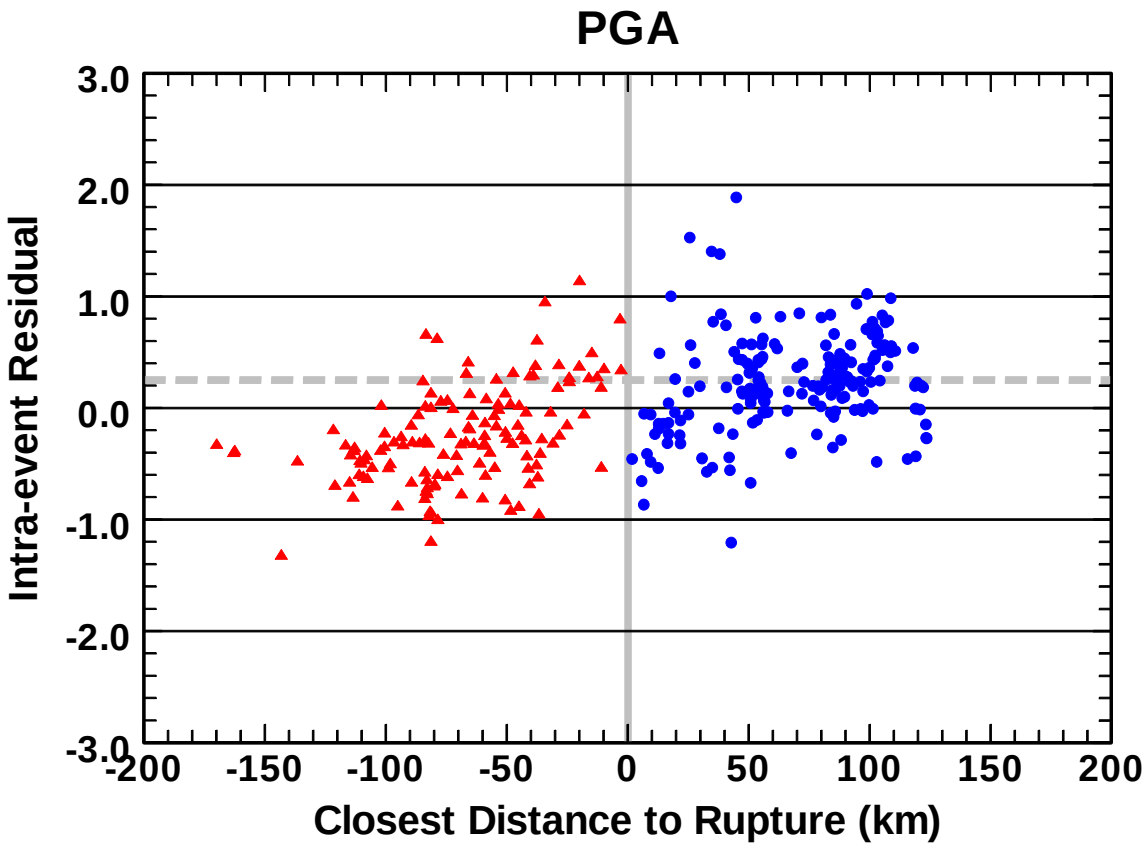

Figure9: Plot of the PGA intra-event residuals from the Campbell-Bozorgnia NGA model for the Chi-Chi mainshock. Recordings are identified as being off the edge of the fault to the north in the direction of rupture (blue circles) or off the edge of the fault to the south in the opposite direction of rupture (red triangles). Southern distances are plotted as negative values for clarity. The vertical solid grey line demarks the transition from the northern sites to the southern sites. The horizontal dashed grey line represents the adjusted baseline after accounting for the source term and the additional bias caused by disallowing over-saturation, where a positive value represents an over-prediction by the model (in this case a significant over-prediction).

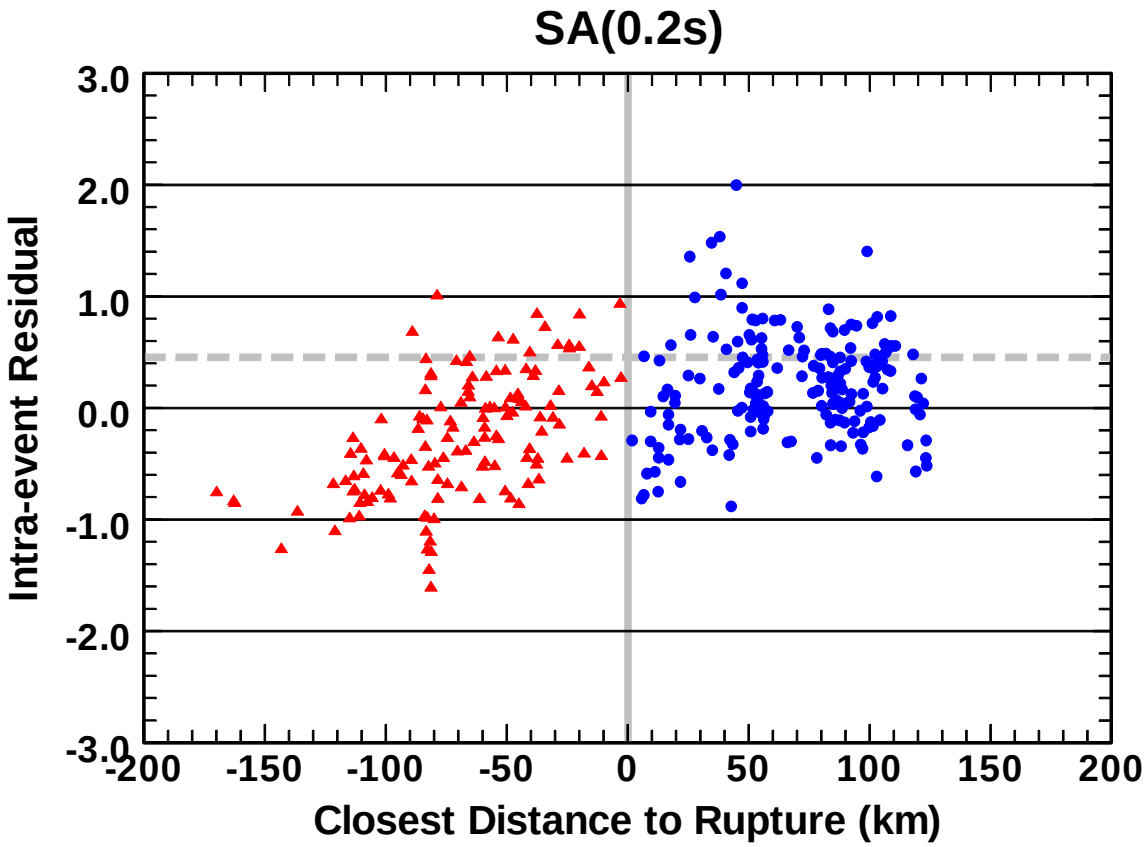

Figure10: Plot of the 0.2s spectral acceleration intra-event residuals from the Campbell-Bozorgnia NGA model for the Chi-Chi mainshock. The symbols and grey solid and dashed lines are the same as in Figure9.

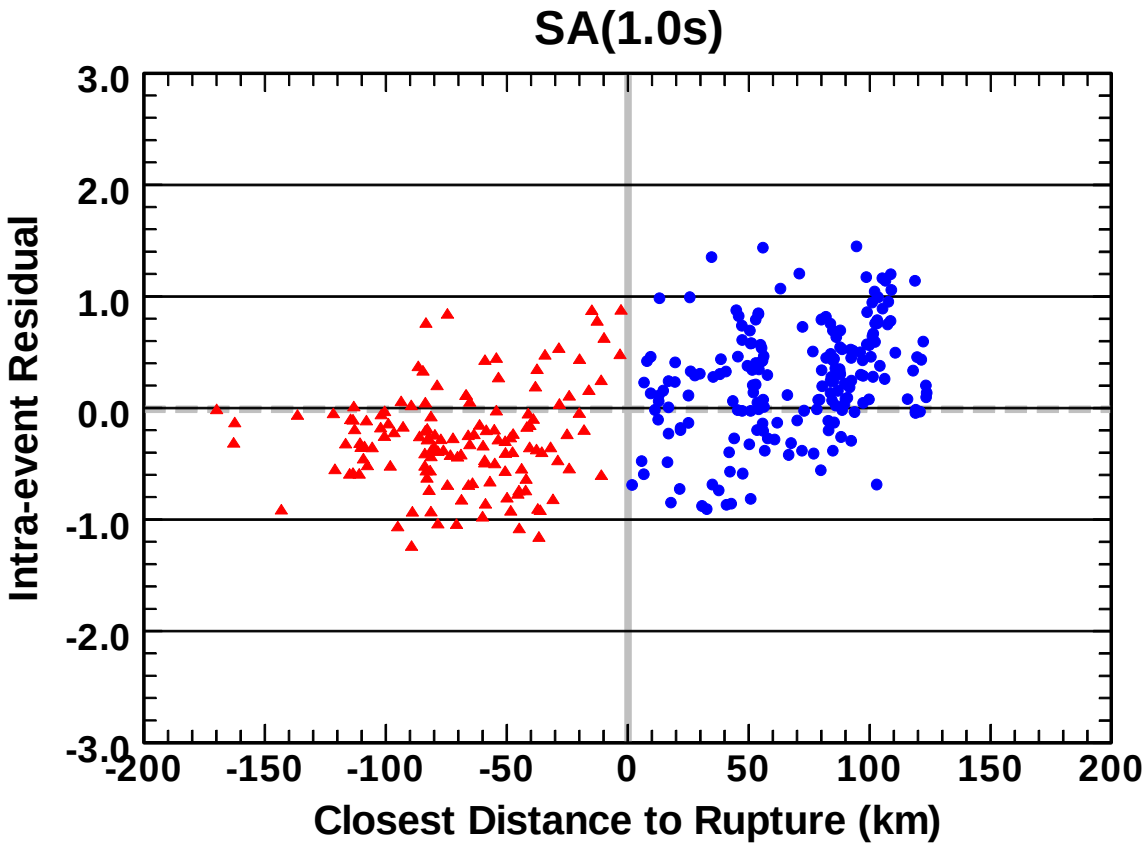

Figure11: Plot of the 1.0s spectral acceleration intra-event residuals from the Campbell-Bozorgnia NGA model for the Chi-Chi mainshock. The symbols and grey solid and dashed lines are the same as in Figure9.

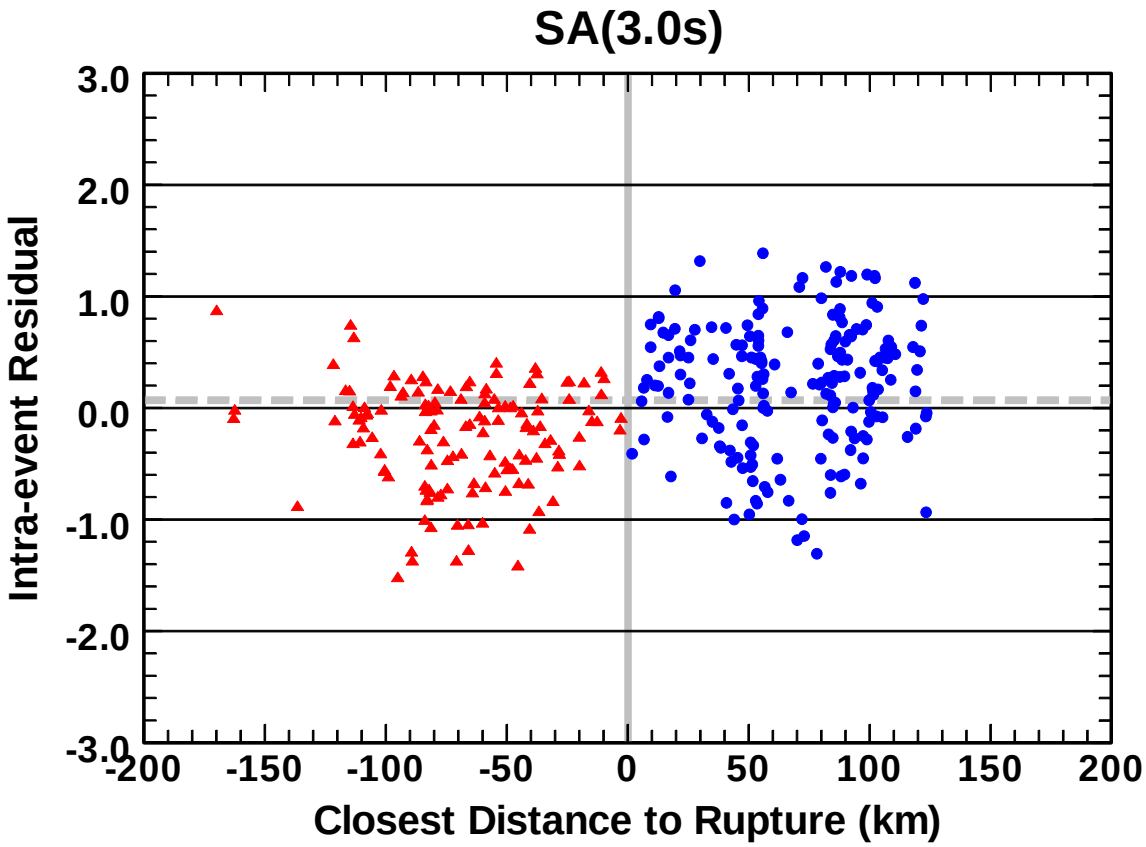

Figure12: Plot of the 3.0s spectral acceleration intra-event residuals from the Campbell-Bozorgnia NGA model for the Chi-Chi mainshock. The symbols and grey solid and dashed lines are the same as in Figure9.

ART FRANKEL'S QUESTION #3

Foot wall term. Chang et al. (BSSA Dec. 2004) shows that there is a dip in residuals of the Chi-Chi footwall motions (at distances less than 15 km) when they are plotted as a function of nearest distance to rupture. This is caused by the fact that the distance to the center of the rupture is farther than the nearest distance for footwall sites. Is this relative dip of footwall ground motions accommodated in the functional forms used in NGA? If not, this could artificially lower ground motions in the distance ranges greater than 15 km. The dip in Chi Chi ground motions is also observed when using RJB. This dip does not appear to be present in the Northridge data. This calls into question the utility of the Chi Chi records for predicting ground motions for large events in other regions (see below).

CHIOU-YOUNGS RESPONSE

We agree with the Campbell-Bozorgnia response; the dip in residuals of the footwall motions at distances less than 15km is an artifact resulting from not having a hanging wall term in Chang et al.'s equation. To verify this claim and to elaborate on the impact of hanging wall term on footwall residuals, we take the same subset of Chi-Chi mainshock data used by Chang et al. and fit two equations to these data. The first equation $ln\, y = a + b\, ln(R_{RUP} + c)$ is identical in form to the equation used by Chang et al. The 2nd equation includes the hanging wall term developed by Chiou and Youngs (2006),

$$ln\, y = a + b\, ln(R_{RUP} + c) + \mathrm{d} \cdot cos^2\, \delta_i \cdot tanh\left(\frac{R_{RUPij}}{2}\right) tan^{-1}\left(\frac{W_i\, cos\, \delta_i}{2(Z_{TORi} + 1)}\right) \frac{1}{\pi / 2} \left\{1 - \frac{R_{JBij}}{R_{RUPij} + 0.001}\right\}$$

The resulting coefficients are listed in Table 1.

Median predictions from these two equations are shown on Figure 1. The hanging wall term has a large influence on parameter *c* because it stops the hanging wall data from pulling the distance curve upward. The larger *c* value in equation 2 results in lower motions at $R_{RUP} < 20$ km, and therefore the dip is no longer present in footwall residuals (Figure 2).

We also want to add that the general form of our distance attenuation model was developed with HW data removed for all earthquakes (this was done only in phase 1 of our model development; see the 'Modeling Steps' section of our report). That decision was motivated by findings similar to the above re-analysis of Chang et al. Removing the hanging wall data helps prevent them from biasing the distance scaling of near-source motions.

Table 1. Coefficients of Equations 1 and 2.

Equation	a	b	c	d	σ
1	3.776	-1.576	19.1	0	0.4123
2	3.926	-1.576	24.6	1.274	0.3097

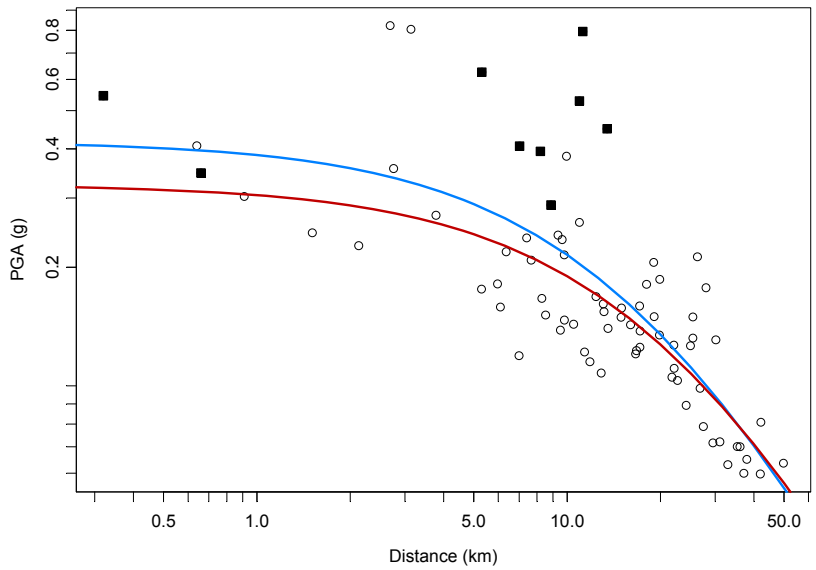

Figure 1: Data and median predictions from equation 1 (blue) and equation 2 (red) for non-hanging wall site. The hanging wall data are shown as solid squares.

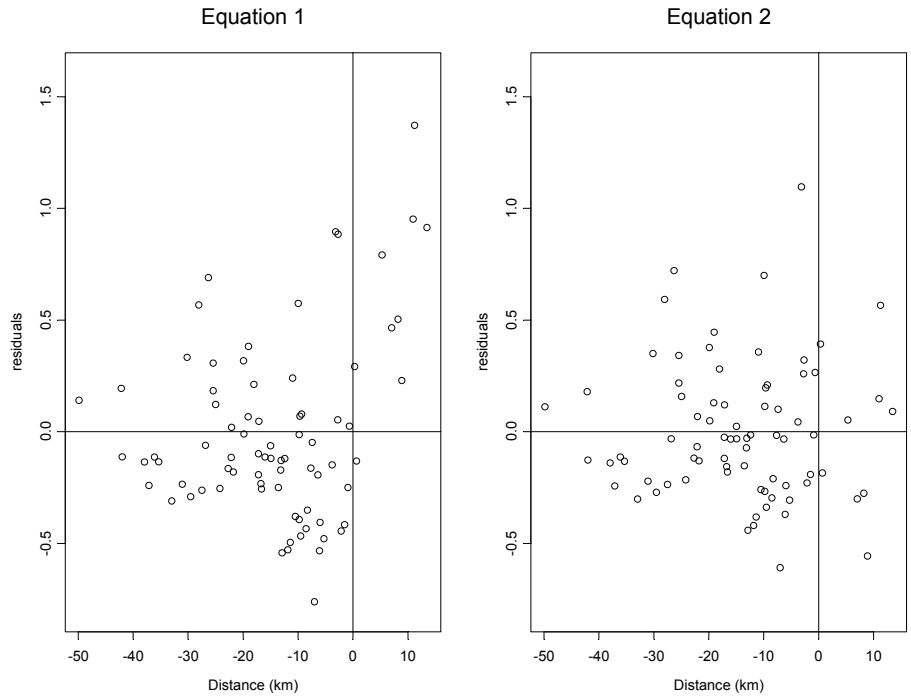

Figure 2: residuals from equations 1 and 2.

ART FRANKEL'S QUESTION #4

Scaling with magnitude. For high frequencies (≥ 5hz), the spectral accelerations for close-in sites (< 10 km JB distance) are far higher for Superstition Hills, Landers, and Kobe earthquakes, than for the Kocaeli earthquake. Here I have chosen only strike slip earthquakes. This suggests there are regional differences in stress drop for strike slip earthquakes.

CAMPBELL-BOZORGNIA RESPONSE

Comments on Regional Differences in Stress Drop

We acknowledge that there are likely to be regional differences in stress drop. The question is whether such differences lead to a bias in the predicted ground motions in regions where the empirical ground motion model will be applied. The earthquakes that you mention come from a variety of tectonic environments. The Kocaeli and Superstition Hills earthquakes occurred in a transtensional stress regime. The Landers earthquake also occurred in what is probably a transtensional stress regime (John Anderson, USGS Workshop, Reno, NV, 2006).[1] The Kobe earthquake occurred in a transpressional stress regime. Seismologists would likely expect the stress drops to be the largest in a transpressional stress regime and smallest in a transtensional stress regime. Of course, there is a large degree of variability in stress drops within a given tectonic environment, so a comparison of a few earthquakes is not really sufficient to derive general conclusions. Nonetheless, in the next section we look to see if there is a systematic bias in our NGA model predictions for these four earthquakes.

Comparison of Model Predictions

In the development of our model, we looked at possible differences in ground motion due to tectonic environment by comparing inter-event residuals (source terms) between extensional and non-extensional tectonic regimes after including coefficients for style of faulting. We didn't find any bias in the residuals of either group, which suggested that, at least for our dataset, there was no systematic difference between these two tectonic regimes that wasn't accounted for by the style-of-faulting factors. In fact, what little effect we saw indicated that ground motions in extensional regimes were possibly larger. However, John Anderson (USGS Workshop, Reno, NV, 2006) has disagreed with the assignment of extensional and non-extensional regimes to several California earthquakes in the NGA database based on the original assessment by Spudich et al. (1997, 1999). He suggests, for example, that earthquakes in the Mojave Desert (e.g., 1992 Landers and 1999 Hector Mine) should be classified as extensional. If this were to be confirmed, we are not sure what difference it would make in our assessment of extensional versus non-extensional tectonic regimes.[6]

Rather than look at the absolute value of ground motion, as you have done, we again look at the residuals for the earthquakes you have mentioned to see if there is a systematic bias in the predictions from our NGA model that is consistent with your suggestion. Absolute values can be deceiving, since they do not take into account differences in predictive variables, such as magnitude and local soil conditions, between earthquakes. In Figure 1 we plot the intra-event

[1] In a subsequent investigation, Paul Spudich and Dave Boore determined that the 1992 Landers, 1999 Kocaeli, and 1999 Hector Mine earthquakes likely occurred in a strike-slip (non-extensional) stress regime.

residuals for PGA versus rupture distance for the 1995 Kobe, 1992 Landers, 1999 Kocaeli, and 1987 Superstition Hills earthquakes over the full range of distances used in our model to see how well the model fits the data overall. Also shown on this plot is the adjusted baselines for these same events after accounting for the inter-event residuals (source term) and the additional bias caused by constraining the model to saturate when over-saturation was predicted. The negative adjusted baselines indicate under-prediction by the model. A larger negative baseline implies a larger under-prediction.

Looking at the adjusted baselines, Figure 1 shows that all four events are under-predicted overall, with the Kobe and Superstition Hills events having the largest under-prediction and the Landers and Kocaeli events having the largest under-prediction. The other interesting observation is that PGA is under-predicted relative to other intra-event residuals for these four earthquakes between distances of around 65–125 km, where one might expect increased ground motions from crustal reflections. (This effect becomes negligible at longer periods). Our functional form does not allow for differences in geometrical attenuation from such reflections because of their complexity and variability with respect to period. Figure 2 shows a similar plot for $R_{JB} \leq 20$ km. This plot extends to a larger distance than you suggested so that there would be enough recordings to make a meaningful comparison. In this distance range, the comparison is quite different than that over all distances. Comparing the intra-event residuals with the adjusted baselines, the Superstition Hills earthquake is clearly under-predicted, but the predictions for the other three earthquakes all appear to be relatively unbiased. Similar results are found for 0.2s spectral acceleration as shown in Figures 3 and4.

If differences in stress drop were causing the differences noted by you and observed in the residual plots for short-period ground motions, these differences should be diminished at longer periods. To test this hypothesis, we show the same residual plots as above for the 1.0 and 3.0s spectral accelerations in Figures5-8. Again, all of the events are under-predicted overall, but now the largest under-prediction is for the Kobe earthquake for 1.0s period (Figure5) and the Landers earthquake for 3.0s period (Figure7), while the other events are all moderately under-predicted with the smallest under-prediction occurring for the Kocaeli event. This ranking for the Kocaeli earthquake does not seem to support the idea that the short-period differences for this event are the result of an unusually low stress drop. At 3.0s, the Landers event is under-predicted at distances beyond about 130 km. Within 20 km, Kocaeli is over-predicted, Kobe is under-predicted, and the other two events are relatively unbiased compared to their adjusted baselines.

Conclusion

We did not find any significant difference in ground motions between extensional and non-extensional tectonic regimes based on an analysis of residuals after accounting for differences due to style of faulting (see our response to Mark Petersen's Question #1). Our residuals also indicate that all four events that you mention are under-predicted by our model, so the Kocaeli earthquake is not unique in this regard, nor does it appear to be an outlier. The Kobe earthquake has the largest under-prediction in our model, which might be consistent with it occurring in a transpressional stress regime. However, it also had a relatively large hypocentral depth (17 km) and its rupture was buried, at least along its northern reaches where most of the recordings were located, which might have also contributed to this under-prediction. At short periods, the

Superstition Hills earthquake, which also had a buried rupture, is under-predicted by our model by about the same amount as the Kobe earthquake. Therefore, one might argue that the relative differences between the residuals for these four earthquakes could be explained by whether they had buried versus surface faulting rather than whether they were affected by regional differences in stress drop. We found this to be the case for reverse faults, but we believed that the data were too ambiguous to allow us to apply such a factor to strike-slip earthquakes at the present time.

Our analysis of residuals suggests that our results either do not support your observation that, for high frequencies, the spectral accelerations for close-in sites (<10 km JB distance) are far higher for Superstition Hills, Landers, and Kobe earthquakes than for the Kocaeli earthquake or that these differences have been reasonably captured in our model. Although we agree that there could be regional differences in stress drop and stress regime for strike slip earthquakes, and our residuals possibly support this, we also believe that this might be just as easily modeled by accounting for differences between buried versus surface faulting. Under the hypothesis that ground motions should be larger in transpressional stress regimes (presumably due to larger stress drops), large strike-slip earthquakes in California from the Big Bend north would be under-predicted by our model; whereas, under the hypothesis that ground motions are smaller for surface-faulting events, these earthquakes would be over-predicted by our model. By not specifically attempting to model one hypothesis over the other, our model allows for the possibility of both hypotheses with a corresponding increase in aleatory variability, which we believe reasonably reflects the uncertainty expressed within the scientific community.

Spudich, P., Fletcher, J., Hellweg, M., Boatwright, J., Sullivan, C., Joyner, W.B., Hanks, T.C., Boore, D.M., McGarr, A.F., Baker, L.M., and Lindh, A.G. (1997). SEA96: a new predictive relation for earthquake ground motions in extensional tectonic regimes. *Seism. Res. Lett*. **68**, 190-198.

Spudich, P., Joyner, W.B., Lindh, A.G., Boore, D.M., Margaris, B.M., and Fletcher, J.B. (1999). SEA99: a revised ground motion prediction relation for use in extensional tectonic regimes. *Bull. Seism. Soc. Am*. **89**, 1156-1170.

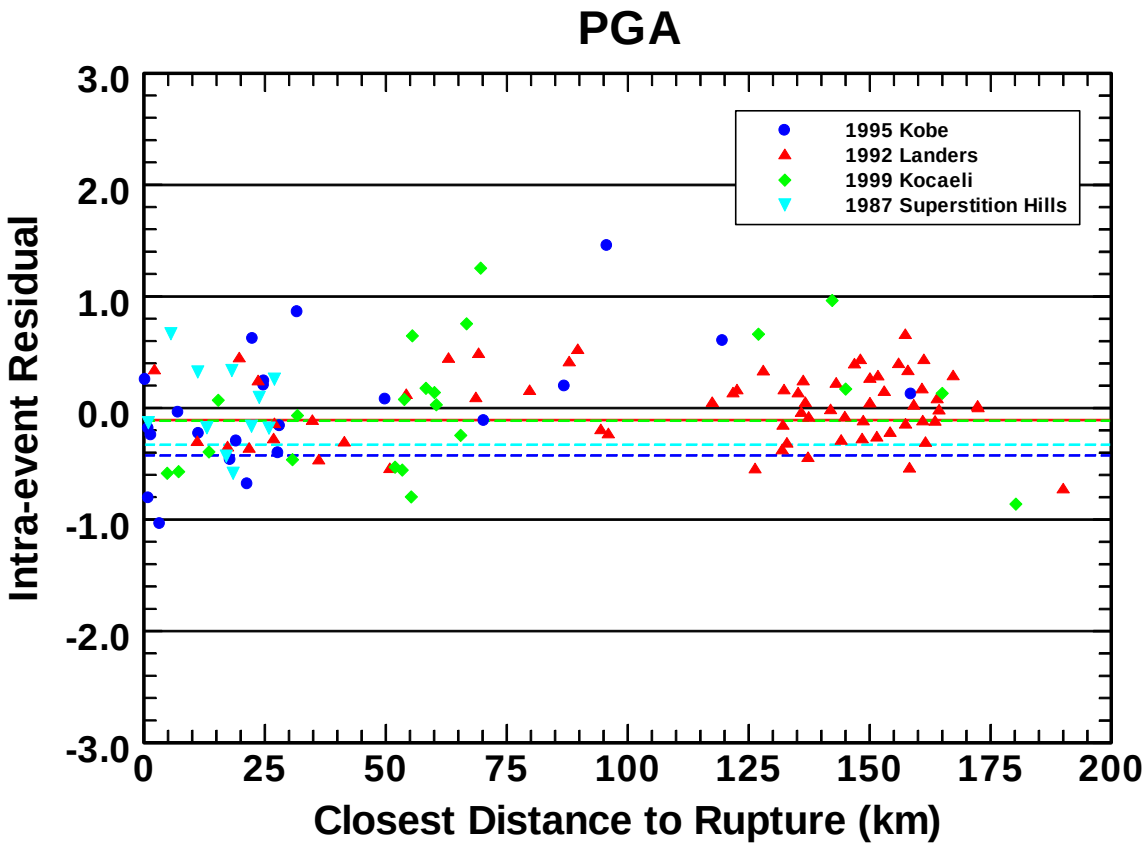

Figure1: Plot of the PGA intra-event residuals from the Campbell-Bozorgnia NGA model for the Kobe (blue circles), Landers (red triangles), Kocaeli (green diamonds), and Superstition Hills (cyan inverted triangles) earthquakes for $R_{RUP} \leq 200$ km. The horizontal dashed lines represent the adjusted baseline for these same earthquakes after accounting for the source term and the additional bias caused by disallowing over-saturation, where a negative value represents an under-prediction by the model.

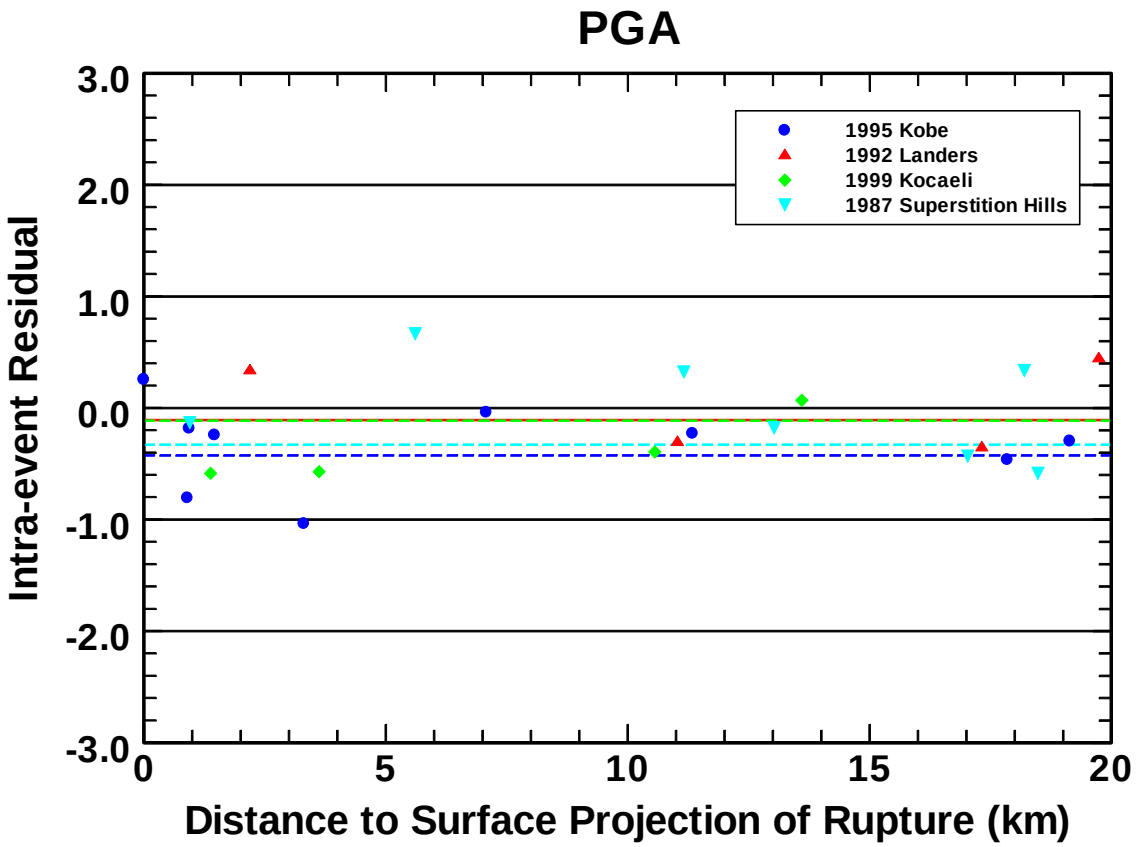

Figure2: Plot of the PGA intra-event residuals from the Campbell-Bozorgnia NGA model for the Kobe (blue circles), Landers (red triangles), Kocaeli (green diamonds), and Superstition Hills (cyan inverted triangles) earthquakes for $R_{JB} \leq 20$ km. The dashed lines are the same as in Figure1.

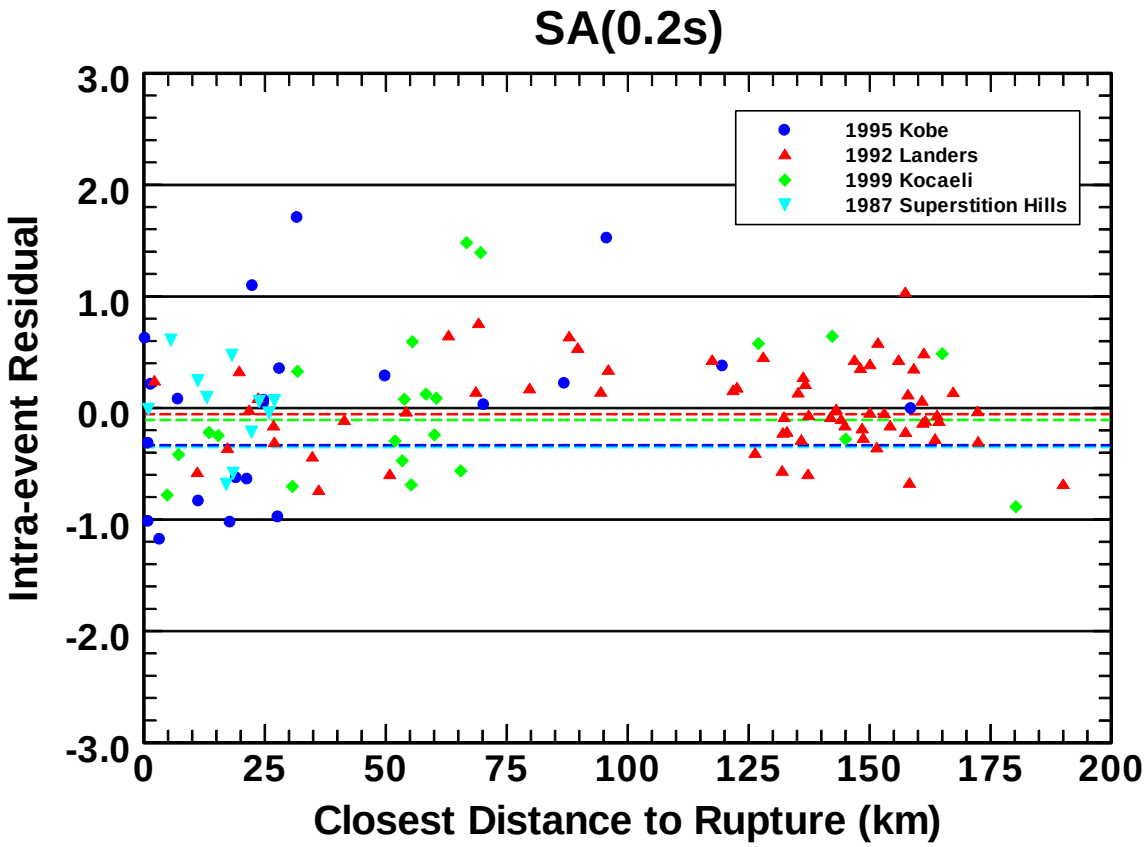

Figure3: Plot of the 0.2s spectral acceleration intra-event residuals from the Campbell-Bozorgnia NGA model for the Kobe (blue circles), Landers (red triangles), Kocaeli (green diamonds), and Superstition Hills (cyan inverted triangles) earthquakes for $R_{RUP} \leq 200$ km. The horizontal dashed lines represent the adjusted baseline for these same earthquakes after accounting for the source term and the additional bias caused by disallowing over-saturation, where a negative value represents an under-prediction by the model.

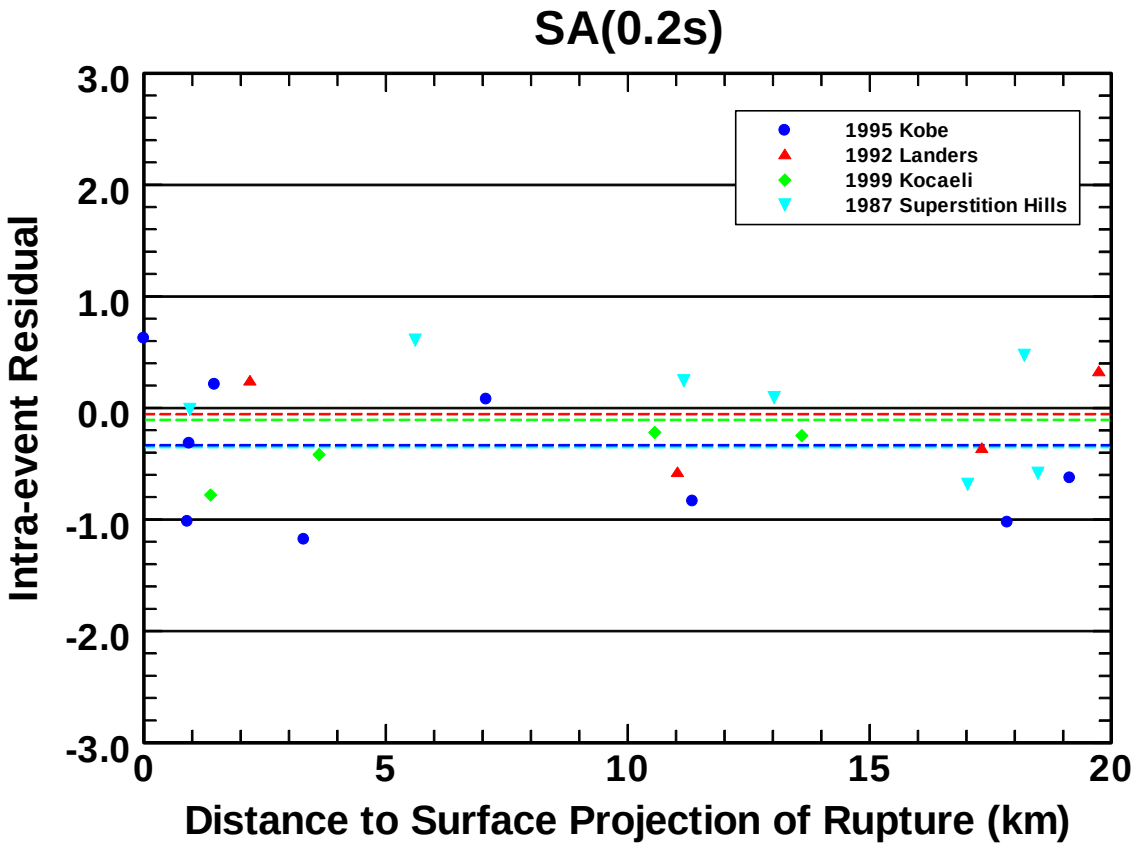

Figure4: Plot of the 0.2s spectral acceleration intra-event residuals from the Campbell-Bozorgnia NGA model for the Kobe (blue circles), Landers (red triangles), Kocaeli (green diamonds), and Superstition Hills (cyan inverted triangles) earthquakes for $R_{JB} \leq 20$ km. The dashed lines are the same as in Figure3.

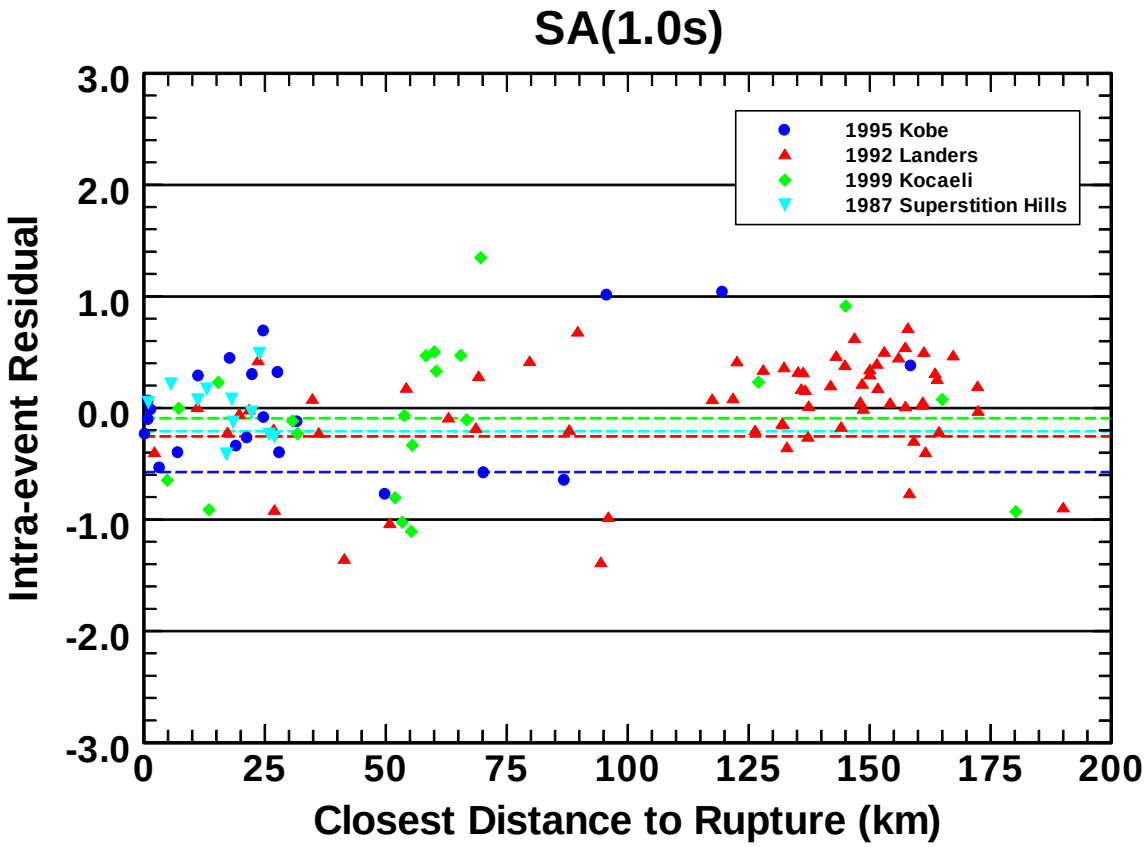

Figure5: Plot of the 1.0s spectral acceleration intra-event residuals from the Campbell-Bozorgnia NGA model for the Kobe (blue circles), Landers (red triangles), Kocaeli (green diamonds), and Superstition Hills (cyan inverted triangles) earthquakes for $R_{RUP} \leq 200$ km. The horizontal dashed lines represent the adjusted baseline for these same earthquakes after accounting for the source term and the additional bias caused by disallowing over-saturation, where a negative value represents an under-prediction by the model.

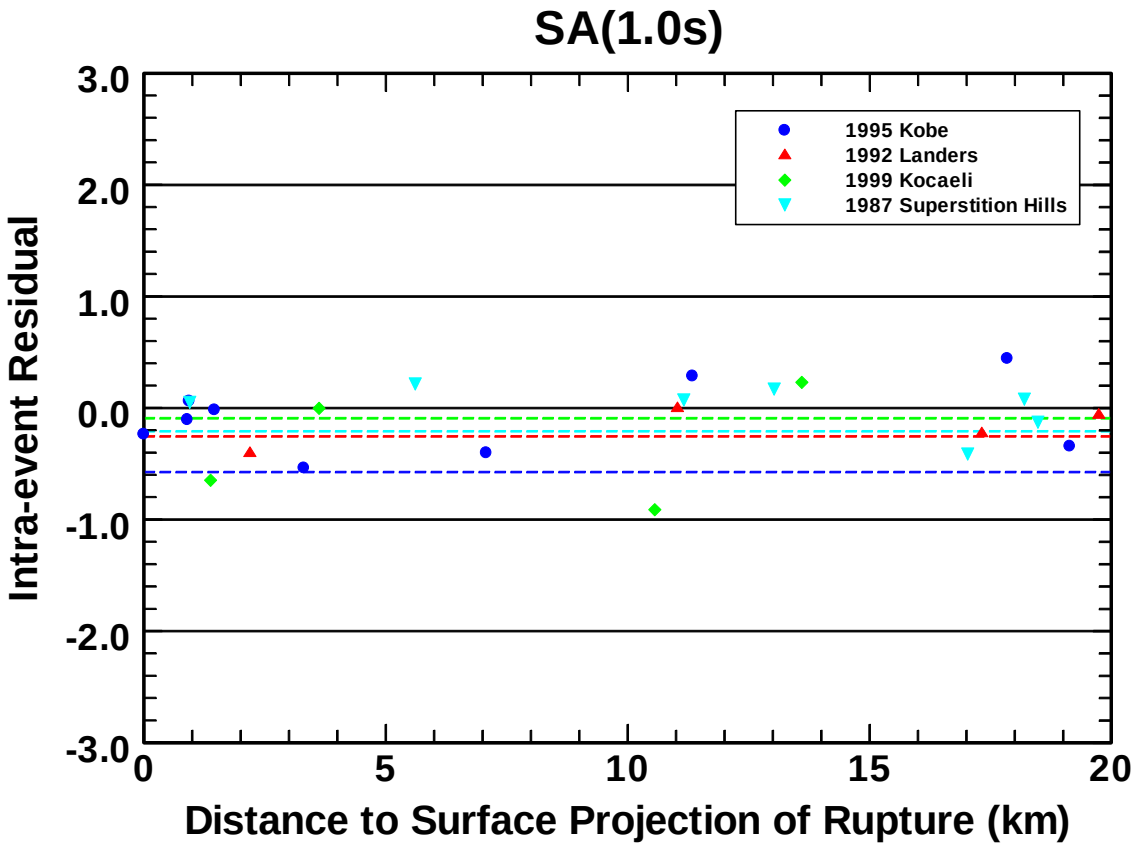

Figure6: Plot of the 1.0s spectral acceleration intra-event residuals from the Campbell-Bozorgnia NGA model for the Kobe (blue circles), Landers (red triangles), Kocaeli (green diamonds), and Superstition Hills (cyan inverted triangles) earthquakes for $R_{JB} \leq 20$ km. The dashed lines are the same as in Figure5.

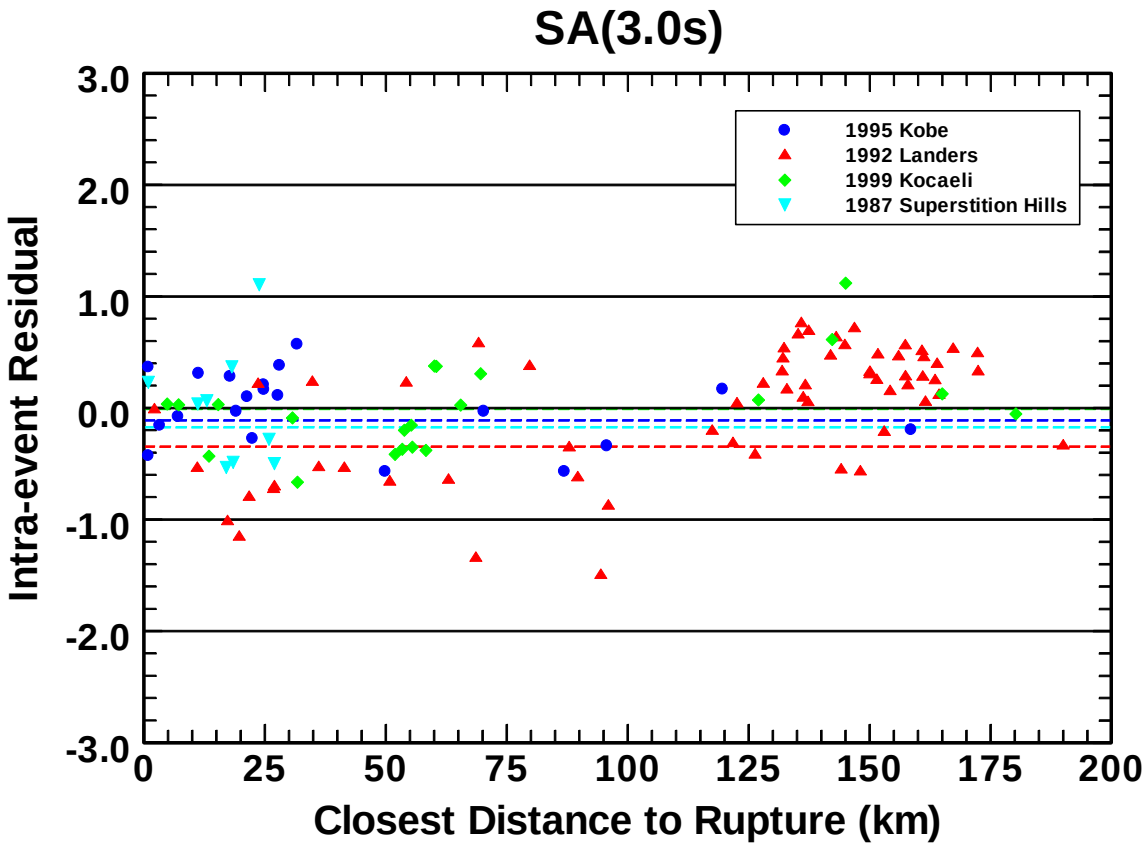

Figure7: Plot of the 3.0s spectral acceleration intra-event residuals from the Campbell-Bozorgnia NGA model for the Kobe (blue circles), Landers (red triangles), Kocaeli (green diamonds), and Superstition Hills (cyan inverted triangles) earthquakes for $R_{RUP} \leq 200$ km. The horizontal dashed lines represent the adjusted baseline for these same earthquakes after accounting for the source term and the additional bias caused by disallowing over-saturation, where a negative value represents an under-prediction by the model.

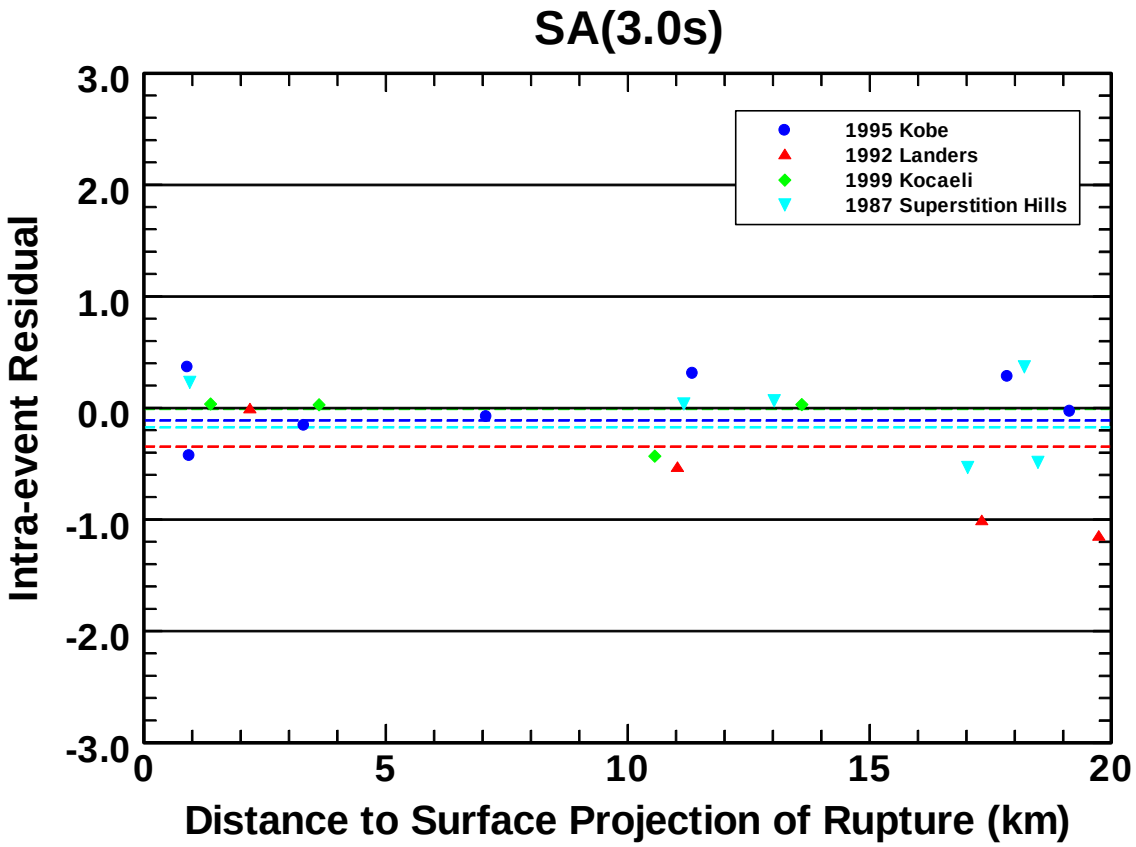

Figure8: Plot of the 3.0s spectral acceleration intra-event residuals from the Campbell-Bozorgnia NGA model for the Kobe (blue circles), Landers (red triangles), Kocaeli (green diamonds), and Superstition Hills (cyan inverted triangles) earthquakes for $R_{JB} \leq 20$ km. The dashed lines are the same as in Figure7.

ART FRANKEL'S QUESTION #4

Scaling with magnitude. For high frequencies (≥ 5hz), the spectral accelerations for close-in sites (< 10 km JB distance) are far higher for Superstition Hills, Landers, and Kobe earthquakes, than for the Kocaeli earthquake. Here I have chosen only strike slip earthquakes. This suggests there are regional differences in stress drop for strike slip earthquakes.

CHIOU-YOUNGS RESPONSE

We concur with the Campbell-Bozorgnia response that comparison of a few earthquakes is not really sufficient to derive general conclusion.

Following the Campbell-Bozorgnia response, plots of intra-event residuals for these four earthquakes are provided below to allow checking of systematic bias or trend. Close-in sites with JB distance less than 10 km are plotted in red.

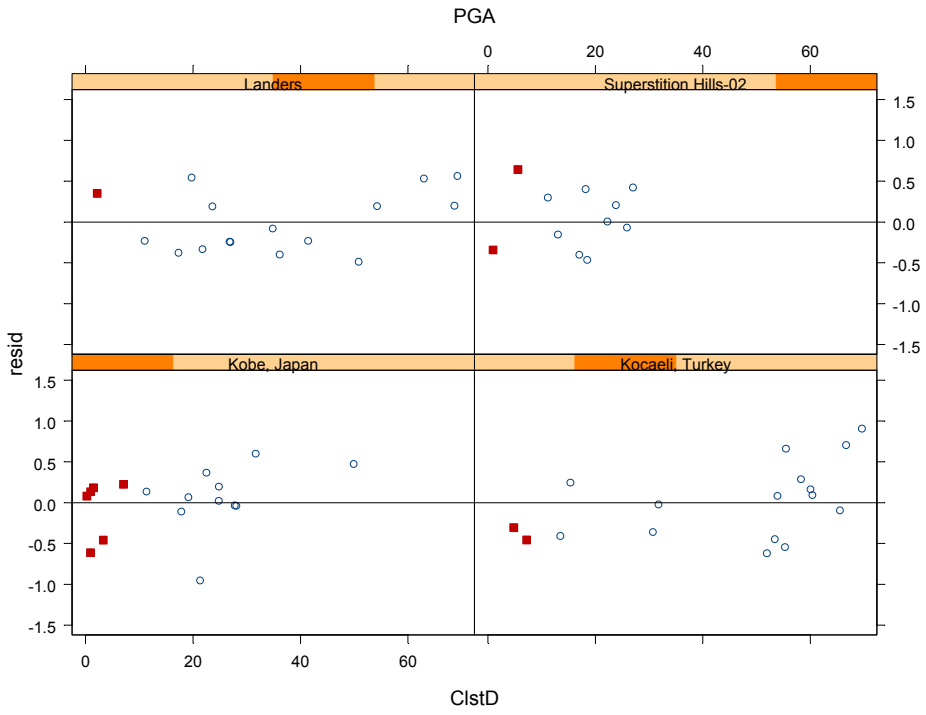

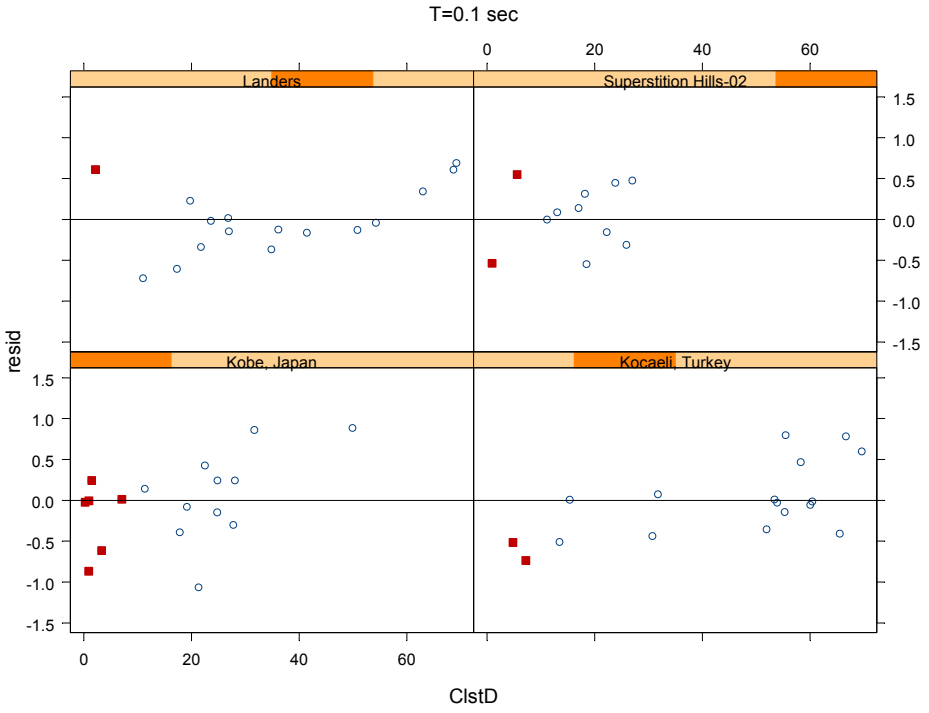
T=0.1 sec
Landers
Superstition Hills-02
Kobe, Japan
Kocaeli, Turkey
resid
ClstD

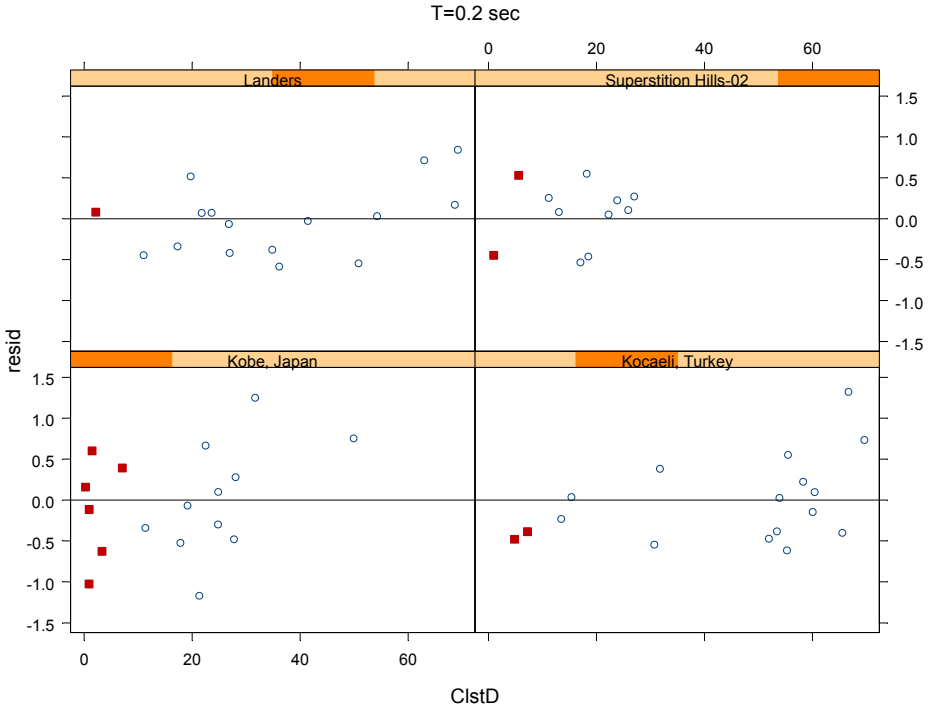
T=0.2 sec
Landers
Superstition Hills-02
Kobe, Japan
Kocaeli, Turkey
resid
ClstD

ART FRANKEL'S QUESTION #5

Changes from previous attenuation relations. There are substantial differences in ground motions from moderate-sized (M6.5) earthquakes at distances of 15-30 km between the NGA relations and the previous relations from the same authors (using the same site conditions). Since there doesn't appear to be very much new data in this magnitude and distance range, why the large differences? An egregious example is Boore-Atkinson (2006) compared to Boore, Joyner and Fumal (1996) for 1 sec S.A. for RJB=0 and M=6.5. There is about a factor of two decrease for BA (2006) compared to Boore et al. 1996. Why?

CAMPBELL-BOZORGNIA RESPONSE

Comparison of NGA and 2003 Models

Figures 3 and 4 in our May 31, 2006 report show that the predictions of PGA from our previous model (CB03) (Campbell and Bozorgnia, 2003) are very similar to those from our NGA model (CB06) for $V_{S30} = 760$ m/s (NEHRP B-C site conditions) and $\mathbf{M} = 6.5$ at all distances of interest. This is largely due to two important properties of the CB03 model: (1) it had a factor for adjusting predictions from generic rock ($V_{S30} = 620$ m/s) to NEHRP B-C site conditions, which avoided an over-prediction of NEHRP B-C ground motions and (2) it incorporated magnitude saturation, which was found to be an important property of the CB06 model based on a much larger dataset. Figures 11 and 12 show similar results for 1.0s spectral acceleration. The biggest differences between the two models are in the predictions for magnitudes of 7.0 and above, for which there was a paucity of data in the previous database. This issue is addressed in the next section.

Differences in Magnitude and Distance Scaling for $\mathbf{M} > 7.0$

The primary difference in the magnitude and distance scaling characteristics of the CB03 and CB06 models is at large magnitudes ($\mathbf{M} > 7.0$). Two factors cause this difference: (1) there was very little data to constrain this scaling in the previous model and (2) the previous model forced magnitude saturation while at the same time fixing the rate of attenuation to be independent of magnitude. This latter property caused the attenuation to be too flat in the critical 10–30 km distance range you mention and, as a result, force too much magnitude scaling at large magnitudes. This was possible because of the lack of data in this magnitude and distance range in the previous database. The relatively large number of recordings for large magnitudes in the NGA database, especially at near-source distances, clearly indicated that we needed to change our functional form to accommodate an attenuation rate that was dependent on magnitude (flattening with increasing magnitude), thus leading to the large difference in the two models at large magnitudes and short distances.

To show that this revision in our NGA model is supported by the available data, please refer to Figures 3–6 in our response to Mark Petersen's Question #2. These figures show the near-source intra-event residuals for our NGA model for PGA and SA at periods of 0.2, 1.0 and 3.0s, respectively. There are no trends in these data that would indicate a bias in our predictions over the critical 15–30 km distance range mentioned in your question. Of course, this only proves that that the attenuation rate is unbiased. There is still the issue of magnitude scaling, which can

decrease or increase the predictions at all distances for a given magnitude. This issue is discussed at length in response to Mark Petersen's Question #1 and will not be repeated here.

Conclusion

We find that the predictions of ground motion from our NGA (CB06) and previous (CB03) empirical ground motion models are similar for $\mathbf{M} = 6.5$ and $V_{S30} = 760$ m/s at all distances. This is due to two factors: (1) we incorporated magnitude saturation in our previous model as in our NGA model and (2) we provided a factor for adjusting ground motions from generic rock to NEHRP B-C site conditions in our previous model. Furthermore, the intra-event residuals from our NGA model show that our revised functional form that predicts magnitude-dependent attenuation is supported by the NGA database, even though it leads to large differences between our NGA and previous models at $\mathbf{M} > 7.0$.

ART FRANKEL'S QUESTION #5

Changes from previous attenuation relations. There are substantial differences in ground motions from moderate-sized (M6.5) earthquakes at distances of 15-30 km between the NGA relations and the previous relations from the same authors (using the same site conditions). Since there doesn't appear to be very much new data in this magnitude and distance range, why the large differences? An egregious example is Boore-Atkinson (2006) compared to Boore, Joyner and Fumal (1996) for 1 sec S.A. for RJB=0 and M=6.5. There is about a factor of two decrease for BA (2006) compared to Boore et al. 1996. Why?

CHIOU-YOUNGS RESPONSE

We believe the large differences noted by Art Frankel can be attributed to the lack of fit of the SAO97 model to the NGA dataset. After SAO97 is updated and the trend in residuals is removed, the median rock motion from the updated SAO97 model is not substantially different from CY2006's prediction. This is particularly true in the case of the 1-sec spectral acceleration. Details are given in the (new) Appendix F, which is attached in the following pages.

APPENDIX F

MODEL SAO2006 – UPDATE OF THE ATTENUATION MODEL OF SADIGH AND OTHERS (1997) USING THE PEER-NGA DATASET OF CHIOU AND YOUNGS (2006)

INTRODUCTION

Comparisons of predicted median motions from Chiou and Youngs (2006) (CY2006) to those from Sadigh and others (1997) (SAO97) are shown in Figures 39 to 44 of the main text. The large differences in high-frequency prediction at $M < 5$ are due to the differences in extrapolation from the differences in magnitude scaling in the two models. Comparisons of CY2006 model to the TriNet PGA data (Appendix D) suggest that extrapolation of CY2006 provides a better fit than extrapolation of SAO97.

It also appears there are substantial differences between the two models at $M > 5.5$. But we feel that the large differences noted in this straight comparison may be misleading because SAO97 was developed more than 10 years ago with less reliable data[1] and without the benefits of the ground-motion research (particularly in the area of soil response) accomplished in the last 10 years. To allow for a more meaningful comparison, we should at least update SAO97 to incorporate the current NGA dataset and implement a few modeling concept that do not require changing SAO97's functional form. This is the main objective of the analysis described in Appendix F. We'll focus our documentation on the rock model because agreement between the two soil models is better than agreement between the two rock models.

In this Appendix, we update the SAO97 attenuation model using the same functional form as SAO97. The model coefficients are modified in order to improve fits to the NGA data. This update effort is not aimed to provide a complete attenuation model that can be used in engineering practice. Rather, it is used only to understand the substantial difference in "rock" motion between CY2006 and SAO97.

We'll show that median predictions of the updated SAO97 model are no longer substantially different from those of CY2006. We attribute the good agreement to the improved fits of updated SAO97 to NGA data.

STRONG-MOTION DATASET AND THE EQUIVALENT V_{S30} FOR ROCK AND SOIL CONDITIONS

We use the same dataset that was selected and used by Chiou and Youngs (2006). The CY2006 dataset consists of 1087 data points from mainshocks at distances less than 70 km. It's important to note that, although the recent large-magnitude data from Taiwan and Turkey are included in this dataset, the bulk of data still comes from California, as shown on Figure F1a.

[1] For example, spectral shape data, instead of spectral acceleration data, were used in the development of SAO97. Also, the old site classification has undergone extensive revision and as a result some rock sites are re-classified as soil sites, and vice versa.

As SAO97, the updated attenuation model is developed for two general site conditions of soft rock and deep soil. The soft rock condition consists of Geomatrix site class A (very thin soil, < 5m, over rock) and B (shallow stiff soil, 5 to 20 m, over rock). The soil condition consists of Geomatrix site class C and D (deep firm soil conditions). Site condition of each recording station is assigned according to the Geomatrix site class given in the PEER-NGA database.

Geometric mean of V_{S30} for the rock and soil categories are listed in Table F1 and the histograms are shown on Figures F1b and F1c. Because the weak-motion soil response in CY2006 is modeled by $ln(V_{S30}/1130)$, we'll use the geometric mean of V_{S30} as the point of comparison with CY2006. The point of comparison is slightly different between PGA and 1-sec period because their V_{S30} distributions are different due to the minimum usable frequency requirement. However, the difference is not large enough to make a difference in the comparison and we'll use 500 m/sec as a compromise[1].

We also want to point out that the V_{S30} distribution of California rock PGA data is bimodal with a geometric mean of 485 m/sec, lower than the full-set value of 505 m/sec. The first mode of the rock data is similar to the soil data. One explanation of this observation is that many of these rock sites happen to be within geological units (such as Qal) where Geomatrix classification is ambiguous in the absence of reliable information on soil depth.

As in CY2006, FW/HW sites are included in the regression analysis. Excluding FW/HW sites will impact the style of faulting effect for reverse event in a manner similar to that described in the 'Modeling Steps' section of Chiou and Youngs (2006).

MODEL EQUATION:

We combine the two model equations for rock and soil of SAO97 and add the random effect of earthquakes ($\tau \cdot z_i$) to the equation. One could consult the paper by Sadigh and others (1997) to connect the new equation with the two original equations. The model equation is

$$
\begin{aligned}
ln(y_{ij}) = \\
& Z_r\left(C^r_1 + C^r_2 M_i + C^r_{2a}(M_i - 6.5,0)_{min} + C^r_3(8.5 - M_i)^{2.5} + C^r_4\, ln\left(R_{rup_{ij}} + exp\left(C^r_5 + C^r_6 M_i + C^r_{6a}(M_i - 6.5,0)_{min}\right)\right)\right) \\
& + Z_s\left(C^s_1 + C^s_2 M_i + C^s_3(8.5 - M_i)^{2.5} + C^s_4\, ln\left(R_{rup_{ij}} + exp\left(C^s_5 + C^s_6 M_i + C^s_{6a}(M_i - 6.5,0)_{min}\right)\right)\right) \\
& + C_{RV} Z_{RV} \\
& + \tau \cdot z_i + \sigma \cdot z_{ij}
\end{aligned}
$$

, where Z_r is the rock condition factor equal to 1 if site is on rock and 0 if otherwise. Z_s is the soil condition factor equal to 1 if site is on soil and 0 if otherwise. Z_{RV} is the reverse faulting factor equal to 1 if $30^o \le \lambda \le 150^o$ and 0 if otherwise.

[1] We used Vs=520 m/sec as the point of comparison in Figures 39 to 44 of our main text. We'll update these figures to Vs=500m/sec when we revise the report in the future.

MODEL DEVELOPMENT:

Followings are descriptions of model development for *PGA* and pseudo spectral acceleration at 1-seconds period. Each model is developed in multiple steps. For convenience of reference, each step is labeled by affixing a lower case letter to "SAO2006." (e.g. SAO2006.a, SAO2006.b, etc.).

Peak Ground Acceleration (Spectral Acceleration at the Period of 0.01 Sec)

Step #1 SAO2006.a: Mixed-Effects Version of SAO97:

In Step #1 all fixed-effects coefficients are set to the SAO97 values, except for coefficients C^r_1, C^s_1, and C_{RV}. The resulting coefficients C^r_1 and C^s_1 are nearly identical to those of SAO97 (not a coincidence?). SAO2006.a is thus effectively a mixed-effects version of SAO97. Models SAO2006.a and SAO97 can be used interchangeably as far as predicting median PGA goes.

The magnitude scaling of SAO2006.a (and SAO97) is appropriate for the NGA dataset (Figure F2a), therefore modifications of coefficients C_2^r, C_{2a}^r, and C_2^s are not necessary. This finding is consistent with the c_2 value in CY2006.

SAO2006.a also adequately models the distance attenuation of soil PGA (Figure F2b). But, under-prediction of rock PGA is noted at $R_{RUP} > 50$km. A hint of over-prediction of rock PGA in the distance range of 5 and 15 km is also noted.

Median predictions from SAO2006.a are shown in Figure F2c. There are substantial differences between SAO2006.a (SAO97) and CY2006. These discrepancies were also noted by Art Frankel (Comment #5 of his June-27-2006 list) in his review of the NGA model.

Step # 2 (SAO2006.b):

The lack of fits noted in Step #1 suggests that an increase (less negative in value) of coefficient C^r_4 is needed. There is another more compelling reason to modify C^r_4. A large difference between C^r_4 and C^s_4, such as that seen in CY2006.a and SAO97, implies strong distance dependence in soil amplification even at large distances where soil response is linear and the soil amplification factor is expected to depend weakly on distance. To hamper the continuous increase of soil amplification with distance, we impose the equality constraint $C^r_4 = C^s_4$ and modify coefficients C^r_5 and C^r_5 to carry the nonlinear response at short distances. Furthermore, with the equality constraint, a large increase of C^r_4 is expected and, consequently, the resulting near-source magnitude scaling would be stronger than the level of near saturation in SAO2006.a (and SAO1997). But such a stronger near-fault magnitude scaling is not supported by the NGA dataset. On the contrary, in lights of the low motions recorded from the recent Turkey and Taiwan earthquakes, one could even make the case for negative near-fault magnitude scaling (i.e. over-saturation). We think over-saturation is such a dramatic change in modeling concept and in engineering practice that its acceptance requires more careful studies. Therefore, we keep the near-fault magnitude saturation by imposing C^r_6=1.1/ C^r_4 and C^s_6=1.0/ C^s_4. Changes to C^r_6 and C^s_6 also trigger the needs to modify near-fault magnitude scaling for M < 6.5 (C^r_{6a} and C^s_{6a}).

In summary, all coefficients except C^r_2 and C^s_2 are modified in this step, with coefficients C^s_4, C^r_6 and C^s_6 being constrained by the conditions explained above. The resulting coefficients for soil are close to the old values in SAO97, as expected. The new estimate of C^r_4 is -1.6, close to the old soil value of -1.7 in SAO97. We notice better fits to data in the distance range of 5 km ≤ R_{RUP} ≤ 15 km and R_{RUP} > 50 km compared to SAO2006.a (Figure F3.a). We also see a slight drop in intra-event standard error.

Median predictions from SAO2006.b are shown on Figure F3.b. Also shown on Figure F3.b are median predictions from CY2006 (solid lines). The discrepancies of rock predictions noted in the previous step and by Art Frankel are now much smaller. For M=6.5, the magnitude mentioned in Art's comments, SAO2006.b and CY2006 are within 5% of each other.

Note that SAO2006.b still has problem with the near-fault prediction for M = 5.5 and smaller. This problem can be fixed by implementing a better magnitude scaling for lower M, such as the one used by CY2006. But we feel the analysis so far have already met the goals stated in the introduction. Therefore we will stop here and move on to the model development for 1-seconds spectral acceleration.

Spectral Acceleration at the Period of 1 Sec

Model development of the 1-sec spectral acceleration is similar in concept to that of PGA, but the process is a lot simpler because the main update is related to magnitude scaling, which does not significantly affect other coefficients.

Step #1 (SAO2006.a:, A Mixed-Effects Version of SAO97:

This is the first of a sequence of regression analysis. All fixed-effects coefficients are set to the SAO97 values, except for coefficients C^r_1, C^s_1, and C_{RV}. The resulting coefficients C^r_1 and C^s_1 are nearly identical to those of SAO97 (another coincidence?). SAO2006.a is effectively a mixed-effects version of SAO97. SAO2006.a and SAO97 can be used interchangeably as far as predicting median motion goes.

We notice a lack of fit to inter-event terms (Figure F4a), suggesting SAO97's magnitude scaling for 1-sec period needs to be revised. The predicted median rock motions differ from those of CY2006 by about 20% to 50% (Figure F4b). This large discrepancy is also noted and questioned by Art Frankel (2006) in his review of the NGA model.

Step #2 (SAO2006.b):

To improve the deficiency in magnitude scaling, coefficients C^r_3 and C^s_3 are added to the list of free coefficients and the regression is repeated. The resulting inter-event terms are shown on Figure F5a. The magnitude trend noted in Step #1 is not present. As a result of improved fits, the inter-event standard error (τ) is about 16 % smaller than the value of previous step.

The predicted medina motion is shown on Figure 5b. Discrepancy with CY2006 in the distance range of 10 km ≤ R_{RUP} ≤ 50 km and M ≥ 5.5 is now less than 5%. There are still large differences between the two models at R_{RUP} < 10 km and at R_{RUP} > 70 km. We notice that

SAO2006.b under-predict data at distances $R_{RUP} < 10$ km (Figure F5c). Adjustment to coefficients C^r_5 and C^s_5 is thus conducted next to improve the overall fits at $R_{RUP} < 10$ km.

Step #3 (SA2006.c):

In this step, coefficients C^r_5 and C^s_5 are added to the list of free coefficients. The resulting model significantly improves the fits at $R_{RUP} < 10$ km (Figure F6b) and, as a result, the agreement in median rock prediction with CY2006 (Figure 6a) is also much closer than the agreement achieved in previous steps.

CONCLUSIONS

We've shown that median predictions of the updated SAO97 model are not substantially different from those of CY2006. We attribute the good agreement to the improved fits of updated SAO97 to NGA data.

Table F1a. Summary Statistics of V_{S30} in CY2006's PGA dataset.

Geomatrix Site Class	Arithmetic Mean of Vs_{30} (m/sec)	Geometric Mean of Vs_{30} (m/sec)	Number of Data
Soft Rock (A+B)	543	506	419
Deep Soil (C+D)	371	316	633
E	212	204	35

Table F1b. Summary Statistics of Vs30 in CY2006's 1-Sec dataset.

Geomatrix Site Class	Arithmetic Mean of V_{S30} (m/sec)	Geometric Mean of Vs_{30} (m/sec)	Number of Data
Soft Rock (A+B)	537	500	407
Deep Soil (C+D)	328	315	625
E	212	204	35

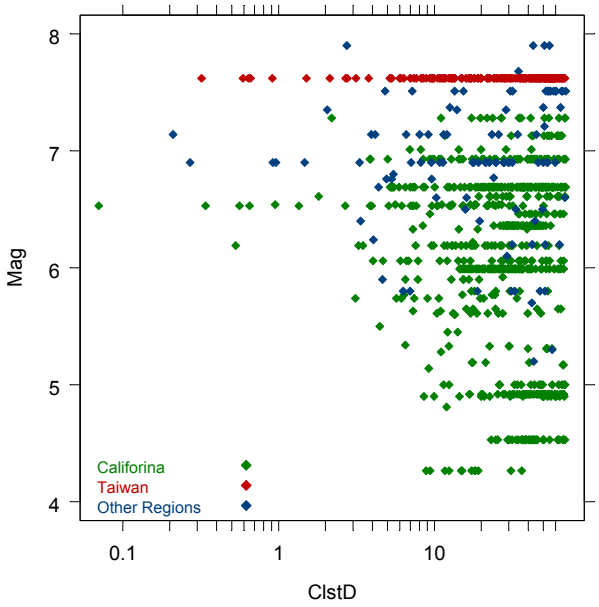

Figure F1a: Magnitude-distance-region distribution of data used in the development of CY2006 and in this study.

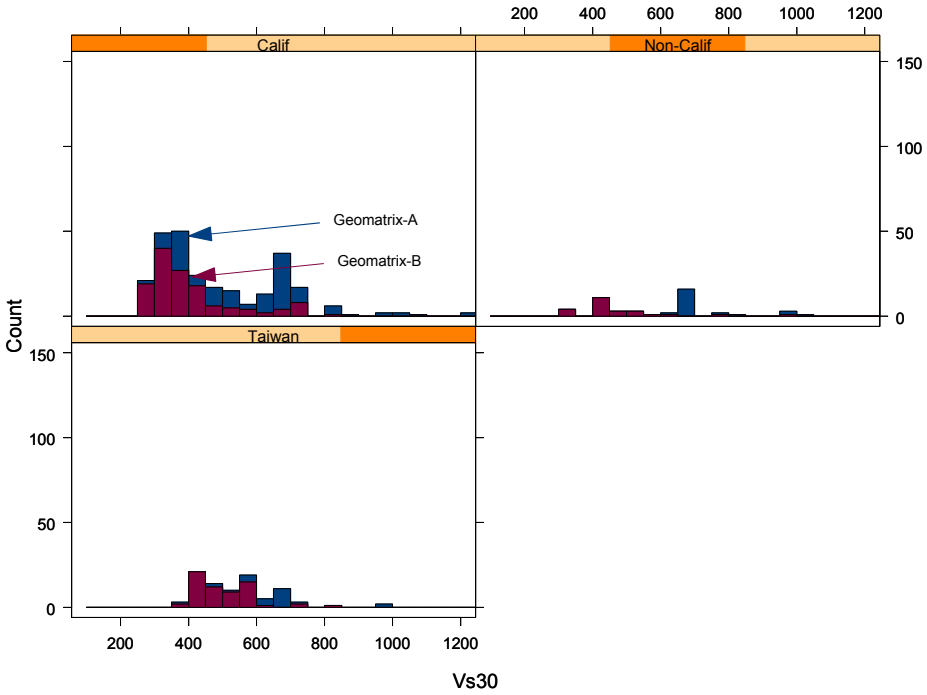

Figure F1b: Vs30 histogram of rock (Geomatrix A+B category) PGA data.

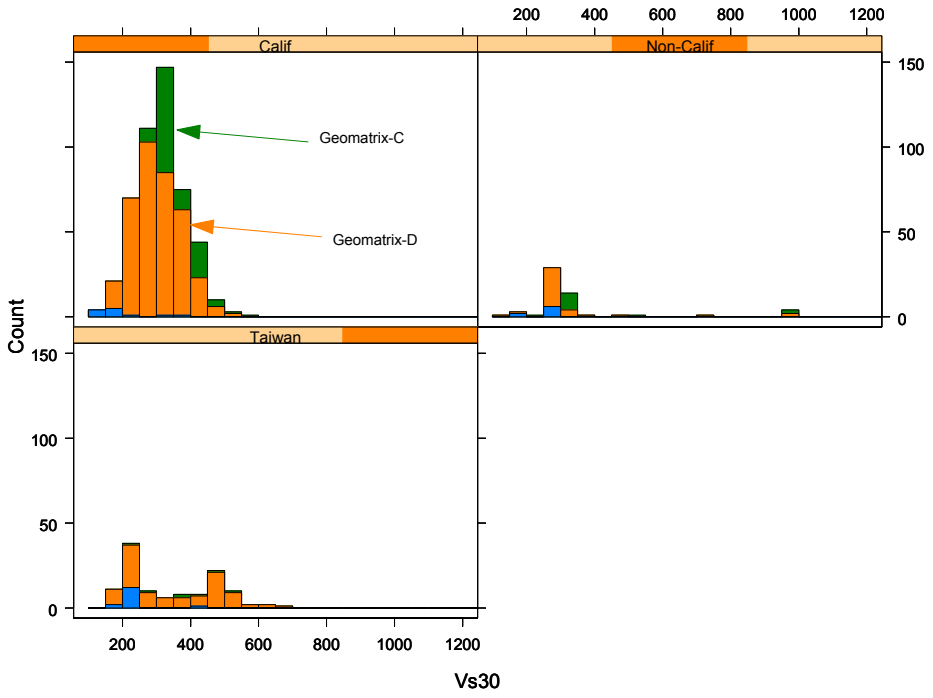

Figure F1c: Vs30 histograms of soil (Geomatrix C+D) PGA data. Geomatrix's E category is denoted by the blue color.

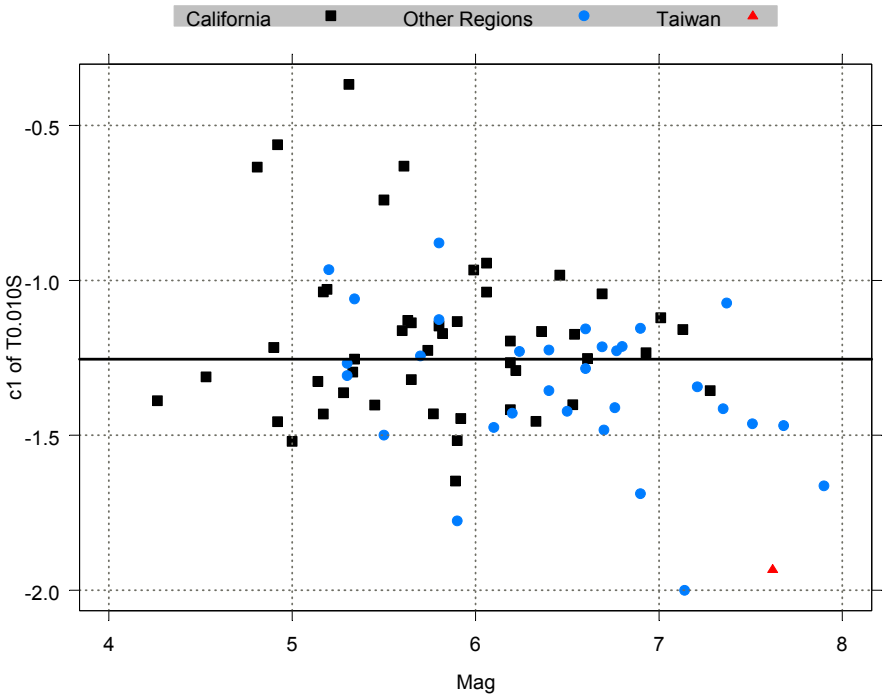

Figure F2a: The random earthquake effects of PGA from SAO2006.a. The horizontal line denotes the population mean. Difference between population mean and individual value represents the random inter-event residual.

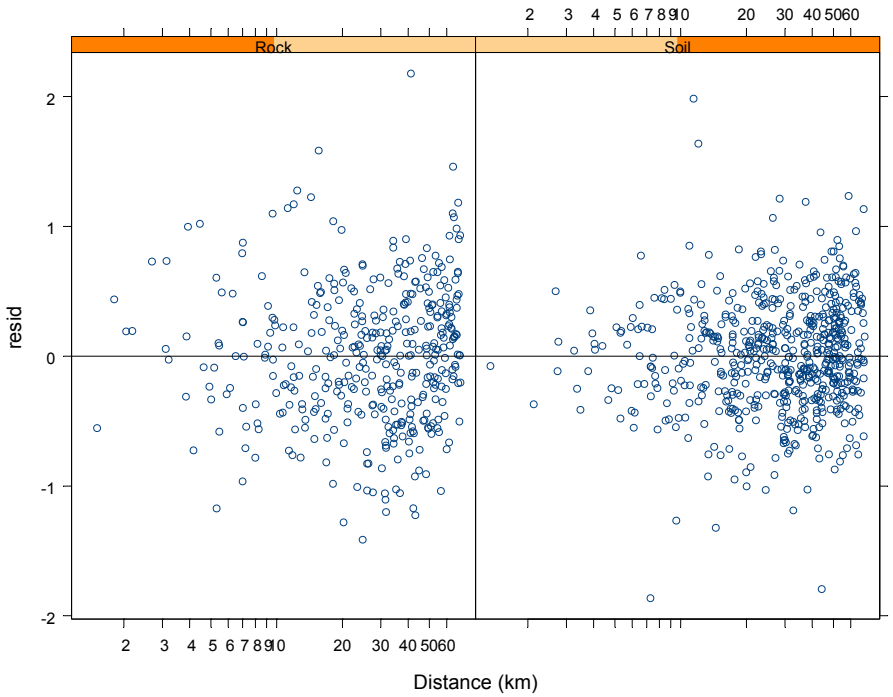

Figure F2b: Intra-event residuals from SAO2006.a for PGA.

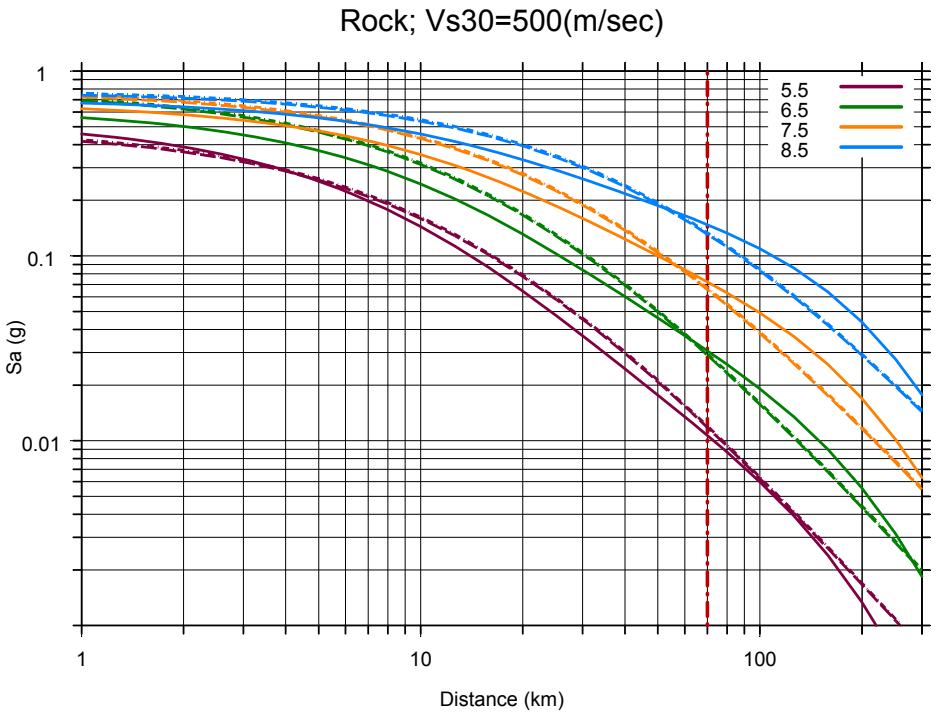

Figure F2c: Comparison of predicted median rock PGA by CY2006 (solid curves), SAO2006.a (dotted-dashed lines), and SAO97 (dashed lines). The read vertical line denotes the cut-off distance of the dataset.

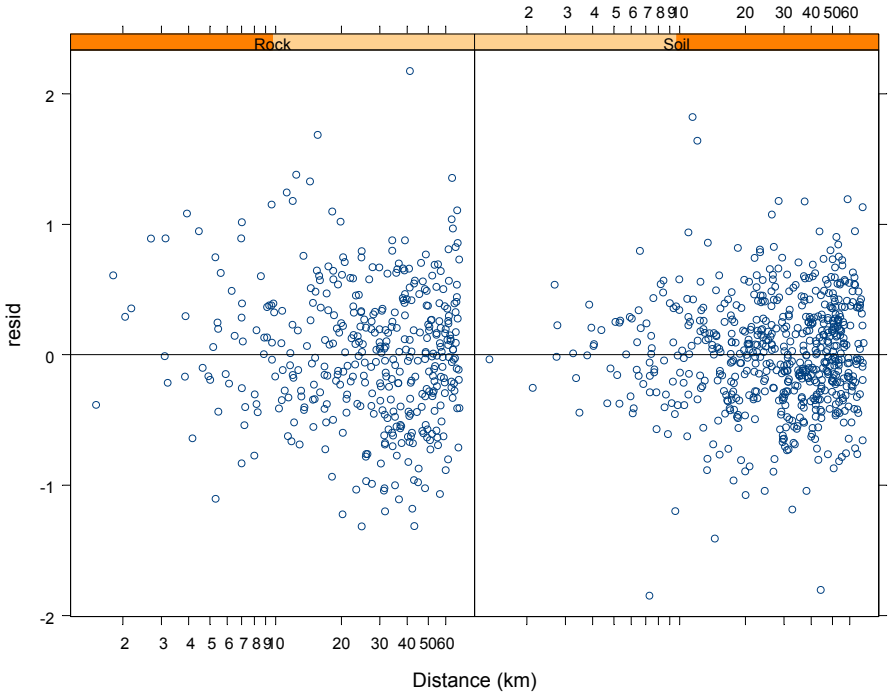

Figure F3a: Intra- event residuals from SAO2006.b for PGA.

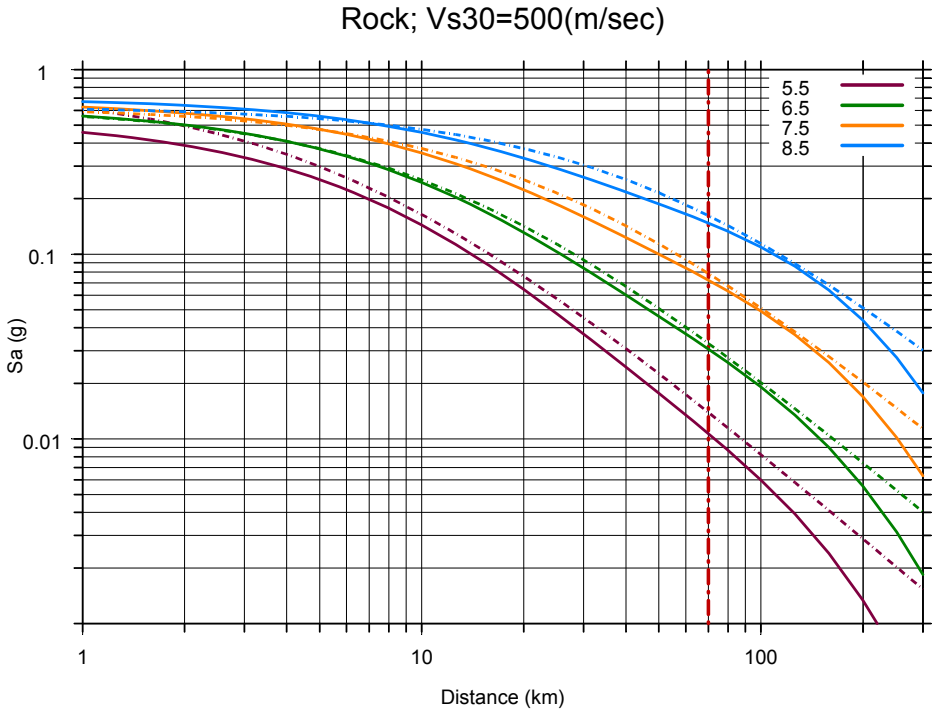

Figure F3b: Comparison of predicted median rock PGA by CY2006 (solid curves) and SAO2006.b (dotted-dashed lines). The red vertical line denotes the cut-off distance of the dataset.

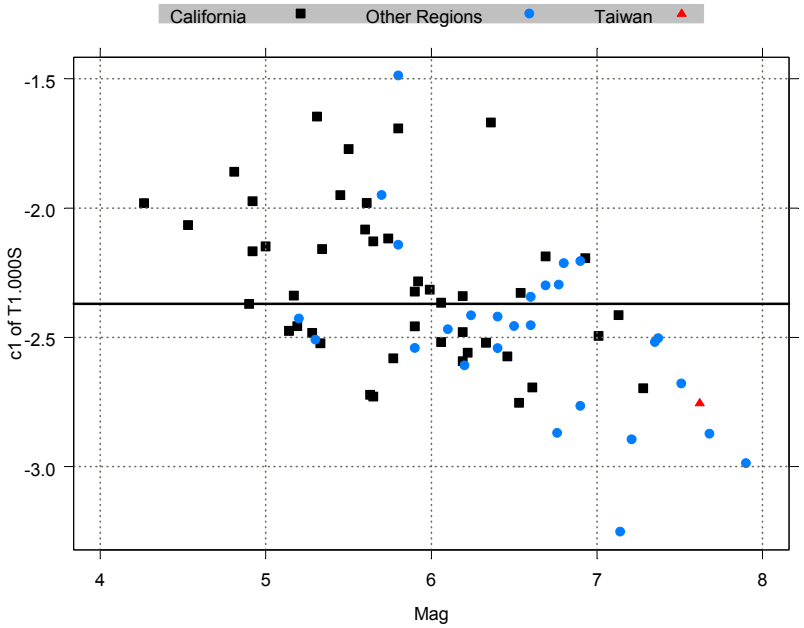

Figure F4a: Random earthquake effects of the 1-sec spectral acceleration from SAO2006.a. The horizontal line denotes the population mean. Difference between population mean and individual value represents the random inter-event residual.

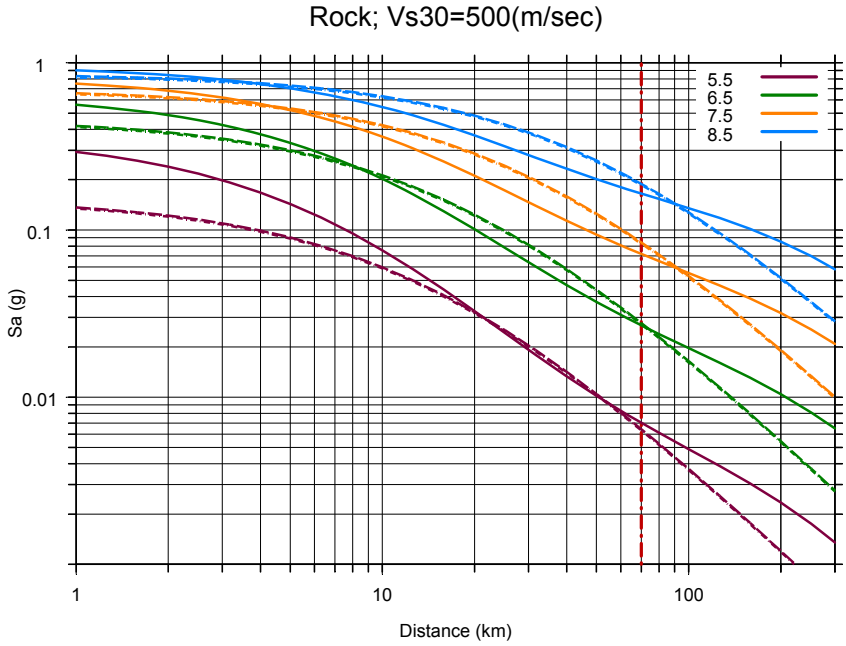

Figure F4b: Comparison of 1-sec rock spectral accelerations predicted by the CY2006 model (solid curves), by the baseline model SAO2006.a (dotted-dashed curves), and SAO97 (long dashed curves). The read vertical line indicates the cut-off distance of the dataset.

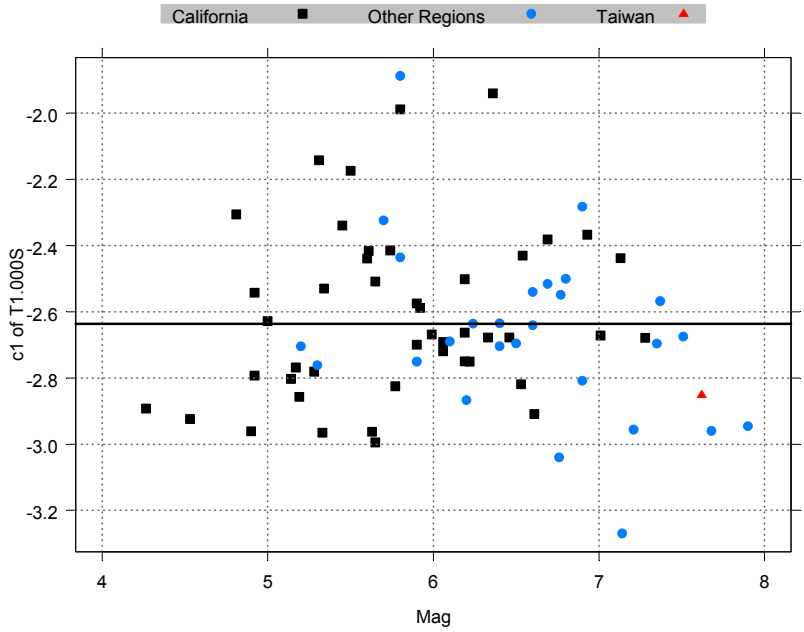

Figure F5a: Random earthquake effects of the 1-sec spectral acceleration from SAO2006.b. The horizontal line denotes the population mean. Difference between population mean and individual value represents the random inter-event residual.

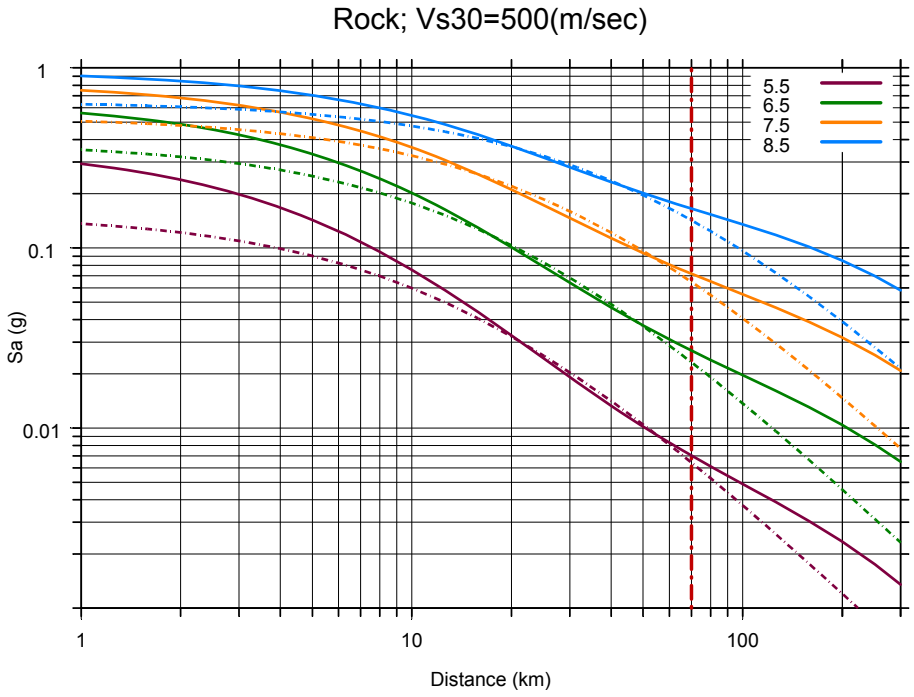

Figure F5b: Comparison of predicted median 1-sec spectral acceleration by CY2006 (solid curves) and by SAO2006.b (dotted-dashed curves) for soft rock condition. The red vertical line indicates the cut-off distance of the dataset.

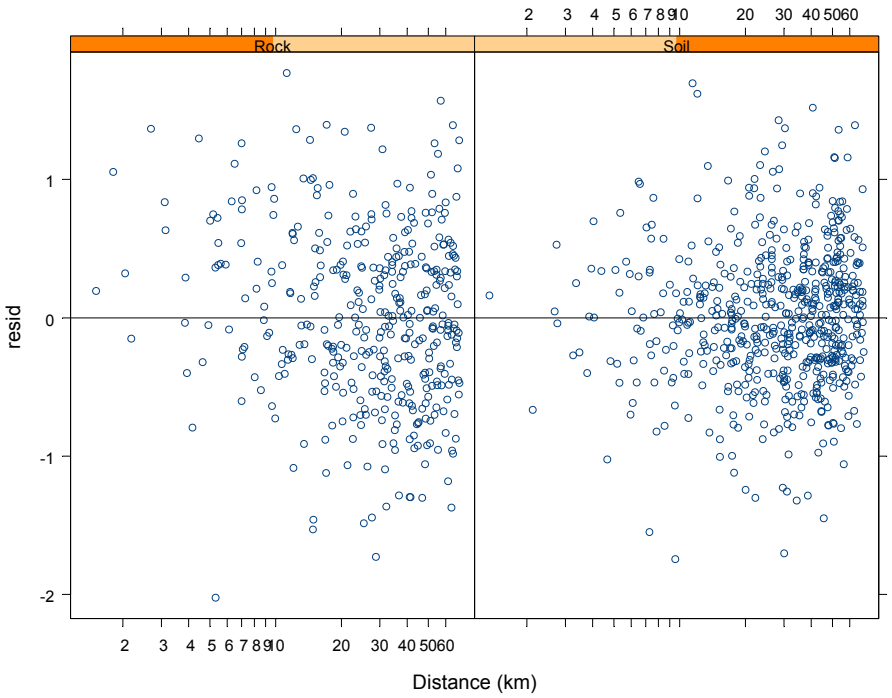

Figure F5c: Intra- event residuals from SAO2006.b for 1-sec spectral acceleration.

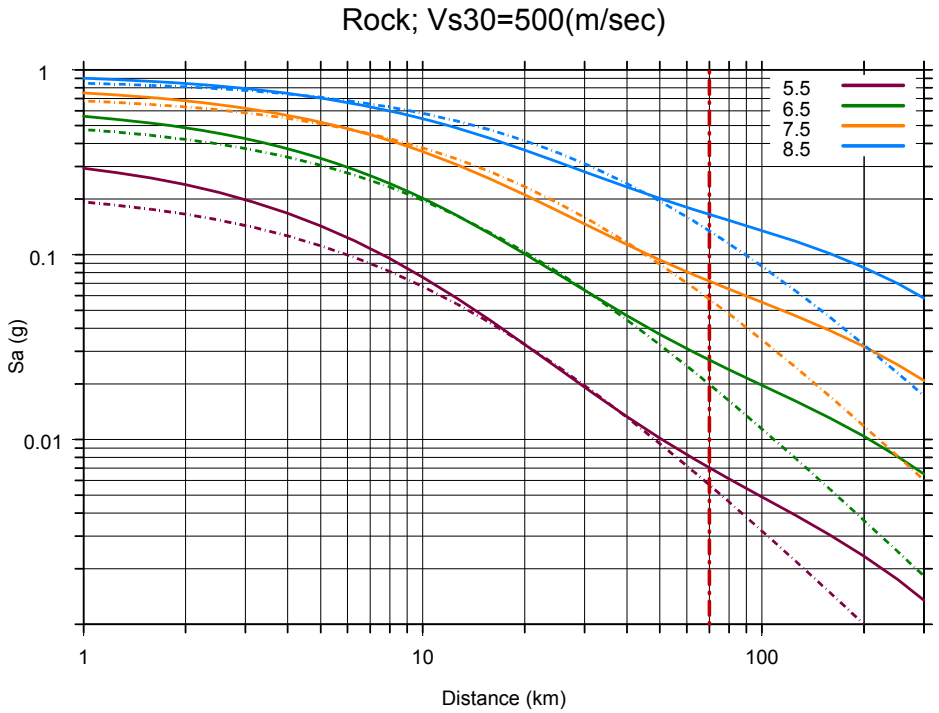

Figure F6a: Comparison of predicted median 1-sec spectral acceleration by CY2006 (solid curves) and by SAO2006.c (dotted-dashed curves) for soft rock condition. The read vertical line indicates the cut-off distance of the dataset.

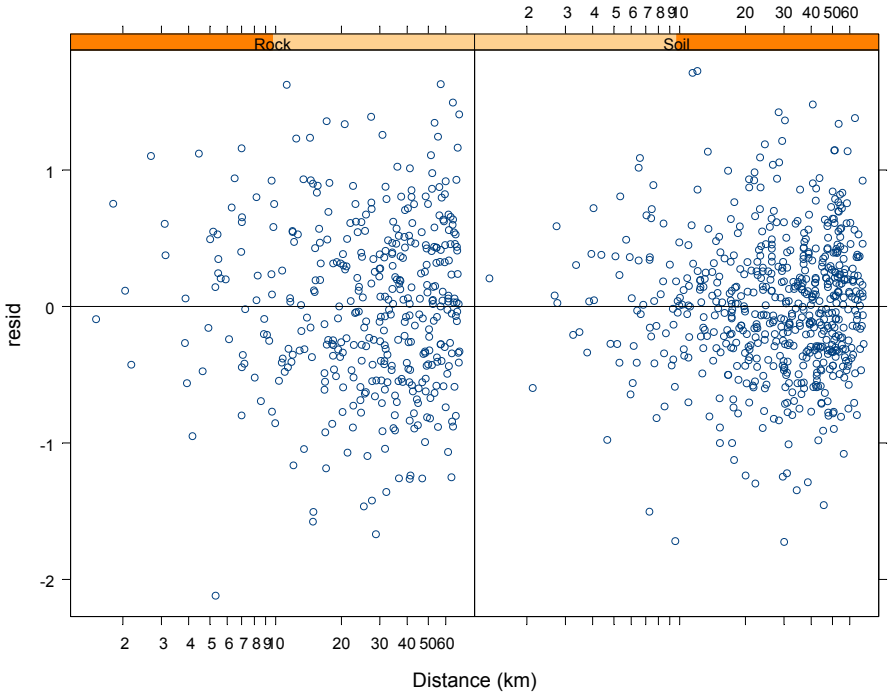

Figure F6b: Intra-event residuals from SAO2006.c for 1-sec spectral acceleration.

ART FRANKEL'S QUESTION #6

Site Amplification. It appears that most of the NGA developers used a similar functional form for the site amplification. How much of the coefficients are derived from numerical modeling and how much are from actually fitting the data? Obviously, using the same functional forms can cause underestimation of the uncertainty.

ABRAHAMSON-SILVA RESPONSE

All of the developers used V_{S30} for shallow site classification. We consider this to be a major advancement, because it allows an unambiguous use of the NGA ground motion models with the NEHRP site categories. This ambiguity has led to unintentional biases in the USGS national seismic hazard maps. For all four models, the linear amplification is modeled as a linear function of the logarithm of V_{S30}. So, the linear amplification does use the same functional form for all of the models. This functional form has been used successfully in both the United States and Japan by many authors to model linear site-response effects.

As you have noted, all of the developers also include non-linear site response. The degree of non-linearity depends on the value of V_{S30} and the level of the input rock motion. The general form of all four models is:

$$Amp = \begin{cases} a \ln\left(\frac{V_{S30}}{V_{ref}(T)}\right) & for\, V_{S30} \geq V_{ref}(T) \\ a \ln\left(\frac{V_{S30}}{V_{ref}(T)}\right) + b(T, V_{S30}) \ln\left(\frac{GM_{rock} + c(V_{S30}, T)}{d(T)}\right) & for\, V_{S30} < V_{ref}(T) \end{cases}$$

Note: Abrahamson & Silva and Campbell & Bozorgnia include an extra term that depends on the ground motion so that the model will approach linear dependence as the value of V_{S30} approaches V_{lin}. This extra term is left out of this general form to make the comparison among the various models easier.

The above equation shows that all of the developers include a non-linear term that depends on the log of the ground motion computed on rock. The V_{S30} dependence of the non-linearity enters the model in either the b-term or the c-term. Table 1 shows how the four sets of developers have modeled the non-linearity for higher ground motion levels (e.g. PGA_{rock} > 0.1g). One key difference is that Chiou & Youngs used the spectral acceleration on rock to define the ground motion level for non-linearity, whereas, the other developers used PGA on rock.

The various developers used different approaches for estimating the non-linear terms. All of the models used some constraints other than the NGA data set. These approaches are compared in Table 2.

Table 1. Models used for the non-linear site response for the higher level of input rock motion.

	b(T,V_{S30})	c(T,V_{S30})	d(T)	GM_{rock}
Abrahamson & Silva	b(T)	$c\left(\frac{V_{S30}}{V_{lin}(T)}\right)^n$	1	PGA_{1100}
Campbell & Bozorgnia	b(T)	$c\left(\frac{V_{S30}}{V_{lin}(T)}\right)^n$	1	PGA_{1100}
Boore & Atkinson	$b_1 \quad for V_{S30} < V_1$ $(b_1 - b_2)\frac{\ln\left(\frac{V_{S30}}{V_2}\right)}{\ln\left(\frac{V_1}{V_2}\right)} \quad for V_1 < V_{S30} < V_2$ $b_2 \frac{\ln\left(\frac{V_{S30}}{V_{ref}}\right)}{\ln\left(\frac{V_2}{V_{ref}}\right)} \quad for V_2 < V_{S30} < V_{ref}$ $0.0 \quad for V_{ref} < V_{S30}$	0	d (0.1g)	PGA_{760}
Chiou & Youngs	$\phi_2(T)\exp\{\phi_3(T)(V_{S30} - 360)\}$	$\phi_4(T)$ (0.1g for PGA)	$\phi_4(T)$	SA_{1130}(T)

Table 2. Methods for Estimating Site Response Coefficients

	Linear Term	Non-linear Terms
Abrahamson & Silva	Estimated from NGA data	All coefficients (b(T), c, n, V_{lin}(T)) constrained from Silva (2004) site response modeling
Campbell & Bozorgnia	Estimated from NGA data	All coefficients (b(T), c, n, V_{lin}(T)) constrained from Silva (2004) site response modeling
Boore & Atkinson	Estimated from NGA data	All coefficients (b_1, b_2, V_1, v_2, V_{Ref}, d) constrained from the Choi and Stewart (2005) model
Chiou & Youngs	Estimated from NGA data	Only coefficient ϕ_4(T) is constrained and its reasonableness is verified against Silva's simulations (2004). Other coefficients (ϕ_2(T), ϕ_3(T)) are estimated from the NGA data.

While all of the developers included non-linearity in their models, they did so in different ways. Even those that used the same non-linear site term found different linear site coefficients (see the response to Vladimir Graizer's Question #5). Therefore, in conclusion, we believe that the difference in non-linear site terms and in linear site coefficients has not artificially constrained the degree of epistemic uncertainty reflected by the models.

ART FRANKEL'S QUESTION #7

Unique aspects of Chi Chi mainshock. The fact that the Chi-Chi aftershocks do not show the same anomalously low high-frequency excitation in the near-source region (< 30 km) as the mainshock (Wang et al., Dec. 2004 BSSA) combined with the observation that regional and teleseismic spectra of the aftershocks and mainshock scale as expected for a constant stress drop model (Frankel, 2006, SSA annual meeting), indicates that there is a bias in the near-source recordings of the Chi-Chi earthquake. This may be due to the low accelerations near the north end of the rupture and/or footwall effects described above. We have previously noted the possible bias introduced by a higher number of stations located near the north end of the rupture compared to the south end. It is worth noting that Kanno et al. (June 2006 BSSA) exclude the Chi Chi mainshock data from their new attenuation relations for Japan (which include some California data), citing propagation differences between Taiwan and Japan. The Kanno et al. (2006) relations appear to be significantly higher than the NGA ones, for large magnitudes and close-in distances.

CAMPBELL-BOZORGNIA RESPONSE

There are four issues raised in this question: (1) that Wang et al. (2004) found anonymously low high-frequency (short-period) ground motions in the near-source region of the Chi-Chi mainshock as compared to its aftershocks, (2) that there might be a bias in the short-period ground motions near the fault because of low accelerations near the north end of the rupture and/or because of footwall effects, (3) that Kanno et al. (2006) excluded Chi-Chi mainshock data from their new empirical ground motion model for Japan, citing possible tectonic differences between Taiwan and Japan, and (4) that the Kanno et al. model appears to predict significantly higher ground motion than the NGA models at large magnitudes and close distances. Each of these issues is discussed below.

Results of Wang et al. (2004) Implying Differences Between Mainshock and Aftershocks

Wang et al. (2004) compared observed ground motions from the mainshock and five large aftershocks of the 1999 Chi-Chi (**M** 7.6) earthquake with predictions from four older empirical ground motion models. They concluded that the observed aftershock motions are in reasonable agreement with the predictions, particularly at distances of 10–30 km, which is in marked contrast to the motions from the mainshock, which are much lower than the predicted motions for periods less than 1.0s. They also concluded that the aftershock motions at distances of 10–30 km are somewhat lower than the predictions, suggesting that the ground motion possibly attenuates more rapidly in this region of Taiwan than it does in the areas represented by these older models.

We did not include Chi-Chi aftershocks in the development of our NGA model, so their specific behavior is not relevant with respect to our predictions. However, the relative difference between these aftershocks and the mainshock, especially at short periods, is potentially important and is addressed here. These authors' conclusions are based on comparing the residuals with respect to a set of older ground motion models, so all that these results really indicate is that the previous models are not consistent with the short-period magnitude scaling from these earthquakes, either because there is a problem with the magnitude scaling predicted

by the models or because there is something different in the short-period behavior of the mainshock. So these results by themselves are equivocal for concluding whether the short-period ground motions from the Chi-Chi mainshock are unusually low with respect to other earthquakes of similar size.

Wang et al. also brought up the possibility that the ground motions might attenuate more rapidly in this part of Taiwan than they do in the areas it is compared with (primarily California). We have addressed that issue in response to your Questions #3 and #5 and Mark Petersen's Question #1, where we show plots that indicate that there is no overall bias in the intra-event residuals with respect to distance in Taiwan (i.e., the Chi-Chi earthquake) or any of the other regions identified in these plots. There are, however, azimuthal differences in the Chi-Chi ground motions as discussed in the next section.

Bias in Short-Period Ground Motions Near the Fault

You have suggested that there might be a bias in the short-period ground motions from the Chi-Chi earthquake near the fault because of low accelerations near the north end of the rupture and/or because of footwall effects. The issue regarding footwall effects was addressed in response to your Question #3. Figures 1 and 2 of that response show that there is no overall positive bias (under-prediction) in PGA or 0.2s spectral acceleration with respect to distance. The only bias is a general over-prediction of ground motions once the inter-event residual (source term) is taken into account. However, as Figures 9 and 10 in response to your Question #3 show, there are relatively strong azimuthal effects that appear to be consistent with your observations. To better address these effects, we have re-plotted these figures over a shorter distance range of 0–40 km in Figures 1 and 2. For purposes of comparison, we also show similar plots for 1.0 and 3.0s spectral accelerations in Figures 3 and 4.

Figures 1 and 2 clearly show that short-period ground motions in the northern direction at distances of 30 km and less are over-predicted by our model, whereas those to the south are under-predicted by our model, relative to the Chi-Chi earthquake as a whole. This is consistent with your observation that short-period ground motions to the north are lower than those to the south. Interestingly, this effect fades out at 1.0s (Figure 3) and the opposite effect occurs at 3.0s (Figure 4). This shift from relatively low short-period ground motions to relatively high long-period ground motions to the north is consistent with both directivity (rupture was primarily to the north) and the increased fault displacement along the northern part of the rupture.

Given that the near-source biases you observed are confirmed by our residuals, the question remains whether they biased our near-source predictions. Again, we refer you to the figures referenced in the previous section, which clearly show that there is no overall bias in our predictions at either near-source or far-source distances. This is due to the large number of recordings from this earthquake, which as a whole provide an unbiased estimate of ground-motion attenuation.

Decision by Kanno et al. (2006) to Exclude Chi-Chi Data

Kanno et al. (2006) chose to exclude recordings from the Chi-Chi earthquake, even though they included recordings from California, the United States, and Turkey, citing three different investigators suggestions that the short-period ground motions from this earthquake were

anonymously low. They performed no independent analyses. They offered two reasons why this might have been the case: (1) that Taiwan is located on a much-fractured continental margin and (2) that seismic wave propagation may be different than in other regions of the crust. We showed in the previous two sections that the second reason is not valid for our dataset. The first observation might be true, but that does not necessarily imply lower attenuation in Taiwan as compared to other active tectonic regions, again as demonstrated by our database.

The Kanno et al. model does appear to predict higher values of PGA than the NGA models for shallow earthquakes at large magnitudes and close distances. These estimates are generally consistent with those predicted by the previous U.S. models (e.g., see their Figure 12 for a comparison with the Boore et al., 1997, model). This is no surprise, since these authors used a traditional magnitude-dependent functional form with the parameter that controls the magnitude scaling at close distances (their e_1) fixed at a value of 0.5 based on previous studies. Furthermore, their magnitude scaling at large magnitudes is linear, whereas most of the recent models have used a quadratic relation, which predicts decreasing magnitude scaling with increasing magnitude at all distances.

By fixing e_1 and using linear magnitude scaling, these authors did not allow their large-magnitude data at either short or long distances to have much influence on the behavior of their model in this critical magnitude range. To show how this decision has biased their predictions, we refer you to their Figure 16c, which plots their inter-event residuals versus magnitude for the shallow events. This figure shows that events with magnitudes between 6.5 and 7.0 are generally under-predicted by their model, whereas those with magnitudes of 7.0 and greater (7 events, including 4 from California) are generally over-predicted by their model. A model that predicts less magnitude scaling for $\mathbf{M} > 6.5$, as our NGA model does, would likely reduce or eliminate this bias.

Conclusion

Based on the discussion provided in the previous sections, we conclude that the Chi-Chi earthquake has not biased the short-period predictions in our NGA model either at near-source or far-source distances. In fact, once the inter-event residuals are taken into account, our model generally over-predicts these short-period ground motions. That is not to say that there are not strong azimuthally dependent attenuation effects, only that there is sufficient data at all azimuths and distances to provide a relatively unbiased estimate of the overall rate of attenuation during this earthquake. Our results also show that overall attenuation during the Chi-Chi earthquake is consistent with our model as well as with the data we used from other regions.

Kanno, T., Narita, A., Morikawa, N., Fujiwara, H., and Fukushima, Y. (2006). A new attenuation relation for strong ground motion in Japan based on recorded data. *Bull. Seism. Soc. Am.* **96** 879-897.

Wang, G.Q., Boore, D.M., Igel, H., and Zhou, X.Y. (2004). Comparisons of ground motions from five aftershocks of the 1999 Chi-Chi, Taiwan, earthquake with empirical predictions largely based on data from California. *Bull. Seism. Soc. Am.* **94**, 2198-2212.

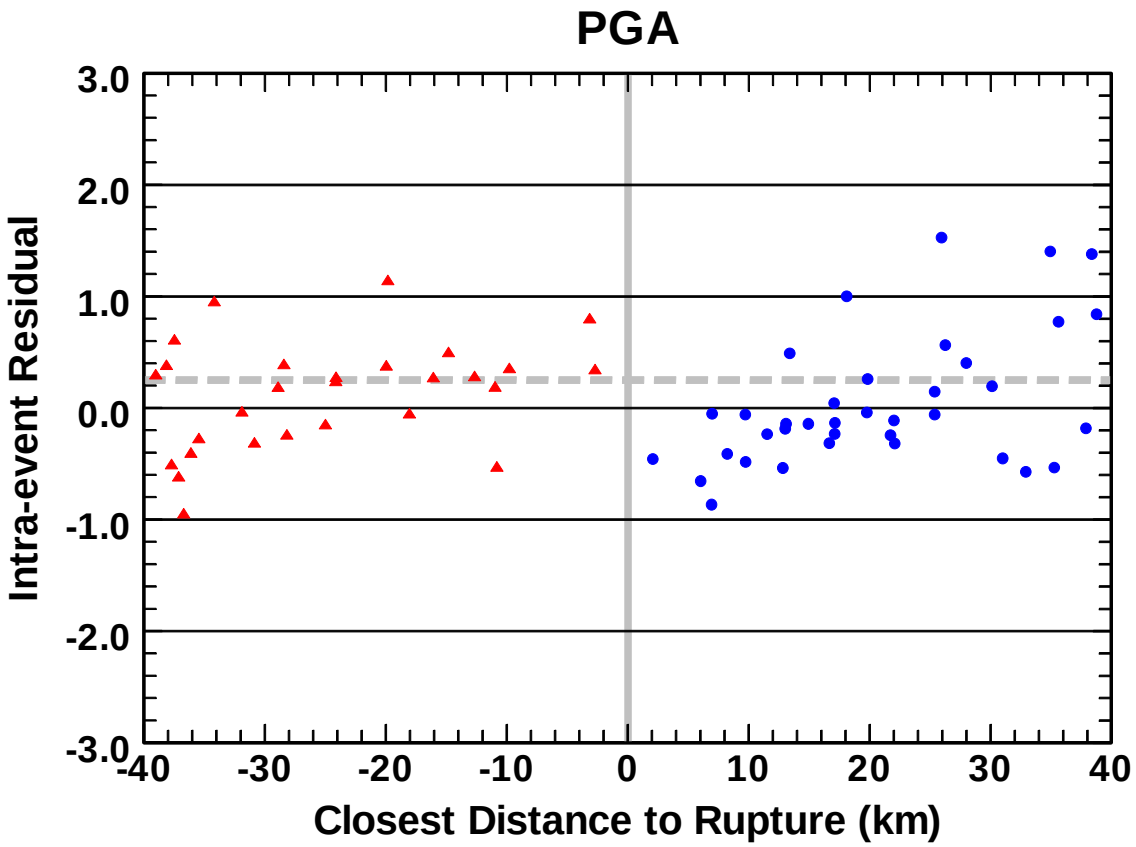

Figure 1: Plot of the PGA intra-event residuals from the Campbell-Bozorgnia NGA model for the Chi-Chi mainshock. Recordings are identified as being off the edge of the fault to the north in the direction of rupture (blue circles) or off the edge of the fault to the south in the opposite direction of rupture (red triangles). Southern distances are plotted as negative values for clarity. The vertical solid grey line demarks the transition from the northern sites to the southern sites. The horizontal dashed grey line represents the adjusted baseline after accounting for the source term and the additional bias caused by disallowing over-saturation, where a positive value represents an over-prediction by the model (in this case a significant over-prediction).

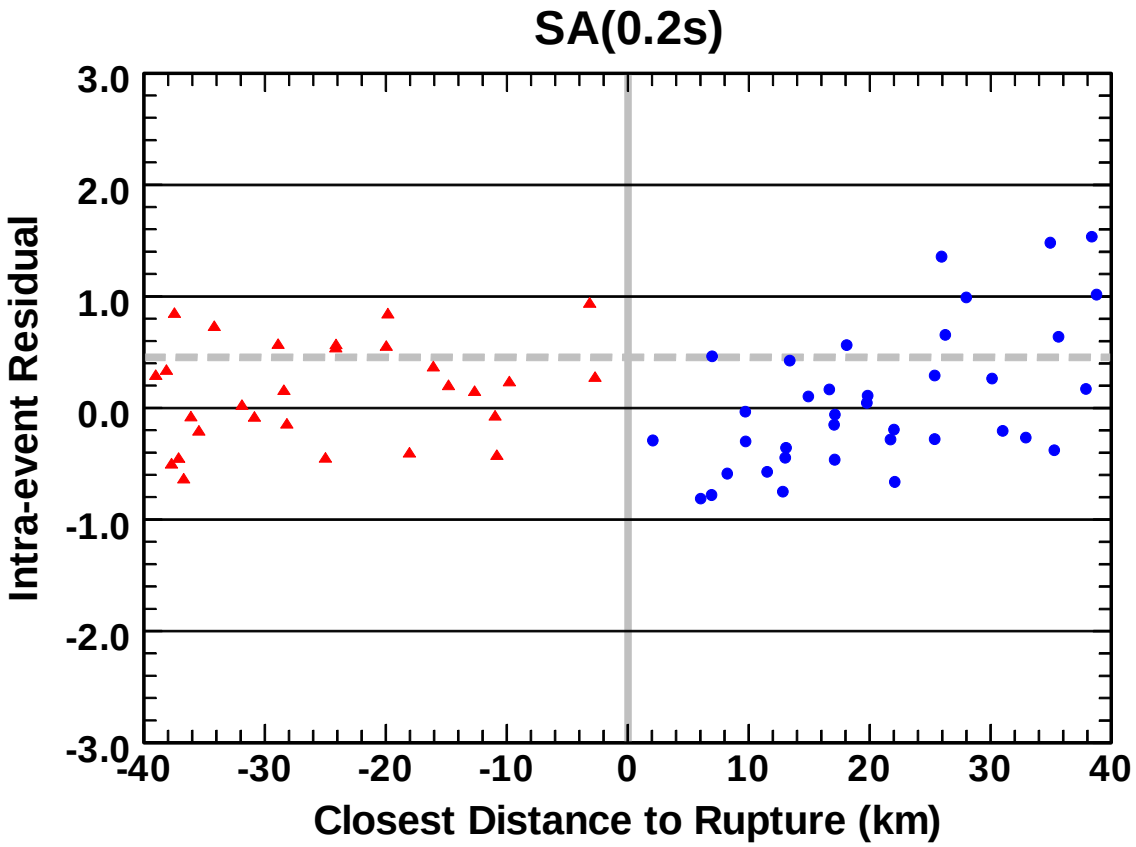

Figure 2: Plot of the 0.2s spectral acceleration intra-event residuals from the Campbell-Bozorgnia NGA model for the Chi-Chi mainshock. The symbols and grey solid and dashed lines are the same as in Figure 1.

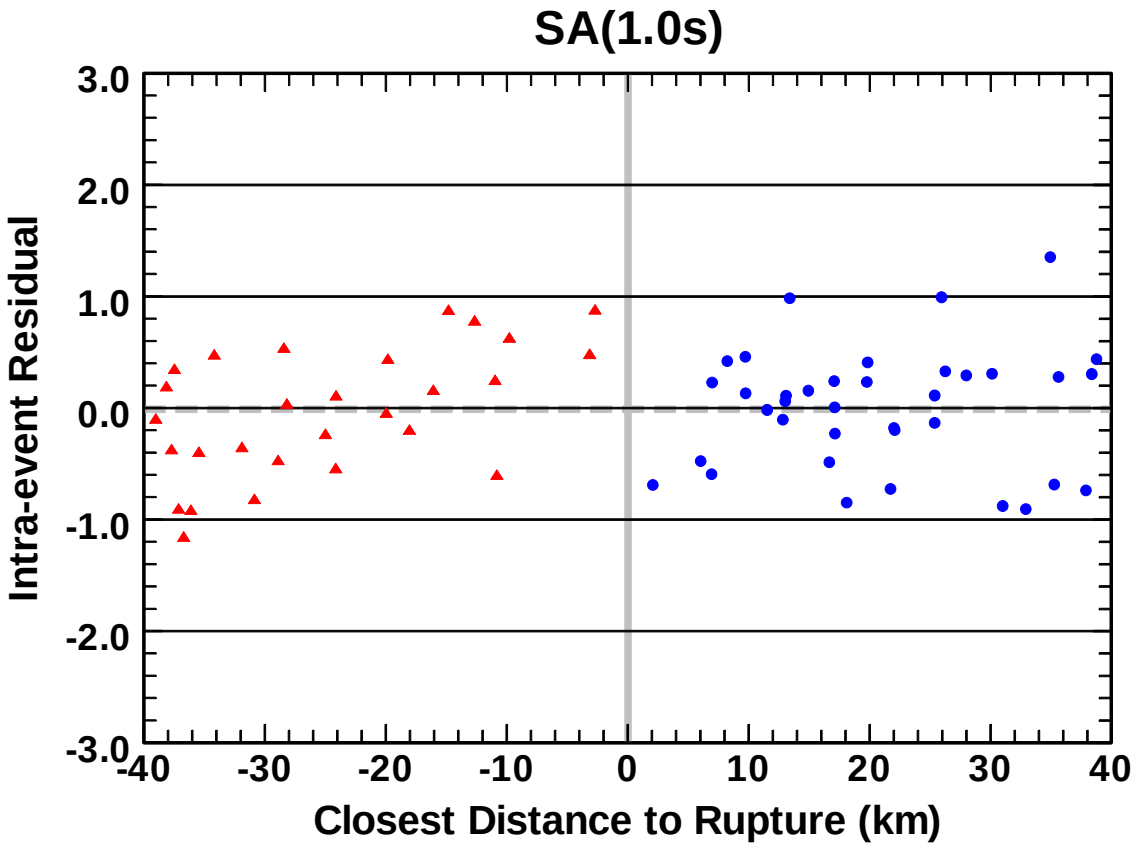

Figure 3: Plot of the 1.0s spectral acceleration intra-event residuals from the Campbell-Bozorgnia NGA model for the Chi-Chi mainshock. The symbols and grey solid and dashed lines are the same as in Figure 1.

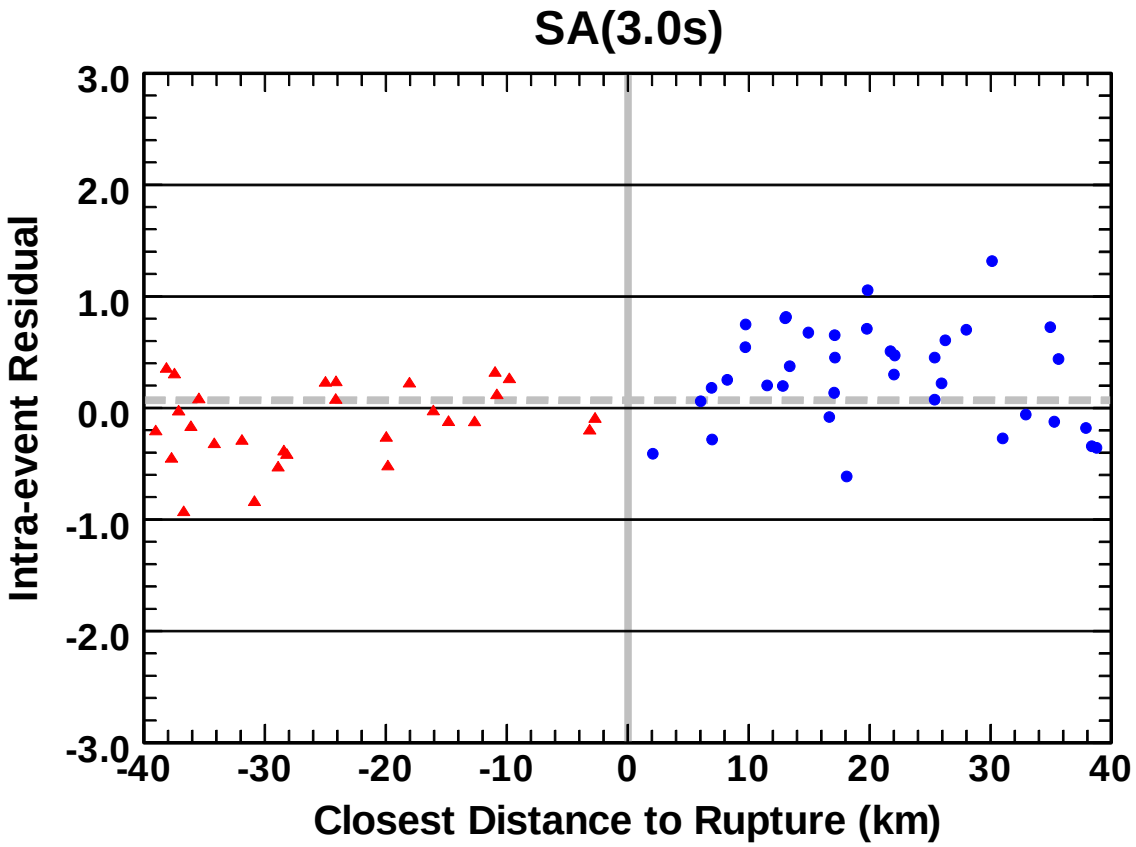

Figure 4: Plot of the 3.0s spectral acceleration intra-event residuals from the Campbell-Bozorgnia NGA model for the Chi-Chi mainshock. The symbols and grey solid and dashed lines are the same as in Figure 1.

ART FRANKEL'S QUESTION #7

Unique aspects of Chi Chi mainshock. The fact that the Chi-Chi aftershocks do not show the same anomalously low high-frequency excitation in the near-source region (< 30 km) as the mainshock (Wang et al., Dec. 2004 BSSA) combined with the observation that regional and teleseismic spectra of the aftershocks and mainshock scale as expected for a constant stress drop model (Frankel, 2006, SSA annual meeting), indicates that there is a bias in the near-source recordings of the Chi-Chi earthquake. This may be due to the low accelerations near the north end of the rupture and/or footwall effects described above. We have previously noted the possible bias introduced by a higher number of stations located near the north end of the rupture compared to the south end. It is worth noting that Kanno et al. (June 2006 BSSA) exclude the Chi Chi mainshock data from their new attenuation relations for Japan (which include some California data), citing propagation differences between Taiwan and Japan. The Kanno et al. (2006) relations appear to be significantly higher than the NGA ones, for large magnitudes and close-in distances.

CHIOU-YOUNGS RESPONSE

Are there propagation differences between Taiwan and California?

"Propagation differences" between Taiwan and Japan were speculated by Kanno et al. (2006), not demonstrated. In fact, based on the evidences described below, we believe differences in magnitude scaling and distance attenuation between Taiwan and California are not likely to be significant. First, we did not find significant difference in Chi-Chi mainshock's γ (anelastic damping) once we account for truncation/incomplete data (Figure 29 of our report is attached). Secondly, we see similarity in PGA attenuation (Figure 1) between the model of Wu et al. (2001)[1], which was derived from Taiwan data only, and the model of Chiou and Youngs (2006), which was derived mainly from California data. Finally, we also see similarity in magnitude scaling between the two models at $R_{RUP} > 50$ km and $M < 6.5$.

However, large differences do exist at $M > 6.5$ and $R_{RUP} < 20$km, where the dataset of Wu et al. is poorly populated (Figure 2). These differences shouldn't be construed as proof of regional difference in near-source motions because the parameter (*h)* controlling the near-source prediction was fixed in Wu et al. [2], whereas the corresponding parameters (c_5 and c_6) in Chiou and Youngs were estimated from strong-motion data.

[1] Wu, Y.M., T.C. Shin, and C.H. Chang (2001). Near real-time mapping of peak ground acceleration and peak ground velocity following a strong earthquake, *Bull. Seism. Soc. Am.* **91**, 1218 – 1228.

[2] The Wu et al. model is $log_{10}(PGA)=0.00215+0.581M_w-log_{10}(R_{RUP}+h) -0.00414R_{RUP}$. Parameter $h=0.0871 x10^{0.5Mw}$ is fixed to the square root of the rupture area determined from a simple relationship between rupture area and M_w.

Unique aspects of Chi-Chi mainshock high-frequency motions and their effect on the Chiou-Youngs model

Several unique aspects of the Chi-Chi high-frequency motions were identified by the reviewers and they were also used by the reviewers to call into questions the utility of the Chi-Chi mainshock data for predicting ground motions of large magnitude event in California.

Some of the of Chi-Chi motions are addressed in our responses to Mark Petersen's question #1 and Art Frankel's question #3. To confirm and provide scientific explanations of the remaining issues would require additional ground-motion data and more in-depth analysis. These studies may be of great scientific interests, but from the standpoint of ground-motion prediction the more relevant question to ask is: do the unique Chi-Chi data bias the estimates of key model parameters?

Throughout our model development we made an attempt to prevent any one earthquake from having a major effect on the estimates of model parameters. For example, we estimated the style of faulting effect with the Chi-Chi mainshock data removed. Another example, the general form of our distance attenuation model was developed with footwall (and hanging) data removed for all earthquakes so that the unique Chi-Chi footwall data will not affect these terms.

The outcome of this practice, we believe, is a model that is not unduly biased by the Chi-Chi data.

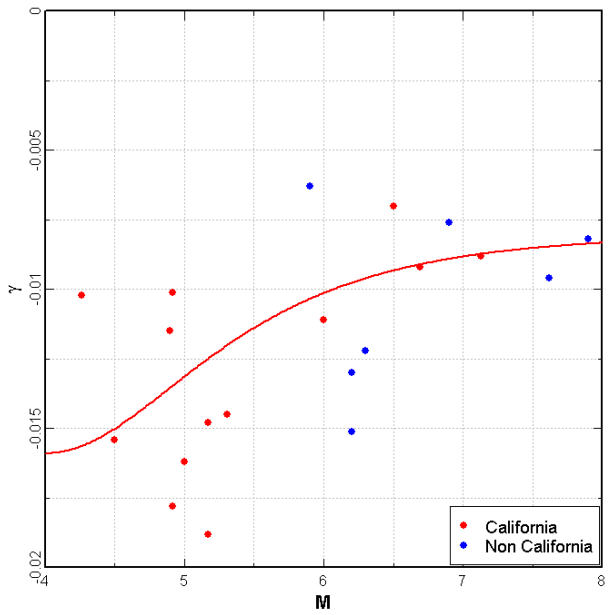

Figure 29 of Chiou and Youngs: Estimates of γ from analysis of the extended data sets (Table 4). Red curve shows the model developed by a fit to the combined California earthquake data set.

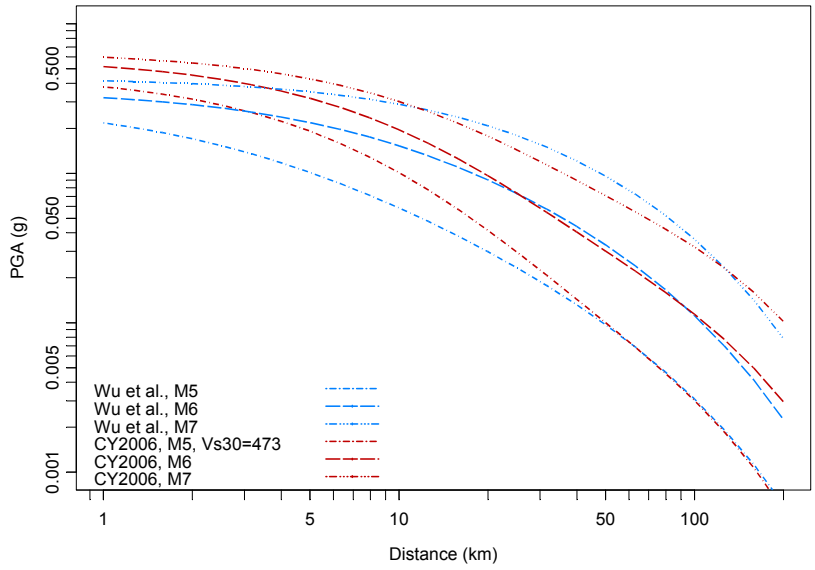

Figure 1: Comparison of median motions predicted by the models of Wu et al. (2001) and Chiou and Youngs (2006). A V_{S30} of 474 m/sec was used to compute motions from Chiou and Youngs.

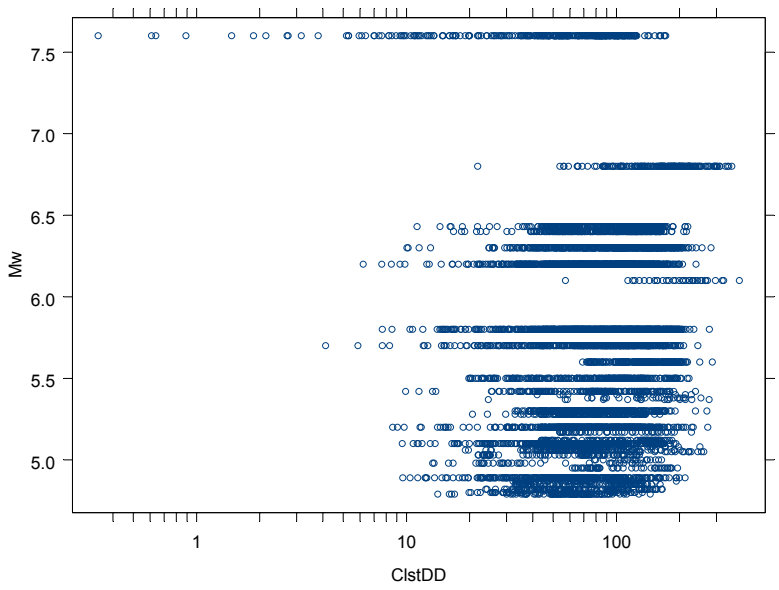

Figure 2: Magnitude-distance distribution of the dataset used in the regression of PGA model by Wu et al. (2001). Note that the regression data set consists of PGA data from 60 earthquakes recorded at 75 telemetered strong-motion stations in Taiwan, plus data recorded by the TSMIP stations at distance less than 30km from the source.

RESPONSES TO VLADIMIR GRAIZER'S QUESTIONS

VLADIMIR GRAIZER'S QUESTION #1

What is the scientific rational for the upper limit of magnitudes: 8.0 for dip-slip and 8.5 for strike-slip? As far as we know, the upper limit on dip-slip faulty style is 7.6 Chi-Chi and for strike-slip it is 7.9 Denali (and Denali has only one record in the near-field).

ABRAHAMSON-SILVA RESPONSE

In the past, published ground motion models often gave limits on the range of magnitudes for which the model was considered to be applicable based on the empirical data set used to derive the models, but these limits were generally ignored in the application of the models in PSHA. Since the users of the models (often people with no ground motion expertise) are going to extrapolate them to magnitudes outside the range of the empirical data, we decided that it would be better to have the model developers decide how their models should be extrapolated.

The specified upper limits on magnitude have nothing to do with the applicable limits of the data. In practice, the models will be applied to whatever magnitudes are included in the source characterization. Using the USGS WG02 model, the largest magnitudes for strike-slip earthquakes in Northern California are larger than M8. For example, for rupture of all four segments of the northern San Andreas, the mean characteristic magnitude can be as large as 8.1. Including aleatory variability about this mean magnitude of 0.24 units leads to a M8.34 earthquake. Therefore, if the WG02 source model is going to be used in a PSHA, ground motions are needed for strike-slip earthquakes up to M8.34. We rounded this to M8.5 for the NGA project. For reverse earthquakes, reverse faults in California can have mean characteristic magnitudes in the high M7 range. For example, the Little Salmon fault has a mean characteristic magnitude of 7.75. Again, including the aleatory variability leads to a magnitudes as large as 8.0.

We recognized that the empirical data would not constrain the ground motion models at these large magnitudes. To help the developers constrain the extrapolation to these very large magnitudes, suites of numerical simulations for rock site conditions were conducted based on 1-D kinematic models. The set of simulation exercises and the magnitude scaling resulting from these simulations are given in Somerville et al (2006)[1].

These simulations were not as useful as we had hoped because the resulting magnitude scaling was not consistent between the three groups that conducted the simulations (URS, Pacific Engineering, and UNR). We are conducting additional work on improving the numerical simulations to address the short-comings from the NGA study, but this work is expected to take several years.

In conclusion, it should be the responsibility of the developers, not the users, to use the information provided during the NGA project and their expertise in ground motions to

[1] Subsequently, the results in Somerville et al (2006) were revised in Collins et al. (2006).

extrapolate their empirical models to the very large magnitudes demanded by the latest PSHA models.

Collins, N., Graves, R., and Somerville, P., 2006, Revised analysis of ID rock simulations for the NGA-E Project, Report to the PEER-Lifelines Program, Project 1C02d by URS Corporation.

Somerville, P. G., Collins, N., Graves, R., Pitarka, A., Silva, W., and Zeng, Y., 2006, Simulation of ground motion scaling characteristics for the NGA-E Project, *Proceedings of the 8th National Conference on Earthquake Engineering,* San Francisco, CA.

VLADIMIR GRAIZER'S QUESTION #2

What is the justification for the upper and lower level of periods 0.01 to 10 sec (0.1 to 100 Hz)? All analog type instruments like SMA-1 have a limit of about 20 Hz (0.05 sec), and it is about 50 Hz for the new digital. For the long-period part, most data before Northridge were processed up to about 5 secs. Only starting with Hector Mine we can justify 10 sec as a cut-off.

ABRAHAMSON-SILVA RESPONSE

As with the magnitude limits discussed in Question 1, the specified limits on period have nothing to do with the applicable limits of the data. In practice, response spectra are required to cover very high frequencies (e.g. for equipment) and very long periods (e.g. for high rise buildings, bridges and tanks). If we only develop the ground motion models for periods that are well constrained by the empirical data, then these spectra will have to be extrapolated to high frequencies and long periods for individual projects. In the past, this extrapolation has been done in inconsistent ways. In many cases, the spectra are extrapolated by people without expertise in ground motions. Therefore, we decided that it would be better to have the NGA developers do the extrapolation to high frequencies and long periods.

To assist the NGA developers, the 1-D rock site simulations discussed in response to Question 1 provided spectral values that covered the specified period range. In addition, scaling of long period spectra values based on 3-D basin simulations were also provided.

In conclusion, It should be the responsibility of the developers to use this information and their expertise in ground motions to extrapolate their empirical models to the high frequencies and long periods demanded by engineers.

VLADIMIR GRAIZER'S QUESTION #2

What is the justification for the upper and lower level of periods 0.01 to 10 sec (0.1 to 100 Hz)? All analog type instruments like SMA-1 have a limit of about 20 Hz (0.05 sec), and it is about 50 Hz for the new digital. For the long-period part, most data before Northridge were processed up to about 5 secs. Only starting with Hector Mine we can justify 10 sec as a cut-off.

CAMPBELL-BOZORGNIA RESPONSE

In order to judge whether our model predicts reasonable spectral values at long periods, we plotted the displacement spectra predicted by our model out to 10s. Although the overall shape of the spectra looked reasonably good, we could see that the long-period spectral behavior at magnitudes less than around 6.5 were not in line with what one might expect from simple seismological principles. In order to better constrain the model at long periods and small magnitudes, we looked at the predicted displacement spectra from ground-motion simulations. Figure 1 gives an example of the displacement spectra predicted by our model. The predictions above M6.5 are generally constrained by the empirical data, so it is only the smaller magnitudes that have been constrained from seismological principles.

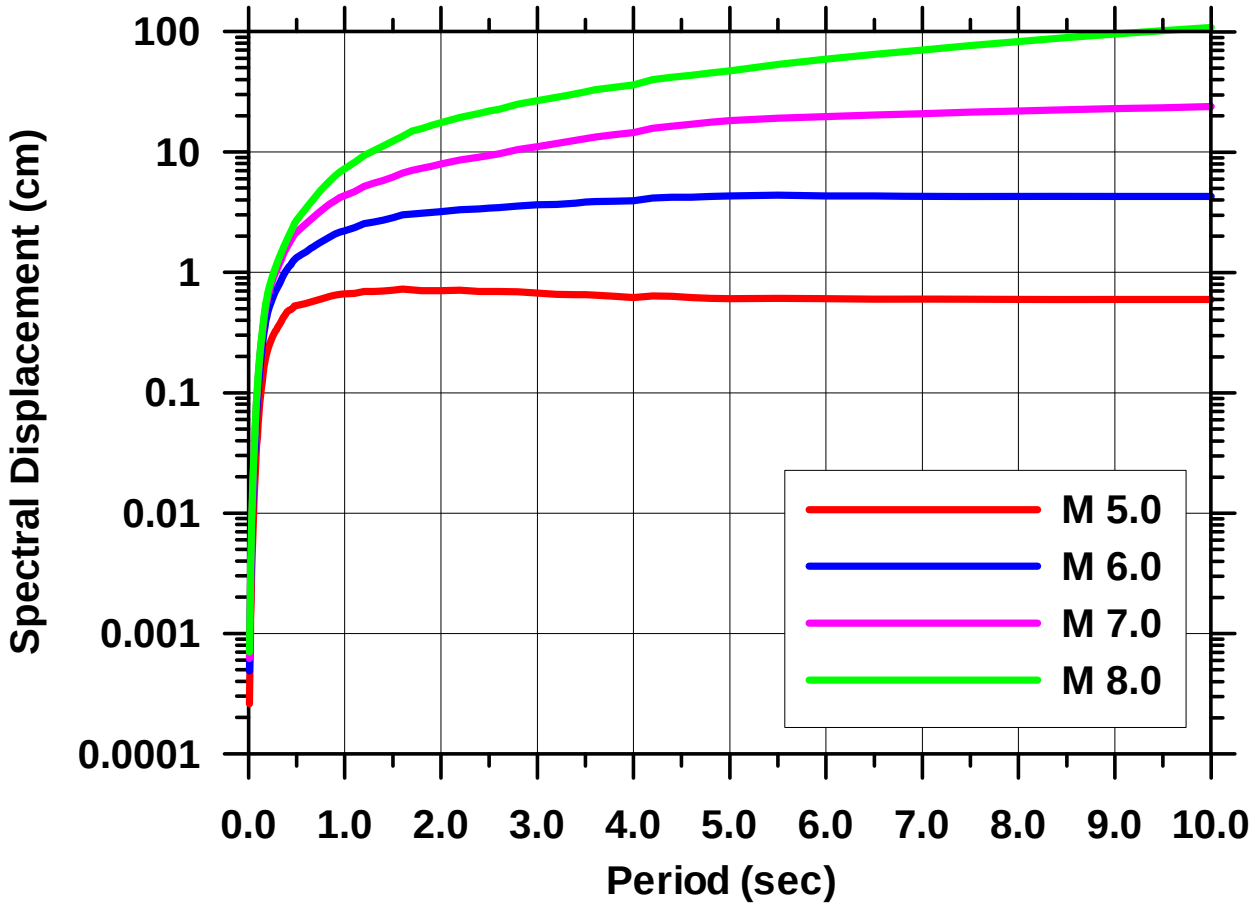

Figure 1: Relative displacement spectra predicted by the Campbell-Bozorgnia NGA model for a distance of 10 km, NEHRP B-C site conditions, and strike-slip faulting.

VLADIMIR GRAIZER'S QUESTION #2

What is the justification for the upper and lower level of periods 0.01 to 10 sec (0.1 to 100 Hz)? All analog type instruments like SMA-1 have a limit of about 20 Hz (0.05 sec), and it is about 50 Hz for the new digital. For the long-period part, most data before Northridge were processed up to about 5 secs. Only starting with Hector Mine we can justify 10 sec as a cut-off.

CHIOU-YOUNGS RESPONSE

We use data with long period information and accounted for bias in sample to extend to 10 sec. At high frequencies, we expect that WUS ground motions at most sites have little energy above 50 Hz. Therefore, 100 Hz is essentially the same as PGA. We recognize that this may be an issue as high V_{s30} sites, which is why we set ground motions to be equal for sites with V_{s30} < 1130 m/sec.

VLADIMIR GRAIZER'S QUESTION #3

Strong motion data are biased toward larger motions at large distances, but data truncation at 60-80 km is really very restrictive. For example, it basically eliminates basin effect, which is extremely important in Southern California (Hector Mine, Landers). How can you justify applicability of the equations up to 200 km by using data set that practically doesn't have surface waves?

ABRAHAMSON-SILVA RESPONSE

The 200 km upper limit on the distance has nothing to do with the applicable limits of the data. In practice, the ground motion models are used for large distances regardless of the limits of applicability that the developers may state. Since the ground motion models will be extrapolated to large distances, we decided that it would be better to have the NGA developers do the extrapolation to large distances. To assist the developers, 1-D rock simulations (as discussed in Question 1) were provided out to distances of 200 km. The Green's functions for two of three sets of simulations include surface waves, but only for rock site conditions (e.g. no surface waves due to basin response).

In addition, an analysis of attenuation from network data (Boatwright, 2005) was provided that could be used to guide the extrapolation to large distances. Finally, the developers were provided recordings from digital accelerograms from several magnitude 5 earthquakes out to distances of several hundred km that could be used to constrain the attenuation at large distances (D. Boore, written communication, 2005).

A few developers opted to truncate the distance used to select the database at a value less than the required 200 km. However, those developers used additional data, such as broadband and other network data, to extrapolate their models to larger distances.

VLADIMIR GRAIZER'S QUESTION #3

Strong motion data are biased toward larger motions at large distances, but data truncation at 60-80 km is really very restrictive. For example, it basically eliminates basin effect, which is extremely important in Southern California (Hector Mine, Landers). How can you justify applicability of the equations up to 200 km by using data set that practically doesn't have surface waves?

CAMPBELL-BOZORGNIA RESPONSE

We were initially concerned that using data out to 200 km would result in a bias in our prediction of near-source ground motions. As a result, we first truncated the database at 60 km as in our 2003 model and performed our analysis. We then added the remaining data and repeated the analysis. The comparison showed that the near-source predictions were not significantly impacted by the more distant data. The largest effect was a much more moderate degree of over-saturation at large magnitudes and short distances when data from all distances were used. Since we chose not to allow over-saturation in our model, we thought that a database that minimized this behavior was preferable over one that did not. Of course, as you suggest in your question, including such data also increased the number of recordings that contributed to our sediment depth (i.e., 3-D basin) term. One adverse impact of using the more distant data is our belief that our model might under-predict the amount of attenuation for the smaller earthquakes, but this only impacts ground motion of little engineering importance. This impact is due in part to the selectiveness of only processing earthquakes and/or recordings with the largest ground motions, especially for earthquakes with magnitudes less than around 6.0.

VLADIMIR GRAIZER'S QUESTION #3

Strong motion data are biased toward larger motions at large distances, but data truncation at 60-80 km is really very restrictive. For example, it basically eliminates basin effect, which is extremely important in Southern California (Hector Mine, Landers). How can you justify applicability of the equations up to 200 km by using data set that practically doesn't have surface waves?

CHOIU-YOUNGS RESPONSE

We constrained the distance scaling for R >70 km using well recorded California earthquakes. We account for the influence of surface waves at larger distances by changing to $R^{-1/2}$ geometric spreading at large distances. Basin effects are incorporated through scaling with $Z_{1.0}$. Out Figure 45 compares the model extrapolated to large distances with data for two well recorded earthquakes.

VLADIMIR GRAIZER'S QUESTION #4

What is the current thinking on large distance data with amplitudes below 0.5% g recorded at non-strong motion networks? It was a long discussion at a couple of meetings and justification for use of these data, and they are not even mentioned in the current reports?

BOORE-ATKINSON RESPONSE

We see nothing wrong with the more distant data. This conclusion is based on the fact that the data we used for the three small earthquakes (Anza, Big Bear City, and Yorba Linda) were not from velocity sensors and thus did not need conversion to acceleration and also from comparing plots of the data vs. distance for the three small events and for the Parkfield earthquake.

The attached Figures 1, 2, and 3 compare pgv, pga, and PSA for 0.1, 0.2, 1.0, and 3.0 sec for Parkfield 2004 (M=6.0), Anza 2001 (M=4.92), Big Bear City 2003 (M=4.92), and Yorba Linda (M=4.27). According to the SCSN web site (http://www.trinet.org/instr.html#analogvsdig), the accelerograph data for the three small earthquakes come from K2 accelerographs. The distance for Park04 is rjb and for others is rep. No site correction has been applied to Park04, but the data for other quakes has been corrected to V30=760 m/s using BJF97 amp factors (no nonlinear correction). The ground-motion intensity measures from the two horizontal components have not been merged---the plots show both the intensity measures for both components for each station. Nothing strange is noted in the distance decay of the three smaller events compared to the Parkfield data, although it is interesting to note that the level of motions at high frequency for Anza and BBC are comparable to Parkfield, although the magnitudes are quite different.

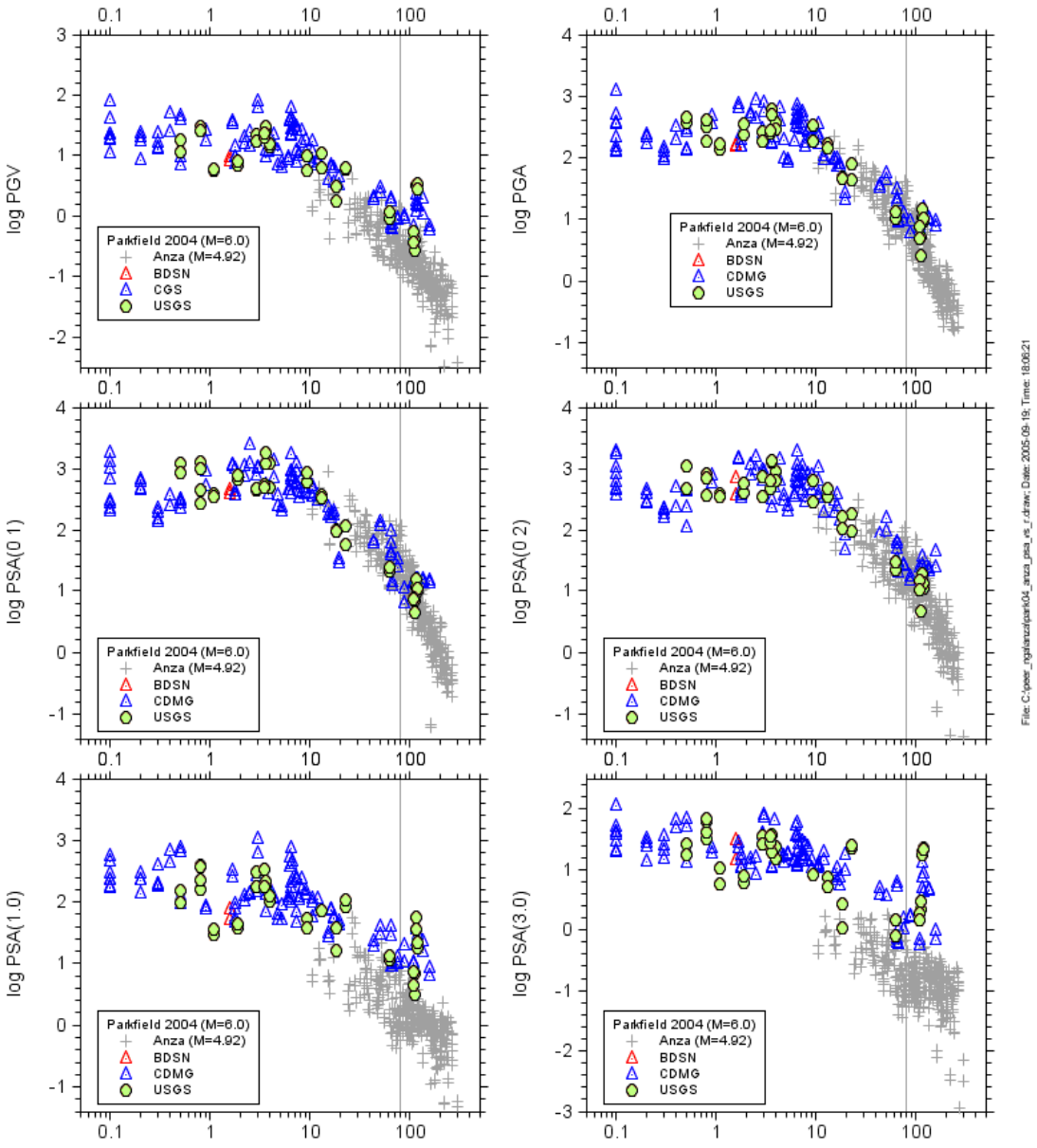

Figure 1. Anza and Parkfield data.

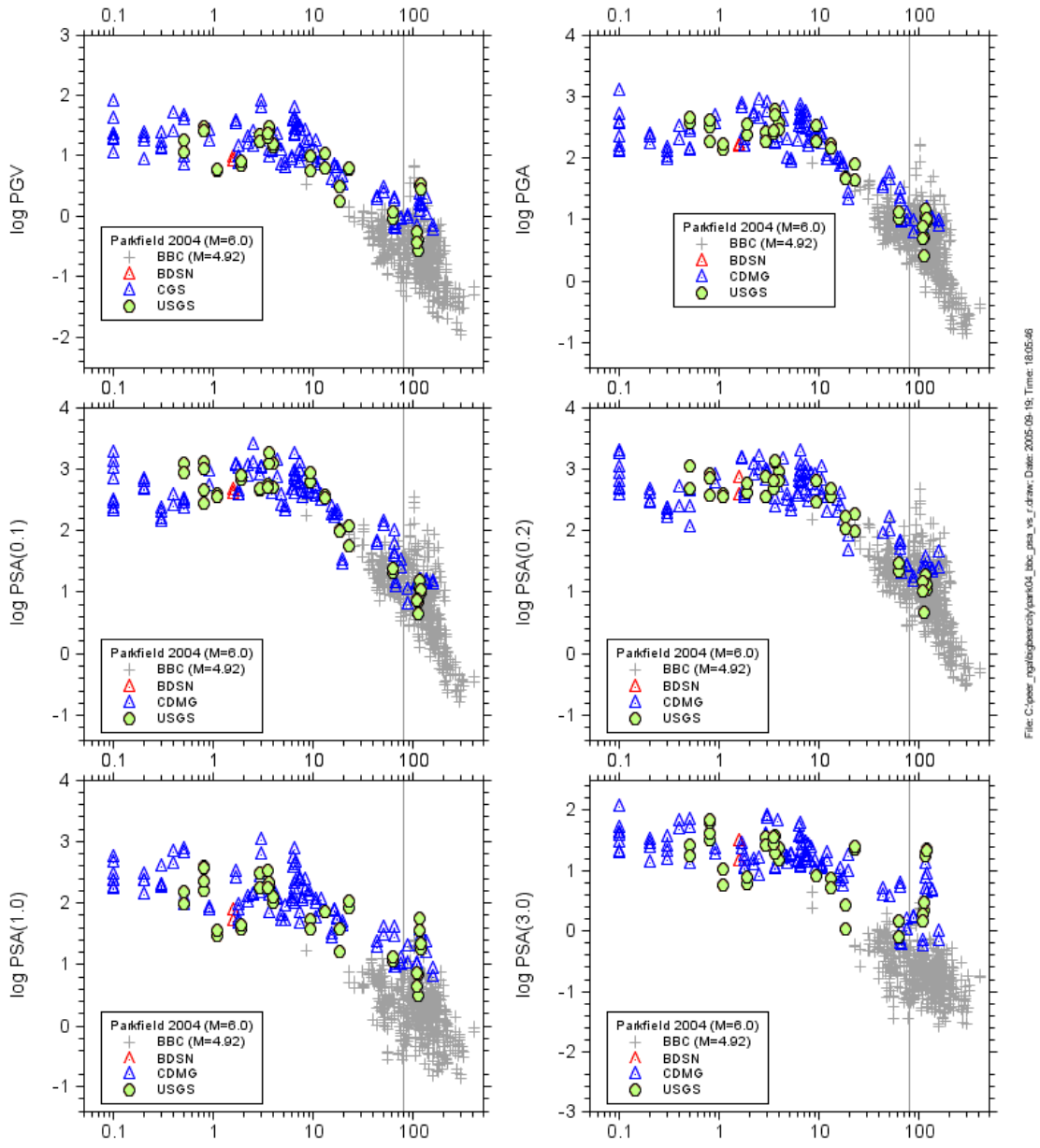

Fig. 2. BBC and Parkfield

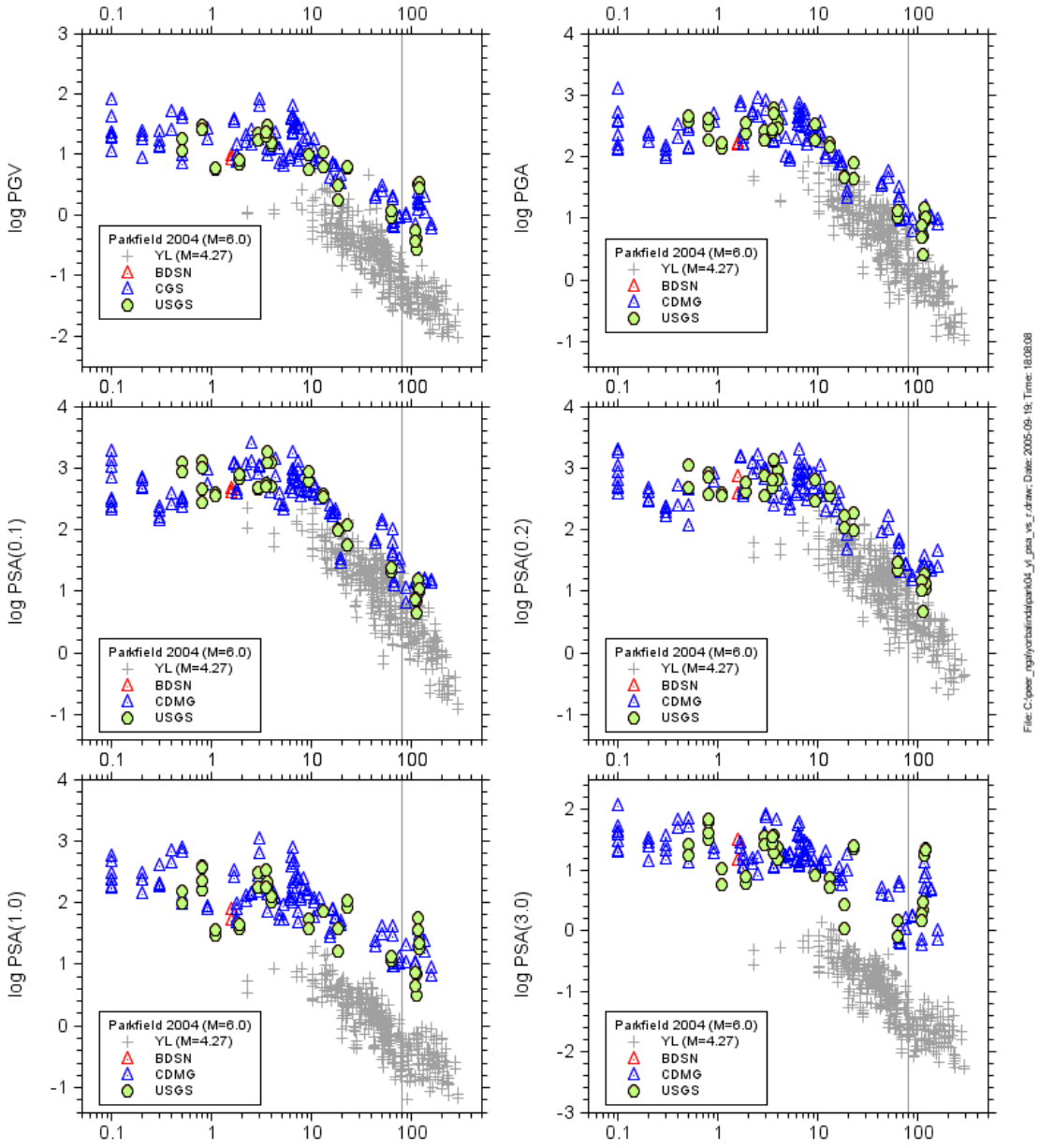

Fig. 3. YL and Parkfield

VLADIMIR GRAIZER'S QUESTION #4

What is the current thinking on large distance data with amplitudes below 0.5% g recorded at non-strong motion networks? It was a long discussion at a couple of meetings and justification for use of these data, and they are not even mentioned in the current reports?

CAMPBELL-BOZORGNIA RESPONSE

The discussions you refer to centered on the validity of these ground motions, considering they potentially come from instruments whose response is flat to velocity rather than acceleration. Such data would require differentiation to obtain acceleration. None of the developers explicitly used such data in their regression analyses. In fact, including data other than that provided through the NGA database development team (the so-called "flatfile") was strictly forbidden. However, data other than that provided by the NGA project was used to various degrees by some developers to help constrain their models, which was allowed. Campbell-Bozorgnia did not use any data other than that provided by the NGA project team (the so-called flatfile) in the development of our model, so the small-amplitude data you refer to did not influence our model.

VLADIMIR GRAIZER'S QUESTION #4

What is the current thinking on large distance data with amplitudes below 0.5% g recorded at non-strong motion networks? It was a long discussion at a couple of meetings and justification for use of these data, and they are not even mentioned in the current reports?

CHIOU-YOUNGS RESPONSE

We use these data, see our Figure 28 and Appendix D. We think that they are an important source of information.

VLADIMIR GRAIZER'S QUESTION #5

What is the seismological justification for using non-linearity in it current form? Is it in accordance to what is known about non-linearity in strong motion:

- *Non-linearity is only proven for amplitudes of ground motion higher than 20-30% g in some earthquakes. (Loma Prieta, Northridge, Chi-Chi), but does not show up for examples in records or Whittier Narrows (Beresnev, 2002).*
- *Non-linearity is a frequency dependent phenomenon shown to take place for frequencies 1.0-5.0 Hz (Field, 2000)*
- *Empirical results of Choi & Stewart (2005) for 5% damped response spectral acceleration show large degree of non-linearity for Vs30<180 m/s, rapidly decreasing with increasing Vs30.*

ABRAHAMSON-SILVA RESPONSE

The developers used different approaches to modeling the non-linearity. All of the approaches are consistent with what is "known" about non-linear behavior in strong motion; however, what the developers consider to be "known" may be different between the different developers. In each case, the developers checked that the non-linearity in their models is consistent with their selected subset of the empirical data. But these data are not sufficient to constrain the non-linear soil behavior at large ground motions and soft sites, so most of the modelers reverted to modeling to some extent to define the models in this region.

Boore & Atkinson Approach: These developers constrained the non-linearity of the site to be consistent with the empirical results of Choi and Stewart (2005). However, they found it necessary to modify the model to smooth through the velocity "steps" built into the Choi and Stewart model and to constrain the model to behave more linearly at small values of PGA.

Abrahamson & Silva; Campbell & Bozorgnia Approach: These developers constrained the non-linearity using analytical geotechnical models of the site response based on modeling by Silva (2005). Using standard 1-D equivalent-linear soil models, the non-linearity of the site response was parameterized as a function of the input rock PGA and Vs30 as described by Walling and Abrahamson (2006). This model leads to some non-linear site response even at PGA values less than the 0.20g-0.30g values cited in the question. This degree of non-linearity is consistent with the non-linearity observed in the aftershocks from the Chi-Chi earthquake.

Chiou & Youngs Approach: These developers used the results of the analytical site response analysis models from Silva (2005) to guide the formulation of their non-linearity terms and allowed the empirical data to constrain the model parameters.

It is often quoted that non-linear soil behavior is observed starting at around a PGA value of 0.2g. These are empirical observations that can only detect non-linearity when it is large enough to be observed above the normal ground-motion variability. Small amounts of non-linearity will go undetected in such observations, so models that predict some degree of non-linearity at smaller ground motions are not necessarily invalid. The 0.2g observational threshold for non-linearity is typically that recorded on soil not firm or hard rock, which is the

site condition used by the developers to determine non-linear soil effects. Rock values will be closer to 0.1g, again relatively consistent with the developers' models

With reference to Choi and Stewart (2005), since their reference site condition is soft rock reflected in empirical attenuation relations (e.g. Geomatrix A and B with a $\overline{V}_S(30m)$ near 500m/sec), a degree of nonlinearity associated with this site condition is already included in their reference site and thereby subtracted from their site amplification. Specifically, the Geomatrix A and B site condition (as a representative of soft rock site $\overline{V}_S(30m)$) is bi-modal with $\overline{V}_S(30m)$ peak at about 370m/sec and a lower peak (fewer recordings) at about 640m/sec. As a result some degree of nonlinearity is likely incorporated in the Choi and Stewart (2005) reference site, potentially reducing the apparent degree of nonlinearity in their amplification factors.

Choi, Y. and Stewart, J.P. 2005, Nonlinear site amplication as function of 30 m shear wave velocity, *Earthquake Spectra*, 21, 1-30.

Silva, W.J. 2005, Site response simulations for the NGA project. Report prepared for the Pacific Earthquake Engineering Research Center.

Walling, M., and Abrahamson, N., 2006, Non-linear soil response model, *Proc. 8th Nat. Conf. Earthquake Eng.*, San Francisco, CA.

VLADIMIR GRAIZER'S QUESTION #5

What is the seismological justification for using non-linearity in it current form? Is it in accordance to what is known about non-linearity in strong motion:

- *Non-linearity is only proven for amplitudes of ground motion higher than 20-30% g in some earthquakes. (Loma Prieta, Northridge, Chi-Chi), but does not show up for examples in records or Whittier Narrows (Beresnev, 2002).*
- *Non-linearity is a frequency dependent phenomenon shown to take place for frequencies 1.0-5.0 Hz (Field, 2000)*
- *Empirical results of Choi & Stewart (2005) for 5% damped response spectral acceleration show large degree of non-linearity for Vs30<180 m/s, rapidly decreasing with increasing Vs30.*

CAMPBELL-BOZORGNIA RESPONSE

Because NEHRP E sites can be subject to unique site-response characteristics, we have recommended that our model not be used for values of Vs30 less than 180 m/sec, unless the user believes that his site will not be subject to such unique site-response characteristics.

Choi, Y. and Stewart, J.P. 2005, Nonlinear site amplication as function of 30 m shear wave velocity, *Earthquake Spectra*, 21, 1-30.

VLADIMIR GRAIZER'S QUESTION #5

What is the seismological justification for using non-linearity in it current form? Is it in accordance to what is known about non-linearity in strong motion:

- *Non-linearity is only proven for amplitudes of ground motion higher than 20-30% g in some earthquakes. (Loma Prieta, Northridge, Chi-Chi), but does not show up for examples in records or Whittier Narrows (Beresnev, 2002).*
- *Non-linearity is a frequency dependent phenomenon shown to take place for frequencies 1.0-5.0 Hz (Field, 2000)*
- *Empirical results of Choi & Stewart (2005) for 5% damped response spectral acceleration show large degree of non-linearity for Vs30<180 m/s, rapidly decreasing with increasing Vs30.*

CHIOU-YOUNGS RESPONSE

We think that our model is consistent with the data (see our Figure 36).

Choi, Y. and Stewart, J.P. 2005, Nonlinear site amplication as function of 30 m shear wave velocity, *Earthquake Spectra*, 21, 1-30.

VLADIMIR GRAIZER'S QUESTION #6

All three reports use Choi and Stewart (2005) for the site amplification effect but the coefficients for the linear part vary: it is 0.36 in B&A, 0.34 in C&B, and 0.48 in C&Y. Why is it so different if it is based on the same source?

ABRAHAMSON-SILVA RESPONSE

The Abrahamson and Silva (A&S) model has a linear site term for PGA equal to 0.47, similar to that of C&Y. Note that all of these coefficients are actually negative to accommodate a reference site velocity in the denominator of the site velocity term. Not all of the developers used Choi and Stewart (2005) for their site-amplification term as indicated in the response to your Question 5, so one would not necessarily expect them to also have the same linear site term. This term will depend on the degree of non-linearity predicted by the model, the reference site velocity, the selected database, and other factors.

The four models all determine the linear site term from the empirical data. Since the models use different empirical subsets, the linear terms will be different. For example, Chiou & Youngs and Abrahamson & Silva include the Chi-Chi aftershocks in the determination of the site response, but Boore & Atkinson and Campbell & Bozorgnia do not include the these aftershocks. Given the large number of recordings from the Chi-Chi aftershocks, this data set difference could lead to a significant difference in the linear site terms.

Choi, Y. and Stewart, J.P. 2005, Nonlinear site amplication as function of 30 m shear wave velocity, *Earthquake Spectra*, 21, 1-30.

VLADIMIR GRAIZER'S QUESTION #6

All three reports use Choi and Stewart (2005) for the site amplification effect but the coefficients for the linear part vary: it is 0.36 in B&A, 0.34 in C&B, and 0.48 in C&Y. Why is it so different if it is based on the same source?

CAMPBELL-BOZORGNIA RESPONSE

Our linear soil coefficients of -0.34 and -0.73 for PGA and 1.0s spectral acceleration are very similar to the values of -0.37 and -0.70 originally derived by Boore et al. (1997). Although this doesn't prove our values are correct, it does imply that the non-linear site model we adopted from Walling and Abrahamson (2006) has not strongly biased our linear site term. We also checked our residuals and found, at least for NEHRP D and stiffer sites for which we consider our model valid, that our non-linear site term removed the tendency for our linear model to over-predict short-period ground motions on NEHRP C and D sites at the largest observed values of PGA without under-predicting at smaller values of PGA.

Boore, D.M., Joyner, W.B., and Fumal, T.E., 1997, Equation for estimating horizontal response spectra and peak accelerations from western North American earthquakes: a summary of recent work, *Seismol., Res. Lett*. 68, 128-153.

Choi, Y. and Stewart, J.P. 2005, Nonlinear site amplication as function of 30 m shear wave velocity, *Earthquake Spectra*, 21, 1-30.

Walling, M., and Abrahamson, N., 1996, Non-linear soil response model, *Proc. 8th Nat. Conf. Earthquake Eng.*, San Francisco, CA.

VLADIMIR GRAIZER'S QUESTION #6

All three reports use Choi and Stewart (2005) for the site amplification effect but the coefficients for the linear part vary: it is 0.36 in B&A, 0.34 in C&B, and 0.48 in C&Y. Why is it so different if it is based on the same source?

CHIOU-YOUNGS RESPONSE

We do not use Choi and Stewart, only compare model with theirs. Our φ1 from the full data set is consistent with φ1 computed from the ABY broadband data.

Choi, Y. and Stewart, J.P. 2005, Nonlinear site amplication as function of 30 m shear wave velocity, *Earthquake Spectra*, 21, 1-30.